Published for SISSA by Springer
Received: *September 25, 2020*
Accepted: *November 20, 2020*
Published: *January 18, 2021*

Elastic positivity vs extremal positivity bounds in SMEFT: a case study in transversal electroweak gauge-boson scatterings

Kimiko Yamashita,[a] **Cen Zhang**[a,b,c] **and Shuang-Yong Zhou**[d,e]

[a] *Institute of High Energy Physics, Chinese Academy of Sciences, 19B Yuquan Road, Beijing 100049, China*
[b] *School of Physical Sciences, University of Chinese Academy of Sciences, 19B Yuquan Road, Beijing 100049, China*
[c] *Center for High Energy Physics, Peking University, 209 Chengfu Road, Beijing 100871, China*
[d] *Interdisciplinary Center for Theoretical Study, University of Science and Technology of China, 96 Jinzhai Road, Hefei, Anhui 230026, China*
[e] *Peng Huanwu Center for Fundamental Theory, 96 Jinzhai Road, Hefei, Anhui 230026, China*

E-mail: kimiko@ihep.ac.cn, cenzhang@ihep.ac.cn, zhoushy@ustc.edu.cn

Abstract: The positivity bounds, derived from the axiomatic principles of quantum field theory (QFT), constrain the signs of Wilson coefficients and their linear combinations in the Standard Model Effective Field Theory (SMEFT). The precise determination of these bounds, however, can become increasingly difficult as more and more SM modes and operators are taken into account. We study two approaches that aim at obtaining the full set of bounds for a given set of SM fields: 1) the traditional elastic positivity approach, which exploits the elastic scattering amplitudes of states with arbitrarily superposed helicities as well as other quantum numbers, and 2) the newly proposed extremal positivity approach, which constructs the allowed coefficient space directly by using the extremal representation of convex cones. Considering the electroweak gauge-bosons as an example, we demonstrate how the best analytical and numerical positivity bounds can be obtained in several ways. We further compare the constraining power and the efficiency of various approaches, as well as their applicability to more complex problems. While the new extremal approach is more constraining by construction, we also find that it is analytically easier to use, numerically much faster than the elastic approach, and much more applicable when more SM particle states and operators are taken into account. As a byproduct, we provide the best positivity bounds on the transversal quartic-gauge-boson couplings, required by the axiomatic principles of QFT, and show that they exclude $\approx 99.3\%$ of the parameter space currently being searched at the LHC.

Keywords: Effective Field Theories, Beyond Standard Model

ArXiv ePrint: 2009.04490

https://doi.org/10.1007/JHEP01(2021)095

JHEP01(2021)095

Contents

1 Introduction

The dimension-8 (dim-8) Wilson coefficients [1–3] that give rise to s^2 dependence of a two-to-two scattering amplitude in the Standard Model Effective Field Theory (SMEFT) are not allowed to take arbitrary values [4–10]. By assuming that the SMEFT admits a UV

JHEP01(2021)095

completion that satisfies the fundamental principles of quantum field theory (QFT), including analyticity, unitarity, crossing symmetry, locality and Lorentz invariance, the so-called positivity bounds can be derived [11–44], determining the signs of certain linear combinations of dim-8 coefficients (plus possible dim-6 coefficients at the squared level). Since the ultimate goal of the SMEFT is to determine its UV completion, one should restrict the search for operators only within these bounds, and optimize the search strategy accordingly.

Alternatively, one might also use these bounds to experimentally test the fundamental principles of QFT [10, 45]. An even more important application of positivity is to infer or to exclude possible UV states using precision measurements, analyzed at the dim-8 level, in a completely model-independent way [10], which potentially provides an answer to the "inverse problem" [46–48]. In particular, if experimental observation continues to agree with the SM, this allows to set exclusion limits on all UV states up to certain scales, which cannot be lifted by cancellations among various UV particles [10]. Dim-8 operators and their positivity nature are thus crucial for SM tests. In either case, as the LHC has started to probe the dim-8 SMEFT operators in many occasions [49–53], and more opportunities can be foreseen at the future lepton colliders [10, 54, 55], it has become increasingly important to understand the positivity bounds on their coefficients.

In SMEFT, there are at least two approaches to derive positivity bounds, which we dub "elastic positivity bounds" and "extremal positivity bounds" in this paper. The first is the conventional approach which makes use of the *elastic* 2-to-2 forward scattering amplitude. Using analyticity of the amplitude, the Froissart bound and the optical theorem, one can show that its second order derivative is positive:

$$M^{ij} \equiv \frac{d^2}{ds^2}\bar{M}(ij \to ij)(s, t = 0) \geq 0 \tag{1.1}$$

where $\bar{M}(ij \to ij)$ is the elastic scattering amplitude between states $|i\rangle$ and $|j\rangle$, with poles subtracted (to be explained later) and s, t are the standard Mandelstam variables. The i, j indices label the SM modes. Since M^{ij} involves only low-energy physics, it can be computed within the SMEFT. This leads to, at the tree level, a set of linear homogeneous inequalities for dim-8 coefficients C_α [4, 5, 7]:

$$\sum_\alpha C_\alpha p_\alpha^{ij} \geq 0 \tag{1.2}$$

where p_α^{ij} only involve SM parameters. These are exactly a set of positivity bounds on SMEFT Wilson coefficients. While the squared contribution of the dim-6 coefficients may also enter the l.h.s., in this work we will mainly focus on dim-8 coefficients, for reasons that will be discussed later. We will, however, investigate the impact of the dim-6 coefficients in section 6.

The above results depend on the choice of basis for particle states. While physics is independent of the basis for states, the notion of elasticity is not. The elastic amplitude in one basis (e.g. the mass-eigenstate basis) may involve non-elastic amplitude components when transformed to a different basis (e.g. the gauge-eigenstate basis). To maximize the constraining power, one should consider all basis, or equivalently, consider the elastic scattering of arbitrarily superposed states, e.g. the scattering of $u^i |i\rangle$ and $v^j |j\rangle$ states, with

JHEP01(2021)095

u, v arbitrary complex vectors. This leads to the following infinite set of bounds:

$$\sum_{\alpha} C_\alpha p_\alpha(u, v) \geq 0 \tag{1.3}$$

where u, v are arbitrary complex vectors, and $p_\alpha(u, v)$ are quartic polynomials of u, v, u^*, v^*. C_α needs to satisfy a number of inequalities for the above to hold for all possible values of u, v, and it is this set of inequalities that we call elastic positivity bounds. Since all superpositions are explored, the full set of elastic positivity bounds is basis-independent, and so one can start from an arbitrary particle basis. While this approach is convenient when the number of particle states (or the dimension of u, v) is small, identifying the full set of bounds can quickly become difficult as the number of states increases. One way to see this is that eq. (1.3) is equivalent to the determination of the positive semi-definiteness of a quartic polynomial of u, v, which is a NP-hard problem.

The second approach that we will discuss in this work is the extremal positivity approach that has been recently proposed by some of the authors [9]. This approach has the advantage that one is guaranteed to obtain the best bounds allowed by the fundamental QFT principles. Indeed, bounds tighter than the elastic positivity eq. (1.3) can potentially be obtained, and an explicit example has been presented in [9]. In this approach, instead of using elastic channels to probe the bounds, which are the boundary/facets of the allowed parameter space, one first constructs the edges, or the *extremal rays* (ERs), of the allowed space. The convex hull of these rays determines the bounds. This is efficient because the ERs can be directly written down via group theoretical considerations. The approach essentially describes the allowed parameter space as a convex cone via the *extremal representation* of cones, and thus its name. When the cones are polyhedral, positivity bounds are the facets of the cones, and can be identified through a vertex enumeration algorithm.

The systematic application of both approaches to the SMEFT dim-8 operators is currently very limited. Positivity bounds in most literature come from the elastic positivity approach, exploiting no or only limited superpositions of states. A particular interesting topic is the positivity bounds for anomalous quartic gauge-boson couplings (aQGC), as these couplings are currently being used as a theory framework to interpret the vector boson scattering (VBS) and the tri-boson production measurements at the LHC [56]. In refs. [4, 5], following the elastic positivity approach, we worked in the mass eigenstate basis (i.e. in the broken phase of the SM electroweak symmetry), but only considered the superposition of various polarization states. The mixing between different gauge components and between W and B were not considered. This already significantly constrains the physical space of the aQGCs, with only about 2% of the total space satisfying the bounds.[1] In addition, the authors of [7] worked in the unbroken phase, and considered the superposition of Higgs and Goldstone bosons but not that of the gauge modes. This gives a set of complementary constraints. On the other hand, the extremal representation approach has been so far only considered in ref. [9], where simple examples have already shown that it is efficient and powerful at least for cases in which low energy modes lie within the same

[1] This 2% is computed without including the operators $O_{T,10}$ and $O_{T,11}$, which have been missing in the conventional aQGC parameterization, see section 2.

JHEP01(2021)095

irreducible representation (irrep) (such as for the Higgs doublet or the W-boson triplet). More general applications of this approach are yet to be explored.

In this work, we apply both approaches — the elastic positivity from all superposed states, and the extremal representation approach — to the set of the dim-8 operators that parameterize the transversal aQGCs, i.e. the couplings of four W-bosons, of four B-bosons, and of two W- and two B-bosons. Our goal is three-fold:

1. We will use the aQGC operators as a realistic case, to establish the methodology for both approaches. We focus on the potential difficulties that arise when one aims to extract the best positivity constraints that involve a large number of particle states. For the elastic approach, the main difficulty is that all possible superpositions of the following modes need to be explored:

$$W_x^1, W_y^1, W_x^2, W_y^2, W_x^3, W_y^3, B_x, B_y \tag{1.4}$$

   where the subscripts x, y for W, B are the transversally polarized modes, and the superscripts of W are the SU(2) index in the **3** representation. The u, v vectors are thus elements of $\mathbb{C}^8$, and together they have 32 real degrees of freedom. One then needs to exhaust all possible directions in a 32 dimensional space, to check if a given set of coefficients can be excluded by some u, v vectors. Alternatively, for the extremal approach, the main difficulty is that when both W and B are involved, degenerate irreps show up, and so there are multiple ERs that are continuously parameterized by some real parameters. One needs to find a way to identify the boundary spanned by these "continuous rays". In both cases, we will discuss how to deal with the difficulties and to solve the problem both analytically and numerically. The latter allows us to quantify the accuracy of any approximations we will use in the analytical approach.

2. We will compare several aspects of both approaches, to understand their advantages and disadvantages. In terms of the final results, we know that the extremal approach gives tighter constraints, and we will quantify the actual improvement in this realistic case. Another important aspect to be compared, is to what extend these approaches can be implemented algorithmically, and thus made applicable to more general and complicated problems (e.g. full set of bounds for the entire SMEFT). Finally, the speed and accuracy of the numerical approaches are also important.

3. We will obtain the best positivity bounds on the transversal aQGCs, which alone are a very important physics result. Searching for possible beyond the SM physics in the form of aQGC is one of the main goals of the current electroweak program at the LHC. These couplings can be measured in the VBS or the tri-boson production channels. Knowing their bounds from positivity will undoubtedly provide guidance for future theoretical and experimental studies. Existing results [4, 5, 7] followed the elastic approach and only explored limited superpositions. In this work we will unify and supersede these results, by exploring the elastic channels of all possible superposed states. On the other hand, the extremal positivity approach has only been considered for 4-W-boson operators, but it already gives better bounds than

JHEP01(2021)095

the conventional elastic approach [9]. We will show that this continues to hold when both W and B-bosons are taken into account.

The paper is organized as follows. In section 2, we will list the full set of effective operators that are relevant in this study. In section 3, we will present the theoretical basis of this work — the two approaches to positivity bounds. In particular, in section 3.2 we will present a geometric interpretation for the positivity problem, based on which we will explain the elastic positivity approach in section 3.3 and the extremal positivity approach in section 3.4, using 4-Higgs and 4-W operators as toy examples. In section 4 and section 5, we will tackle the problem using the elastic approach and the extremal approach, respectively. In both cases we will present analytical and numerical results. The quadratic dim-6 contributions will be discussed in section 6. Finally, we will discuss all the results and compare the two approaches in section 7, and summarize in section 8. For readers who are mainly interested in the physics results, i.e. positivity bounds on aQGC coefficients, our best analytical results are given in eqs. (5.27)–(5.45).

2 Effective operators

The aQGCs already appear at dim-6 in the SMEFT. They are however not independent of the triple gauge-boson couplings at dim-6, which are often assumed to be severely constrained through other channels such as the di-boson production. Dim-8 Wilson coefficients are thus used to parameterize the truly independent aQGCs, which are measured in the VBS and tri-boson processes. They are also used to cover all possible helicity combinations involved, and to account for cases in which the dominant effects are beyond dim-6, possibly due to loop-suppression at dim-6[2] or the helicity selection rule [57]. Experimental studies have been extensively performed, by both the ATLAS and the CMS collaborations at the LHC, to set limits on the sizes of aQGCs, and we refer to [51–53] for some recent progresses. A compilation of current limits on aQGC can be found in [58]. The HL-LHC projection for the dim-8 aQGC operator sensitivities can reach the TeV level and beyond [59].

The dim-8 aQGC operators are often categorized in three different types: the S-type, M-type, and T-type operators [60–62]. The S-type operators have a schematic form of $(D\Phi)^4$, where $D\Phi$ is the covariant derivative of the Higgs doublet. The M-type operators involve two covariant derivatives of the Higgs doublet and two field strengths, schematically forming $(D\Phi)^2F^2$. The T-type operators are constructed by four field strength tensors, F^4.

In this paper, we focus on the T-type operators, which involve four transversal gauge modes. There are 10 such operators. Using the convention in [61], we define

$$\hat{W}^{\mu\nu} \equiv ig\frac{\sigma^I}{2}W^{I,\mu\nu}, \quad \hat{B}^{\mu\nu} \equiv ig'\frac{1}{2}B^{\mu\nu} \tag{2.1}$$

and

$$\tilde{W}_{\mu\nu} \equiv ig\frac{\sigma^I}{2}\left(\frac{1}{2}\epsilon_{\mu\nu\rho\sigma}W^{I,\rho\sigma}\right), \tilde{B}_{\mu\nu} \equiv ig'\frac{1}{2}\left(\frac{1}{2}\epsilon_{\mu\nu\rho\sigma}B^{\rho\sigma}\right), \tag{2.2}$$

[2]There are three independent degrees of freedom at dim-6, two of which can only be generated at the loop level, in a weakly coupled UV completion.

JHEP01(2021)095

$O_{T,0} = \mathrm{Tr}[\hat{W}_{\mu\nu}\hat{W}^{\mu\nu}]\mathrm{Tr}[\hat{W}_{\alpha\beta}\hat{W}^{\alpha\beta}]$	$O_{T,1} = \mathrm{Tr}[\hat{W}_{\alpha\nu}\hat{W}^{\mu\beta}]\mathrm{Tr}[\hat{W}_{\mu\beta}\hat{W}^{\alpha\nu}]$
$O_{T,2} = \mathrm{Tr}[\hat{W}_{\alpha\mu}\hat{W}^{\mu\beta}]\mathrm{Tr}[\hat{W}_{\beta\nu}\hat{W}^{\nu\alpha}]$	$O_{T,10} = \mathrm{Tr}[\hat{W}_{\mu\nu}\tilde{W}^{\mu\nu}]\mathrm{Tr}[\hat{W}_{\alpha\beta}\tilde{W}^{\alpha\beta}]$
$O_{T,5} = \mathrm{Tr}[\hat{W}_{\mu\nu}\hat{W}^{\mu\nu}]\hat{B}_{\alpha\beta}\hat{B}^{\alpha\beta}$	$O_{T,6} = \mathrm{Tr}[\hat{W}_{\alpha\nu}\hat{W}^{\mu\beta}]\hat{B}_{\mu\beta}\hat{B}^{\alpha\nu}$
$O_{T,7} = \mathrm{Tr}[\hat{W}_{\alpha\mu}\hat{W}^{\mu\beta}]\hat{B}_{\beta\nu}\hat{B}^{\nu\alpha}$	$O_{T,11} = \mathrm{Tr}[\hat{W}_{\mu\nu}\tilde{W}^{\mu\nu}]\hat{B}_{\alpha\beta}\tilde{B}^{\alpha\beta}$
$O_{T,8} = \hat{B}_{\mu\nu}\hat{B}^{\mu\nu}\hat{B}_{\alpha\beta}\hat{B}^{\alpha\beta}$	$O_{T,9} = \hat{B}_{\alpha\mu}\hat{B}^{\mu\beta}\hat{B}_{\beta\nu}\hat{B}^{\nu\alpha}$

Table 1. T-type aQGC operators.

where $\epsilon_{\mu\nu\rho\sigma}$ is the Levi-Civita tensor,

$$W^I_{\mu\nu} = \partial_\mu W^I_\nu - \partial_\nu W^I_\mu + g\epsilon_{IJK}W^J_\mu W^K_\nu, \;\; B_{\mu\nu} = \partial_\mu B_\nu - \partial_\nu B_\mu, \tag{2.3}$$

and g and g' are $\mathrm{SU}(2)_L$ and $\mathrm{U}(1)_Y$ gauge couplings, respectively. With these notations, the T-type dim-8 aQGC operators are listed in table 1. Note that two operators, $O_{T,10}$ and $O_{T,11}$, are included in addition to the conventional T-type aQGC operators. These two operators are conventionally missed in the set of aQGC operators, and this has been pointed out recently by ref. [7]. They are also included in refs. [2, 3].

We do not consider parity-odd operators. The effective Lagrangian for the aQGC interactions is:

$$\mathcal{L}_{aQGC} = \sum_i \frac{F_{T,i}}{\Lambda^4}\mathcal{O}_{T,i}, \tag{2.4}$$

where $F_{T,i}$ is the Wilson coefficient for the corresponding operator $\mathcal{O}_{T,i}$, and Λ is the characteristic scale of new physics.

The scattering amplitude of two transversal gauge bosons could also receive contributions at the s^2/Λ^4 level from the dim-6 operators. These contributions are proportional to the squares of the dim-6 Wilson coefficients. They come from diagrams in which triple-gauge-boson couplings (or potentially the HVV couplings) can be inserted twice. In the Warsaw basis [63], such a contribution only comes from the O_W operator:

$$O_W = \varepsilon^{IJK}W^{I\nu}_\mu W^{J\rho}_\nu W^{K\mu}_\rho. \tag{2.5}$$

We define $\bar{a}_W \equiv a_W/g^2$ for convenience, where a_W is the coefficient of this operator.

Finally, all scattering amplitudes used in this paper are computed at the tree level using standard tools [64–67].

3 Theoretical framework

The positivity bounds derived from forward scattering amplitudes have been well established and widely used, for example, in refs. [11, 26]. A generalization to the non-forward case has been discussed in refs. [13, 18, 21–23]. However, in the SMEFT, non-forward scatterings at the leading order do not lead to new bounds on the s^2 dependence of the amplitudes. In this work we thus focus on the forward case.

JHEP01(2021)095

In this section, we will first derive a dispersion relation for general non-elastic forward scatterings. We will then present a geometric interpretation for the parameter space allowed by this dispersion relation, and show that positivity bounds arise from the latter. We will show that both the elastic approach and the extremal approach can be easily understood from this geometric picture. Toy examples, including four-Higgs operators and four-W operators, will be discussed to demonstrate how the full set of bounds can be extracted following both approaches. Finally, for the elastic approach, we will also show that the superposition of low energy modes only needs to take real values. This is an important simplification for the elastic approach.

3.1 Dispersion relation

Positivity bounds arise from the dispersion relation, which has been extensively discussed in the literature (see e.g. refs. [5, 9]). Here we only give a brief outline, skipping unnecessary details. The main difference is that here we consider inelastic scattering amplitudes.

Let us denote $\tilde{M}^{ijkl}$ as the second-order s derivative of the scattering amplitude $ij \to kl$ with low-energy poles subtracted

$$\tilde{M}^{ijkl} = \frac{1}{2}\frac{d^2}{ds^2}M(ij \to kl)\left(s = \frac{M^2}{2}, t\right) + c.c. \tag{3.1}$$

where $c.c.$ stands for the complex conjugate of the previous term. i, j, k, l indices run through either a subset or the full set of SM modes. Using the analyticity of the amplitude and the Froissart-Martin bound, a contour integral around a low energy point $M^2/2$ can be deformed to go around the branch cuts and the infinity, which leads to

$$\tilde{M}^{ijkl} = \int_{M_{\rm th}^2}^{\infty}\frac{ds}{2i\pi}\frac{\text{Disc}M(ij \to kl)(s,t)}{(s-\frac{1}{2}M^2)^3} + \int_{-\infty}^{-(M_{\rm th}^u)^2}\frac{ds}{2i\pi}\frac{\text{Disc}M(ij \to kl)(s,t)}{(s-\frac{1}{2}M^2)^3} + c.c. \tag{3.2}$$

where $M_{\rm th}$ and $M_{\rm th}^u$ are the s and u channel threshold scale for process $ij \to kl$, and $M^2 \equiv m_i^2 + m_j^2 + m_k^2 + m_l^2$. We can calculate the amplitude to a desired accuracy within an EFT up to energy scale $\epsilon\Lambda$ (with $\epsilon \lesssim 1$), so we can subtract the dispersive integral up to $\epsilon\Lambda$, and get

$$M^{ijkl} = \int_{(\epsilon\Lambda)^2}^{\infty}\frac{ds}{2i\pi}\frac{\text{Disc}M(ij \to kl)(s,t)}{(s-\frac{1}{2}M^2)^3} + \int_{-\infty}^{-(\epsilon\Lambda)^2}\frac{ds}{2i\pi}\frac{\text{Disc}M(ij \to kl)(s,t)}{(s-\frac{1}{2}M^2)^3} + c.c. \tag{3.3}$$

For inelastic scattering between particles with different masses, the forward limit $\theta = 0$ is generally not the same as the limit $t = 0$. However, since the integral starts from $\epsilon\Lambda \gg m_i$, we can take the approximation $s \gg m_i^2$, in which the forward limit $\theta = 0$ becomes the same as $t = 0$ and we can make use of the simple crossing relation $\text{Disc}M(ij \to kl)(s,0) \simeq -\text{Disc}M(il \to kj)(s,0)$. Also, by the same token, we approximate the denominator $s - M^2/2 \simeq s$. (Note that M^2 depends on the indices i, j, k, l.) These approximations are consistent with $M^2 \ll \Lambda^2$, which is the condition for a SMEFT expansion to be valid. Any deviations from them are a higher order effect in the SMEFT. We then have

$$M^{ijkl} = \int_{(\epsilon\Lambda)^2}^{\infty}\frac{ds}{2i\pi}\frac{\text{Disc}M(ij \to kl)(s)}{s^3} + (j \leftrightarrow l) + c.c. \tag{3.4}$$

JHEP01(2021)095

Thanks to Hermitian analyticity $M(kl \to ij)^*(s+i\varepsilon) = M(ij \to kl)(s-i\varepsilon)$ and the (generalized) optical theorem $M(ij \to kl) - M(kl \to ij)^* = i\sum'_X M(ij \to X)M(kl \to X)^*$, where $\sum'_X$ denotes the sum of all possible states X together with their phase space integration, we can re-write the dispersion relation as

$$M^{ijkl} = \int_{(\epsilon\Lambda)^2}^{\infty} \sum_X{}' \sum_{K=R,I} \frac{d\mu\, m_K{}_X^{ij} m_K{}_X^{kl}}{\pi\mu^3} + (j \leftrightarrow l) \tag{3.5}$$

where we have defined $M(ij \to X) \equiv m_{R_X}^{ij} + i m_{I_X}^{ij}$, with m_{RX} and m_{IX} both real matrices. Eq. (3.5) is the master equation on which all positivity bounds discussed in this work are based.

In a model-independent EFT, we shall make no assumption on $m_{K_X}^{ij}$, and so a priori they can be arbitrary matrix functions of s and the phase space of X. However, since all other factors in the integrand are non-negative, the dispersion relation implies that M^{ijkl} is not allowed to take arbitrary values, i.e. there are bounds on M^{ijkl}. The easiest way to see this is to consider an elastic scattering amplitude. When $i = k$ and $j = l$, the integrand of the r.h.s. is a sum of squares and hence positive semi-definite (PSD). We have

$$M^{ijij} \geq 0 \tag{3.6}$$

i.e. the 2nd s derivative of the (subtracted) elastic scattering amplitude is non-negative.

More generally, consider two arbitrary vectors $u, v \in \mathbb{C}^n$, where n is the number of low energy modes being considered. Contracting eq. (3.5) with $u^i v^j u^{*k} v^{*l}$, we find

$$u^i v^j u^{*k} v^{*l} M^{ijkl} = \int_{(\epsilon\Lambda)^2}^{\infty} \sum_X{}' \sum_{K=R,I} \frac{d\mu}{\pi\mu^3} \left[|u \cdot m_{K_X} \cdot v|^2 + |u \cdot m_{K_X} \cdot v^*|^2 \right] \geq 0 \tag{3.7}$$

where the summation over repeated i, j, k, l indices is omitted. Defining a quartic polynomial

$$P(u, v) \equiv u^i v^j u^{*k} v^{*l} M^{ijkl}, \tag{3.8}$$

we find that the dispersion relation implies $P(u, v) \geq 0\ \forall u, v \in \mathbb{C}^n$. In other words, $P(u, v)$ is a quartic PSD polynomial on $\mathbb{C}^{2n}$.

The above statement can be thought of as coming from the 2nd order derivative of the elastic channel $M(ab \to ab)$, where the states a, b are superposed states characterized by the u, v vectors:

$$|a\rangle = u^i |i\rangle\,, \quad |b\rangle = v^i |i\rangle \tag{3.9}$$

We have essentially shown that positivity bounds can be derived from the elastic scattering of any superposed states that mix possibly different helicities and other quantum numbers, as the fact that $u^i v^j u^{*k} v^{*l} M^{ijkl} \geq 0$ only requires eq. (3.5).

In the SMEFT, M^{ijkl} can be computed in terms of higher-dimensional operators. At the tree level, since M^{ijkl} is defined as the 2nd order s derivative, its leading contribution comes from either a subset of the dim-8 Wilson coefficients (which give rise to s^2 dependence in the amplitude, see [7]) at the linear level, or, potentially, also from dim-6 coefficients but at the squared level. Neglecting the latter, we can write

$$M^{ijkl} = \Lambda^{-4} C_\alpha M_\alpha^{ijkl} \tag{3.10}$$

JHEP01(2021)095

where C_α's are the dim-8 coefficients and the summation over α is implicit. Defining the 4-th order polynomials

$$p_\alpha(u,v) \equiv M_\alpha^{ijkl} u^i v^j u^{*k} v^{*l} \tag{3.11}$$

the elastic positivity then simply requires $C_\alpha p_\alpha(u,v) \geq 0$. This condition constrains the possible values of C_α. While plugging any given u, v vectors into this relation will lead to a valid bound, our goal, however, is to derive the full set of necessary and sufficient conditions for:

$$C_\alpha p_\alpha(u,v) \geq 0, \quad \forall\ u, v \in \mathbb{C}^n \tag{3.12}$$

which is independent of the basis of particle states. This problem is equivalent to the determination of a PSD quartic polynomial, which is a NP-hard problem. Its difficulty grows with n, the number of modes. In section 3.3, we will show that one in fact only needs to consider $C_\alpha p_\alpha(u,v) \geq 0$ for real u, v. This is an extremely useful simplification, because it halves the number of variables to be considered.

Eq. (3.12) is exactly how we extract the elastic positivity bounds. As for the extremal positivity approach, we postpone the discussion to section 3.4, which will be more intuitive based on the geometric picture that we will introduce in the next section.

Before proceeding, let us briefly comment on other contributions to M^{ijkl} that might arise in the SMEFT. First, we have so far neglected the quadratic contribution from the dim-6 coefficients. In practice, this is a useful simplification as it leads to compact results on the dim-8 aQGC operators. Furthermore, these results are still valid in general: as we have shown in ref. [5], the removal of dim-6 contributions only makes these bounds more conservative, at least in the elastic positivity approach. On the other hand, including these contributions is also straightforward with all the methods we will demonstrate in this work. For simplicity, we will postpone a discussion about the dim-6 contributions to section 6, while for the rest of the paper we will not consider such contributions, and aim at deriving the full set of bounds for the dim-8 coefficients. On a different ground, in section 6, we will demonstrate that, even in the extremal positivity approach, neglecting dim-6 contributions is a safe approximation, as it only makes the bounds more conservative.

In addition, beyond the tree level, eq. (3.10) needs to be augmented with loop corrections, from the SM and even dim-6 operators. Some of these effects are discussed in ref. [5]. For example, the SM corrections are shown to be not important given the current experimental sensitivity, but they might play a role in the future. In any case, positivity bounds should be viewed as bounds on the amplitude M^{ijkl}: the latter can be mapped to the SMEFT coefficients to any desired order by an explicit SMEFT calculation, but such a calculation beyond the tree level is by itself a separate and nontrivial problem. Since the goal of this work is to study the methodology for extracting bounds, in the rest of the paper we will only use tree level expressions for M^{ijkl}, namely eq. (3.10). If loop-level amplitudes are available in the SMEFT, our approaches can be easily improved by a loop-level matching from M^{ijkl} to the Wilson coefficients.

JHEP01(2021)095

3.2 A geometric interpretation of positivity

A convex geometric perspective can provide useful guidance for the extraction of bounds. Let us first introduce a few basic concepts and facts about convex geometry.

- A *convex cone* (or simply a *cone*) is a subset of some vector space, closed under additions and positive scalar multiplications. A *salient* cone is a cone that does not contain any straight line. In other words, if $\mathcal{C}$ is salient, then having $x \in \mathcal{C}$ and $-x \in \mathcal{C}$ implies $x = 0$.

- An *extremal ray* (ER) of a cone $\mathcal{C}_0$ is an element $x \in \mathcal{C}_0$ that cannot be a sum of two other elements in $\mathcal{C}_0$. If we write an extremal ray as $x = y_1 + y_2$ with $y_1, y_2 \in \mathcal{C}_0$, then we must have $x = \lambda y_1$ or $x = \lambda y_2$, with λ some a real constant. The extremal rays of a polyhedral cone are its edges.

- The *convex hull* of a given set $\mathcal{X}$ is the set of all convex combinations of points in $\mathcal{X}$, where a convex combination is defined as a linear combination of points, where all the combination coefficients are non-negative and sum up to 1.

- The *conical hull* of a given set $\mathcal{X}$ is the set of all positive linear combinations of elements in $\mathcal{X}$, denoted by $\text{cone}(\mathcal{X})$. Obviously, $\text{cone}(\mathcal{X})$ is a convex cone, and its extremal rays are a subset of $\mathcal{X}$.

- The *dual cone* $\mathcal{C}_0^*$ of the cone $\mathcal{C}_0$ is the set $\mathcal{C}_0^* \equiv \{y \mid y \cdot x \geq 0,\ \forall x \in \mathcal{C}_0\}$, where $\cdot$ represents inner product. We have $(\mathcal{C}_0^*)^* = \mathcal{C}_0$, and if $\mathcal{C}_1 \subset \mathcal{C}_2$, then $\mathcal{C}_1^* \supset \mathcal{C}_2^*$.

With these in mind, we observe from eq. (3.5) that the dispersion relation implies that M^{ijkl}, viewed as a vector, live in a convex cone. To see this, note that the integration is a limit of summation and all other factors in the integrand are positive, so M^{ijkl} is a positively weighted sum of $m^{ij}m^{kl}+m^{il}m^{kj}$, where m^{ij} is a $n\times n$ matrix, with n the number of low energy particles in the EFT. Since we do not assume any specific UV completion, m^{ij} is arbitrary. Therefore all possible values of M^{ijkl} must live in the following set $\mathcal{C}$:

$$\mathcal{C} \equiv \text{cone}\left(\left\{m^{ij}m^{kl} + m^{il}m^{kj}\right\}\right) \tag{3.13}$$

An immediate important fact is that $\mathcal{C}$ is a salient cone, i.e. it does not contain any straight line. This can be seen by contracting its elements with $\delta^{ik}\delta^{jl}$, which always gives a positive summation in the integrand of the r.h.s., $m^{ij}m^{ij} > 0$, unless the element itself vanishes. So if x is in $\mathcal{C}$, $-x$ is not. Thus, intuitively, the $\mathcal{C}$ cone constrains M^{ijkl} to be in certain (positive) directions in the total parameter space, and this constraint applies to all directions. In other words, the $\mathcal{C}$ cone represents the "directional information" of the amplitude that can be extracted out of the dispersion relation. In this view, the goal of finding all possible positivity bounds can be achieved by finding the boundary of $\mathcal{C}$. In the SMEFT, all particles are charged under the SM gauge symmetries, so m^{ij} is not totally arbitrary but subject to constraints from symmetries. Nevertheless, eq. (3.13) represents all requirements from the axiomatic principles.

JHEP01(2021)095

The convex cone $\mathcal{C}$ defined by eq. (3.13) can be characterized in two ways. Positivity bounds are directly related to the *inequality* representation, which follows from the Hahn-Banach separation theorem. The theorem states that $\mathcal{C}$ is an intersection of half-spaces, each described by a linear inequality. These inequalities are exactly what we call positivity bounds. Therefore, in this view, our goal is to find the inequality representation of $\mathcal{C}$. Alternatively, the *extremal* representation follows from the Krein-Milman theorem, which implies that a *salient cone* $\mathcal{C}$ is a convex hull of its ERs. The extremal approach proposed in ref. [9] simply follows this representation, and it determines $\mathcal{C}$ by first finding its ERs.

The two representations of a convex cone are connected by the concept of dual cones: the bounds of $\mathcal{C}$ are the ERs of $\mathcal{C}^*$, and vise versa. In other words, the inequality representation of $\mathcal{C}$ is the extremal representation of $\mathcal{C}^*$. To see this, note that $(\mathcal{C}^*)^* = \mathcal{C}$ implies $\mathcal{C}$ is described by a set of inequalities,

$$\mathcal{C} = \{M \mid M \cdot T \geq 0,\ \forall T \in \mathcal{C}^*\} \tag{3.14}$$

The extremal representation of $\mathcal{C}^*$ allows any element $T \in \mathcal{C}^*$ to be written as a positively weighted sum of $E_i \in \mathcal{E}$, where $\mathcal{E}$ is the set of ERs in $\mathcal{C}^*$, so the above is equivalent to

$$\mathcal{C} = \{M \mid M \cdot E \geq 0,\ \forall E \in \mathcal{E}\} \tag{3.15}$$

This defines $\mathcal{C}$ as a set of bounds, each represented by an ER of $\mathcal{C}^*$. This is exactly the inequality representation of $\mathcal{C}$ that we are looking for.

Note that although eqs. (3.14) and (3.15) describe the same cone $\mathcal{C}$, eq. (3.14) consists of an infinite number of inequalities, most of which are redundant, as $M \cdot T \geq 0$ is guaranteed by $M \cdot E \geq 0$. In contrast, eq. (3.15) is the complete and independent set of inequalities that are required to describe $\mathcal{C}$. Thus our goal is to find $\mathcal{E}$, the set of all ERs of $\mathcal{C}^*$. In fact, the idea of the elastic positivity approach is to first construct explicitly a subset of $\mathcal{C}^*$ (see eq. (3.21)), and identify its ERs. This leads to a set of conservative bounds, which we denote by $\mathcal{C}^{el}$. It is conservative because $\mathcal{C}^{el*} \subset \mathcal{C}^*$ implies $\mathcal{C}^{el} \supset \mathcal{C}$.

On the other hand, in the extremal approach, one first finds the ERs of $\mathcal{C}$, $\{e_i\}$. This can be greatly simplified by taking into account the SM symmetries. One can essentially replace the $m^{ij}m^{kl}$ tensor with the projector operators of the irreps within which the intermediate states are charged, and rewrite the dispersion relation [9]

$$M^{ijkl} = \int_{(\epsilon\Lambda)^2}^{\infty} \mathrm{d}\mu \sum_{X \text{ in } \mathbf{r}}{}' \frac{|\langle X|\mathcal{M}|\mathbf{r}\rangle|^2}{\pi\mu^3} P_{\mathbf{r}}^{i(j|k|l)} \tag{3.16}$$

where $\mathbf{r}$ runs through all irreps of the SO(2) rotation around the forward scattering axis and the $\mathrm{SU}(3)_C \times \mathrm{SU}(2)_L \times \mathrm{U}(1)_Y$ symmetries; X runs through all intermediate states in the irrep $\mathbf{r}$; $P_{\mathbf{r}}^{ijkl} \equiv \sum_\alpha C_{i,j}^{\mathbf{r},\alpha}(C_{k,l}^{\mathbf{r},\alpha})^*$ are the projective operators of $\mathbf{r}$; $C_{i,j}^{\mathbf{r},\alpha}$ are the Clebsch-Gordan coefficients for the direct sum decomposition of $\mathbf{r}_i \otimes \mathbf{r}_j$, with $\mathbf{r}_i(\mathbf{r}_j)$ the irrep of particle $i(j)$, and α the label of states in $\mathbf{r}$; $i(j|k|l)$ means that the j, l indices are symmetrized; see [9] for more details. With this the cone $\mathcal{C}$ becomes

$$\mathcal{C} \equiv \mathrm{cone}\left(\left\{P_{\mathbf{r}}^{i(j|k|l)}\right\}\right) \tag{3.17}$$

JHEP01(2021)095

So the ERs are a subset of $\{P_{\mathbf{r}}^{i(j|k|l)}\}$, and can be easily determined. This gives the extremal representation of $\mathcal{C}$.

In order to extract bounds, the next step is to convert the extremal representation to the inequality representation. For polyhedral cones, recall that the ERs (edges) of $\mathcal{C}$ are the bounds (facets) of $\mathcal{C}^*$ and vice versa. This conversion can be done by a procedure called *vertex enumeration*: it determines the edges of a polyhedral cone ($\mathcal{C}^*$) from its facets, and this is equivalent to determining the facets of $\mathcal{C}$ from its edges or ERs. There are efficient algorithms to perform this computation, such as the reverse search algorithm of [68, 69], which allows for easy transformation between the two representations. More generally, for non-polyhedral cones with curved boundaries, one will have to deal with a continuous version of this problem. We will discuss this in section 5.

The symmetries we have considered so far are not always sufficient to fully determine the dynamics. In the SMEFT, the physical amplitude M^{ijkl} can be expanded by the operators, $M^{ijkl} = \sum_\alpha C_\alpha M_\alpha^{ijkl}$, where C_α are the dim-8 Wilson coefficients, and this defines a subspace $\mathcal{S}$ of $\{M^{ijkl}\}$ that is allowed by the SMEFT at the tree level. Elements in $\mathcal{S}$ is represented by a vector of coefficients: $\vec{C} = (C_1, C_2, \dots)$, and we also define the vector of amplitudes from individual operators O_i, $\vec{M} = (M_1, M_2, \dots)$, with superscript $ijkl$ suppressed. Now $\mathcal{C}$ represents the requirement from the dispersion relation, while $\mathcal{S}$ represents the requirement from dynamics, so our goal is to identify their intersection, which is also a convex cone, $\mathcal{C}_S = \mathcal{C} \cap \mathcal{S}$ (or $\mathcal{C}_S^{el} = \mathcal{C}^{el} \cap \mathcal{S}$). Specifically, elements of $\mathcal{C}_S$ needs to satisfy

$$\vec{C} \cdot \vec{M}^{ijkl} T^{ijkl} \geq 0, \ \forall T \in \mathcal{C}^* \tag{3.18}$$

This defines $\mathcal{C}_S$ as the dual cone of

$$\mathcal{C}_S^* = \left\{ \vec{M}^{ijkl} T^{ijkl}, T \in \mathcal{C}^* \right\} \tag{3.19}$$

(Strictly speaking, the elements of the dual of the r.h.s. are the vectors $\vec{C}$, while $\mathcal{C}_S$ is a set of $\vec{C} \cdot \vec{M}^{ijkl}$, but we consider them to be equivalent, as M_α^{ijkl} form a linearly independent basis.) In the elastic approach, it may be more convenient to work directly with $\mathcal{C}_S^{el}$, because its dual can be directly written down by replacing the T in the above equation by a subset of $\mathcal{C}^*$ (see again eq. (3.21)). On the other hand, it is also possible to work with $\mathcal{C}$, as the bounds of $\mathcal{C}$ can be easily converted to the bounds of $\mathcal{C}_S$, by a matching calculation of the physical amplitude.

Before concluding this section, let us mention several notations that we use to denote various sets of bounds. In general, we use $\mathcal{C}$ with sub/superscripts for the set of dim-8 Wilson coefficients allowed by some set of bounds. Our goal is to identify $\mathcal{C}_S = \mathcal{C} \cap \mathcal{S}$. Without any approximations, the extremal positivity gives $\mathcal{C}_S$, while elastic positivity relaxes it to $\mathcal{C}_S^{el}$. Due to the complexity of the problem, our analytical and numerical results in both approaches are sometimes based on approximations, and are in general not exactly the same as $\mathcal{C}_S$ or $\mathcal{C}_S^{el}$. We will denote the analytical and numerical results as, say, $\mathcal{C}_A^{el}$ and $\mathcal{C}_N^{el}$ respectively.

To compare the constraining power of various sets of bounds, and to assess how accurately they describe the exact parameter space, one notion that will be useful in this

JHEP01(2021)095

work is the "solid angle" of the parameter space allowed by some set of bounds, say $\mathcal{C}_S$. In general, to quantify the constraining power, one can use the volume of the allowed region of the parameter space. The positivity bounds themselves are however projective, as $\mathcal{C}_S$ (as well as other bounds) is closed under multiplication of a global real and positive number. Therefore the volume is infinity, but instead, one can define the "solid angle" of the cone $\mathcal{C}_S$, $\Omega(\mathcal{C}_S)$, normalized to that of the full parameter space.

To compute $\Omega(\mathcal{C}_S)$, an efficient way is to sample the Wilson coefficients, say the 10 aQGC coefficients $F_{T,i}$ with $i = 0, 1, 2, 5, 6, 7, 8, 9, 10, 11$, on a 9-sphere, and count the number of points that satisfy all bounds. To sample $F_{T,i}$ uniformly on a n-sphere, it is sufficient to simply let $F_{T,i}$ sample the standard normal distribution, thanks to the Muller method and that the bounds are projective. The Monte Carlo sampling error can be estimated by the square root of the variance. Suppose one uniformly samples N points in the 9-sphere and $N_{\mathcal{C}_S}$ points satisfy positivity. Our solid angle is defined by $\Omega(\mathcal{C}_S) = N_{\mathcal{C}_S}/N$, and its error can be estimated by the square root of the sampling variance of $\Omega(\mathcal{C}_S)$, which is

$$\frac{1}{\sqrt{N}}\sqrt{\frac{[N_{\mathcal{C}_S}(1-\Omega(\mathcal{C}_S))^2 + (N-N_{\mathcal{C}_S})(0-\Omega(\mathcal{C}_S))^2]}{N-1}} \simeq \sqrt{\frac{(1-\Omega(\mathcal{C}_S))\Omega(\mathcal{C}_S)}{N}} \simeq \frac{\Omega(\mathcal{C}_S)}{\sqrt{\Omega(\mathcal{C}_S)N}} \tag{3.20}$$

where in the last $\simeq$ we have assumed $\Omega(\mathcal{C}_S) \ll 1$. To achieve a relative error of 0.1%, one needs $N\Omega(\mathcal{C}_S)$ to be greater than 10^6. The above discussion applies not only to $\mathcal{C}_S$ but also to all other bounds that we will present.

3.3 The elastic positivity approach

In the elastic positivity approach, bounds are derived from elastic scatterings of superposed states. Conceptually this is a simple way to obtain bounds. The approach however has two drawbacks. The first is that the resulting bounds are not guaranteed to be complete. The second is that the extraction of the full set of bounds quickly becomes difficult as the number of low-energy modes involved increases. We have briefly discussed these bounds in section 3.1.

From the geometric point of view, finding the elastic positivity bounds is equivalent to constructing a subset of $\mathcal{C}^*$:

$$\mathcal{Q} \equiv \text{cone}\left(\left\{u^i v^j u^k v^l\right\}\right) \subset \mathcal{C}^* \tag{3.21}$$

so that

$$\mathcal{C}^{el} = \mathcal{Q}^* \supset \mathcal{C} \tag{3.22}$$

The elements of $\mathcal{Q}$ represent the elastic scattering channels between $u^i|i\rangle$ and $v^i|i\rangle$. The fact that $\mathcal{Q} \subseteq \mathcal{C}^*$ follows eq. (3.7). $M^{ijkl} \in \mathcal{C}^{el}$ is equivalent to $P(u,v) \geq 0$. In addition, $\mathcal{Q}$ is often a proper subset of $\mathcal{C}^*$, see ref. [9], which means that the elastic approach in general only gives conservative bounds. The problem of finding $\mathcal{C}_S$ is then relaxed to finding the dual of $\mathcal{Q}$ projected on $\mathcal{S}$.

$$\mathcal{C}_S^{el} = \text{cone}\left(\left\{\vec{M}^{ijkl}u^i v^j u^k v^l\right\}\right)^* = \text{cone}\left(\vec{p}(u,v)\right)^* \equiv \mathcal{Q}_P^* \tag{3.23}$$

JHEP01(2021)095

where we define the vector of quartic polynomials, $\vec{p}(u,v)$, whose components are $p_\alpha(u,v) \equiv M_\alpha^{ijkl} u^i v^j u^k v^l$. Our final goal is to identify the set of ERs of $\mathcal{Q}_P$ =cone($\vec{p}(u,v)$), which we denote by $\mathcal{E}_P$. The positivity bounds are then given by

$$\vec{C} \cdot \vec{p} \geq 0, \ \forall \vec{p} \in \mathcal{E}_P \tag{3.24}$$

How do we find $\mathcal{E}_P$? It is often possible to identify the bounds of $\mathcal{Q}_P$ by inspecting the structure of $\vec{p}(u,v)$. Often, $\mathcal{Q}_P$ turns out to be a polyhedral cone, and in that case a vertex enumeration will immediately give $\mathcal{E}_P$. To illustrate this, consider the four-Higgs operators as an example. They are the S-type aQGC operators, and are defined as [61]

$$O_{S,0} = [(D_\mu \Phi)^\dagger D_\nu \Phi] \times [(D^\mu \Phi)^\dagger D^\nu \Phi], \tag{3.25}$$
$$O_{S,1} = [(D_\mu \Phi)^\dagger D^\mu \Phi] \times [(D_\nu \Phi)^\dagger D^\nu \Phi], \tag{3.26}$$
$$O_{S,2} = [(D_\mu \Phi)^\dagger D_\nu \Phi] \times [(D^\nu \Phi)^\dagger D^\mu \Phi]. \tag{3.27}$$

Define the real field components

$$\Phi = \begin{pmatrix} \phi_1 + i\phi_2 \\ \phi_3 + i\phi_4 \end{pmatrix}, \tag{3.28}$$

and $u = (u_1, u_2, u_3, u_4)$, $v = (v_1, v_2, v_3, v_4)$ to represent the superposition of the real Higgs components. Assuming they are real for the moment (shortly we will show u, v being complex does not give rise to any new bounds), by an explicit calculation of the $HH \to HH$ amplitude, we find

$$\vec{p}(u,v) \propto (X + Y + Z, Y, X + Y) \tag{3.29}$$
$$X = \frac{1}{2}\left(-u_4 v_1 - u_3 v_2 + u_2 v_3 + u_1 v_4\right)^2 + \frac{1}{2}\left(-u_3 v_1 + u_4 v_2 + u_1 v_3 - u_2 v_4\right)^2 \geq 0 \tag{3.30}$$
$$Y = \left(u_1 v_1 + u_2 v_2 + u_3 v_3 + u_4 v_4\right)^2 \geq 0 \tag{3.31}$$
$$Z = \left(u_2 v_1 - u_1 v_2 + u_4 v_3 - u_3 v_4\right)^2 \geq 0 \tag{3.32}$$

and this defines $\mathcal{Q}_P$ =cone($\{\vec{p}(u,v)\}$) as a triangular cone, with 3 facets

$$\vec{p}(u,v) \cdot (0,-1,1) \geq 0 \tag{3.33}$$
$$\vec{p}(u,v) \cdot (0,1,0) \geq 0 \tag{3.34}$$
$$\vec{p}(u,v) \cdot (1,0,-1) \geq 0 \tag{3.35}$$

Now, any $\vec{p}(u,v)$ could lead to a necessary bound $\sum_i p_i(u,v) F_{S,i} \geq 0$, but our goal is the complete set of independent bounds, which are given by $\mathcal{E}_P$, the ERs of this triangular cone. They can be obtained from the 3 facets by a vertex enumeration: $\mathcal{E}_P = \{(1,0,0), (1,0,1), (1,1,1)\}$. These give the following bounds:

$$F_{S,0} \geq 0\,, \tag{3.36}$$
$$F_{S,0} + F_{S,2} \geq 0\,, \tag{3.37}$$
$$F_{S,0} + F_{S,1} + F_{S,2} \geq 0\,. \tag{3.38}$$

JHEP01(2021)095

It is easy to see that cone($\{\vec{p}(u,v)\}$) fill the entire triangular cone described by eqs. (3.33)–(3.35), and so the three bounds above give indeed the best and valid positivity bounds for the four-Higgs operators.

The example shown here is a simple one with only 3 ERs in a 3-dimensional space, so the problem is somewhat trivial and can be easily solved in other ways. However, formulating the solution with the help of vertex enumeration is convenient, in particular when the dimension of the parameter space and the number of ERs become larger. We will demonstrate this in section 4.2. More generally, $\mathcal{Q}_P$ may not be polyhedral, as for example in the problem considered in this work, where W- and B-bosons are both taken into account. Still, it is possible to identify $\mathcal{E}_P$ by inspecting the boundary of $\mathcal{Q}_P$. We will demonstrate this approach in section 4.2.

We have mentioned that complex values of u, v do not need to be considered, as they lead to no additional bounds. Here we give a proof. First note that according to eq. (3.5), M^{ijkl} has the following crossing symmetries:

$$M^{ijkl} = M^{ilkj} = M^{kjil} = M^{klij} \,. \tag{3.39}$$

For any $u, v \in \mathbb{C}^n$, we write $u = r+is$, $v = p+iq$, with $r, s, p, q \in \mathbb{R}^n$. Let $T^{ijkl} = u^i v^j u^{*k} v^{*l}$. Recall that the elastic positivity eq. (3.8) requires that $P(u,v) = T^{ijkl} M^{ijkl} \geq 0$. Since M is crossing symmetric, we can symmetrize T w.r.t. the same symmetries in eq. (3.39):

$$\begin{aligned} P(u,v) = T^{ijkl} M^{ijkl} &= \frac{1}{4}\left(T^{ijkl} + T^{ilkj} + T^{kjil} + T^{klij}\right) M^{ijkl} \\ &= \left(r^i p^j r^k p^l + s^i p^j s^k p^l + r^i q^j r^k q^l + s^i q^j s^k q^l\right) M^{ijkl} \\ &= P(r,p) + P(s,p) + P(r,q) + P(s,q) \end{aligned} \tag{3.40}$$

Since $r, s, p, q \in \mathbb{R}^n$, $P(r,p)$ being PSD for real r, p is a sufficient condition for $P(u,v)$ to be PSD for complex u, v. Thus restricting u, v to $\mathbb{R}^n$ is sufficient.

This condition essentially comes from the crossing symmetry of M, which is present because we work with real modes. For example, if instead of $W^i_{x,y}$ we used the helicity basis, $W^i_{\pm}$, the above would not hold. Fortunately, it is always possible to work with a basis in which the crossing symmetry is manifest. This is exactly why we choose the linear polarization basis for the vector modes. We should also mention that, in section 4.1, we consider u, v to be factorizable in the polarization and gauge spaces, i.e.

$$u^i = x^a \alpha^b, \;\; v^i = y^a \beta^b, \quad i = (a,b) \tag{3.41}$$

with a, b the polarization index and the gauge index, respectively, so that the problem of determining a PSD polynomial can be simplified. In this case the crossing symmetry for one set of variables is lost, and so in principle we must consider complex values. In practice, as we will see, with the factorization assumption, this does not significantly increase the difficulty.

3.4 The extremal positivity approach

The extremal positivity approach proposed recently in ref. [9] directly constructs the allowed parameter space as the convex hull of a set of "potential" ERs (PERs), which can be

JHEP01(2021)095

identified as the projectors of the irreps of the symmetry groups, under which the particles i, j are charged. This approach has the advantage that, in principle, it always gives the best bounds as required by the dispersion relation.

To illustrate this idea, consider the W-boson-only case which has been already discussed in ref. [9]. Briefly, following eq. (3.17), one needs the projection operators for $\mathbf{3} \otimes \mathbf{3} = \mathbf{1} \oplus \mathbf{3} \oplus \mathbf{5}$ in $\mathrm{SU}(2)_L$,

$$P^{(1)}_{\alpha\beta\gamma\sigma} = \frac{1}{N}\delta_{\alpha\beta}\delta_{\gamma\sigma}, \qquad P^{(2)}_{\alpha\beta\gamma\sigma} = \frac{1}{2}\left(\delta_{\alpha\gamma}\delta_{\beta\sigma} - \delta_{\alpha\sigma}\delta_{\beta\gamma}\right),$$
$$P^{(3)}_{\alpha\beta\gamma\sigma} = \frac{1}{2}\left(\delta_{\alpha\gamma}\delta_{\beta\sigma} + \delta_{\alpha\sigma}\delta_{\beta\gamma}\right) - \frac{1}{N}\delta_{\alpha\beta}\delta_{\gamma\sigma}, \tag{3.42}$$

where $N = 3$, as well as the projectors of the SO(2) rotation around the forward direction, for $\mathbf{2} \otimes \mathbf{2} = \mathbf{1} \oplus \mathbf{1} \oplus \mathbf{2}$, which is similar but with $N = 2$. Combining both types of projectors with the β, σ indices symmetrized gives 9 PERs, among which 5 are linearly independent and 8 are extremal. Thus $\mathcal{C}$ is determined via the extremal representation, as a 8-edge polyhedral cone $\mathcal{C}$ in a 5-dimensional space.

To obtain bounds, one needs to represent the cone in the inequality representation. Since $\mathcal{C}$ is a polyhedral cone, the problem is a simple vertex enumeration. Once we have the facets of $\mathcal{C}$, taking an intersection with the physical space $\mathcal{S}$ gives $\mathcal{C}_S$ as a cone with 6 facets, each of them representing a linear bound:

$$F_{T,2} \geq 0, \tag{3.43}$$
$$4F_{T,1} + F_{T,2} \geq 0, \tag{3.44}$$
$$F_{T,2} + 8F_{T,10} \geq 0, \tag{3.45}$$
$$8F_{T,0} + 4F_{T,1} + 3F_{T,2} \geq 0, \tag{3.46}$$
$$12F_{T,0} + 4F_{T,1} + 5F_{T,2} + 4F_{T,10} \geq 0, \tag{3.47}$$
$$4F_{T,0} + 4F_{T,1} + 3F_{T,2} + 12F_{T,10} \geq 0. \tag{3.48}$$

The last two bounds, eqs. (3.47) and (3.48), are actually tighter than the best linear bounds from the elastic positivity approach. For illustration, in figure 1 we show this improvement on $F_{T,0}$ and $F_{T,1}$, assuming the other two operators vanish. More discussions about this improvement can be found in ref. [9].

While this approach is powerful and efficient in the above example, difficulties might arise if degenerate irreps appear. For example, a pair of W and a pair of B-bosons can both form a $\mathrm{SU}(2)_L$ singlet, and a projector can be constructed for any linear combination of them. The ERs are then continuously parameterized by a real parameter, r, that represents the mixing of the two irreps. As we will see, when both W and B-bosons are considered, the extremal presentation of $\mathcal{C}$ contains a set of discrete ERs, $\vec{e}_i$, plus a set of continuous ones, $\vec{e}_i(r)$. One then has to determine the convex hull of an infinite number of rays.

Numerically, a possible solution is to sample $\vec{e}_i(r)$ with a sufficiently large number of discrete r values. This gives a set of numerical PERs, which, after intersecting the physical subspace, forms an approximation of $\mathcal{C}_S$, and we will call it $\mathcal{C}_N$. In principle, one could adopt the same vertex enumeration algorithms to find its facets. However, since $\mathcal{C}_N$ is

JHEP01(2021)095

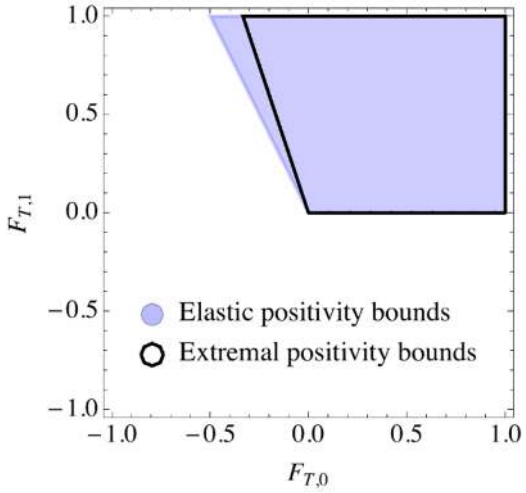

Figure 1. A comparison of elastic positivity bounds and extremal positivity bounds on the $F_{T,0}$-$F_{T,1}$ plane. All other coefficients are fixed to 0.

inscribed to $\mathcal{C}_S$, one has to choose a sufficiently large N, the number of the sampled rays, to avoid over-constraining. The number of facets grows quickly with N, and as a result, this approach becomes not very useful in practice. Instead, we find the following approach more suitable for large N: instead of presenting positivity inequalities and then checking whether a point $\vec{f}$ is included in $\mathcal{C}_N$, we can directly check if there exists a set of positive weights $w_i \geq 0$ and a subset of discretely sampled PERs, $\vec{e}_{\text{num},i}$, such that $\sum_i w_i e_{\text{num},i} = \vec{f}$, i.e. $\vec{f}$ is a positively weighted sum of $\vec{e}_{\text{num},i}$. This problem can be recast into a linear programming problem, and therefore can be solved efficiently with standard tools.

On the other hand, finding the full set of analytical bounds is often difficult if there are many PERs that depend on free real parameters. We will see that the resulting analytical bounds are not simply linear inequalities, but instead they form a series of homogeneous polynomial inequalities with increasing degrees, i.e. linear inequalities, quadratic inequalities, cubic inequalities, and so on. In this work we will show how to derive up to quadratic level bounds for the transversal aQGC operators. Due to this "truncation" at the quadratic order, these analytical results are incomplete and describe a slightly larger cone $\mathcal{C}_A \supsetneq \mathcal{C}_S$. In contrast, the numerical approach describes $\mathcal{C}_N \subsetneq \mathcal{C}_S$, which is slightly over-constraining, so the exact $\mathcal{C}_S$ is bounded by the two methods, with $\Omega(\mathcal{C}_N) < \Omega(\mathcal{C}_S) < \Omega(\mathcal{C}_A)$. By comparing the solid angles $\Omega(\mathcal{C}_N)$ and $\Omega(\mathcal{C}_A)$, we can get a conservative estimate of the errors of both approaches. As we will see, their difference in Ω shows up at the 3rd decimal place, which means that both the numerical bounds and the truncated analytical bounds are extremely close to the truth.

4 The elastic positivity bounds

In this section, we extract the positivity bounds using the conventional elastic positivity approach, i.e. following eq. (3.12). We have shown that u, v only need to be real vectors.

JHEP01(2021)095

Taking this into account, the problem is still a difficult one, equivalent to the determination of a PSD polynomial with 16 variables. Furthermore, these variables are not connected by a single symmetry group: there are two sets of quantum numbers, helicity and gauge, and in addition W and B are not in the same gauge multiplet.

We will consider three different methods. In the first one, we restrict the u, v vectors to those with a specific form, and therefore simplifying the problem, at the cost of a loss in completeness of the resulting bounds. More explicitly, we assume that u, v can be factorized as the tensor products of two vectors, one representing the (complex) superposition in the helicity space, and the other representing the (complex) superposition in the gauge space (including W and B). We will show that by doing so, the problem is factorized into a vertex enumeration problem in the helicity space with 3 variables, plus two quadratic programming problems in the gauge space with 6 variables, both can be solved, analytically and systematically. The results are, of course, only conservative.

A second method is more general and aims at the full set of bounds. Using eq. (3.24) and the definition of an ER, we can directly look for the ERs of $\mathcal{Q}_P$. This approach works well when only the W-boson modes are considered. If the hypercharge boson B is also included, $\mathcal{Q}_P$ becomes not polyhedral, and the identification of its boundary becomes much more difficult. We are not able to find a systematic approach for this identification. Our approach will be based on inspection, but is not always exact. Resulting bounds are therefore, strictly speaking, still incomplete, but we will show that the difference from the complete bounds is tiny, at only the per mille level.

Finally, we will also consider a fully numerical approach, which directly checks if a given set of coefficients are allowed by positivity. It proceeds by minimizing $P(u, v)$ numerically w.r.t. to u, v, and checking that the minimum is positive. This gives in principle the best elastic positivity bounds. The drawback is that no inequalities can be obtained.

The three approaches will be presented in sections 4.1, 4.2, and 4.3.

4.1 The factorization assumption

In this section we will consider the following factorization for the superposition vectors:

$$u^i = x^a \alpha^b, \;\; v^i = y^a \beta^b, \quad i = (a, b) \tag{4.1}$$

where x, y represent superpositions of different polarization states, and α, β represent superpositions of different gauge components, including W and B, such that

$$u^i \left|i\right\rangle = x^1\alpha^1 \left|B_R\right\rangle + \sum_{b=2}^{4} x^1\alpha^b \left|W_R^{b-1}\right\rangle + x^2\alpha^1 \left|B_L\right\rangle + \sum_{b=2}^{4} x^2\alpha^b \left|W_L^{b-1}\right\rangle \tag{4.2}$$

$$v^i \left|i\right\rangle = y^1\beta^1 \left|B_R\right\rangle + \sum_{b=2}^{4} y^1\beta^b \left|W_R^{b-1}\right\rangle + y^2\beta^1 \left|B_L\right\rangle + \sum_{b=2}^{4} y^2\beta^b \left|W_L^{b-1}\right\rangle \tag{4.3}$$

where the subscripts R, L indicate positive and negative helicity states, respectively. This parameterization gives a subset of $\mathcal{Q}_P$, and so the resulting bounds are conservative. We will denote these bounds by $\mathcal{C}^{el}_{AF}$.

JHEP01(2021)095

With this factorized form, $P(u,v)$ can be written as

$$P(u,v) = \sum_{i,k,m,r=1}^{4} \sum_{j,l,n,s=1}^{2} \alpha_i \beta_k \alpha_m^* \beta_r^* x_j y_l x_n^* y_s^* M_{ijklmnrs} \geq 0 \tag{4.4}$$

and we have divided the amplitude by a positive factor $4\alpha^2\pi^2/\Lambda^4$. Explicitly, we find that $P(u,v)$ can be written in a bilinear form:

$$P(u,v) = \sum_{k=1}^{3} \sum_{l=1}^{7} C_{kl}(\{F_{T,i}\}) a_k(x_1, x_2, y_1, y_2) b_l(\alpha_1, \ldots, \alpha_4, \beta_1, \ldots, \beta_4), \tag{4.5}$$

where C_{kl} is a linear function of the coefficients $F_{T,i}$. We omit its explicit form here, and refer to eqs. (A.1)–(A.7) in appendix A. a_k, b_l are quartic polynomials of x, y, x^*, y^*, and of $\alpha, \beta, \alpha^*, \beta^*$, respectively. They can be written as

$$a_1 = |x_1 y_2^* + x_2 y_1^*|^2, \qquad a_2 = |x_1 y_1 - x_2 y_2|^2,$$
$$a_3 = |x_1 y_2^* - x_2 y_1^*|^2, \tag{4.6}$$
$$b_1 = |\langle \vec{u}, \vec{v}^* \rangle|^2, \qquad b_2 = |\langle \vec{u}, \vec{v} \rangle|^2, \qquad b_3 = |\vec{u}|^2 |\vec{v}|^2, \tag{4.7}$$
$$b_4 = \alpha_1 \beta_1 \langle \vec{u}, \vec{v}^* \rangle + c.c., \tag{4.8}$$
$$b_5 = \alpha_1 \beta_1^* \langle \vec{u}, \vec{v} \rangle + c.c., \tag{4.9}$$
$$b_6 = |\beta_1|^2 |\vec{u}|^2 + |\alpha_1|^2 |\vec{v}|^2, \tag{4.10}$$
$$b_7 = |\alpha_1|^2 |\beta_1|^2, \tag{4.11}$$
$$\vec{u} \equiv (\alpha_2, \alpha_3, \alpha_4)^T, \qquad \vec{v} \equiv (\beta_2, \beta_3, \beta_4)^T. \tag{4.12}$$

Here, the inner product is defined by $\langle \vec{u}, \vec{v} \rangle \equiv \vec{u}^\dagger \cdot \vec{v} = \sum_{i=2}^{4} \alpha_i^* \beta_i$. Note that the polarization parameters, x, y, x^*, y^*, are present only in terms of a_1, a_2, and a_3. This can be traced back to the conservations of the total angular momentum and parity. We give a brief explanation in appendix B. The gauge parameters $\alpha, \beta, \alpha^*, \beta^*$ are present only in terms of the b_i variables. $b_{1,2,3}$, $b_{4,5,6}$, and b_7 correspond to the WW, WB and BB scattering channels, respectively.

Now the problem is factorized to the determination of $P(u,v) \geq 0$ w.r.t. the a and b variables separately. To see this, note that a_1, a_2, a_3 can take any real values that satisfy

$$a_1 \geq 0, \ a_2 \geq 0, \ 0 \leq a_3 \leq a_1 + a_2 \,, \tag{4.13}$$

where the last inequality holds because

$$a_1 + a_2 - a_3 = |x_1 y_1 + x_2 y_2|^2 \tag{4.14}$$

These inequalities define a 3-dimensional polyhedral cone $\mathcal{A}$. Defining $M_k = C_{kl} b_l$, we see that $P(u,v) \geq 0$ is equivalent to

$$M_k a_k \geq 0, \ \forall (a_1, a_2, a_3) \in \mathcal{A} \quad \Rightarrow \quad M_k \in \mathcal{A}^* \tag{4.15}$$

JHEP01(2021)095

Since we know the bounds of a_i, which are the facets of $\mathcal{A}$, by vertex enumeration we get the facets of $\mathcal{A}^*$, which are the bounds on M_k, as follows:

$$M_1 \geq 0,\ M_2 \geq 0,\ M_1 + M_3 \geq 0,\ M_2 + M_3 \geq 0 \tag{4.16}$$

So the positivity w.r.t. the helicity superposition is equivalent to a simple vertex enumeration.

To proceed, note that eq. (4.16) implies that 4 linear combinations of $C_{kl}b_l$ must be non-negative, for all possible b's satisfying eqs. (4.7)–(4.11). After a change of variables, the latter can be identified by a set of quadratic inequalities. The problem can hence be turned into a set of quadratically-constrained quadratic programming problems, which are the minimization of a quadratic polynomial of variables that satisfy a set of quadratic inequalities. Due to the symmetries of the problem, it turns out that one needs to solve two such problems with at most 6 variables. These problems can be solved analytically, and details are given in appendix A. In total, we obtain nine linear, three quadratic, and one cubic conditions, for $P(u,v) \geq 0$. These are exactly the bounds that define $\mathcal{C}^{el}_{AF}$. They are:

Linear.

$$2F_{T,0} + 2F_{T,1} + F_{T,2} \geq 0 \tag{4.17}$$
$$F_{T,2} + 4F_{T,10} \geq 0 \tag{4.18}$$
$$4F_{T,1} + F_{T,2} \geq 0 \tag{4.19}$$
$$F_{T,2} \geq 0 \tag{4.20}$$
$$2F_{T,0} + F_{T,1} + F_{T,2} + 2F_{T,10} \geq 0 \tag{4.21}$$
$$2F_{T,8} + F_{T,9} \geq 0 \tag{4.22}$$
$$F_{T,9} \geq 0 \tag{4.23}$$
$$4F_{T,6} + F_{T,7} \geq 0 \tag{4.24}$$
$$F_{T,7} \geq 0 \tag{4.25}$$

Quadratic.

$$\begin{aligned} &4\sqrt{[2(F_{T,0}+F_{T,1})+F_{T,2}](2F_{T,8}+F_{T,9})} \\ &\qquad \geq \max[-2(2F_{T,5}+2F_{T,6}+F_{T,7}), 4F_{T,5}+F_{T,7}] \end{aligned} \tag{4.26}$$
$$2\sqrt{F_{T,9}(F_{T,2}+4F_{T,10})} \geq \max[-(2F_{T,11}+F_{T,7}), 2F_{T,11}] \tag{4.27}$$
$$2\sqrt{[4F_{T,10}+4(F_{T,0}+F_{T,1})+3F_{T,2}](4F_{T,8}+3F_{T,9})} \geq |2F_{T,11}+4F_{T.5}+F_{T,7}| \tag{4.28}$$

Cubic.

$$\begin{aligned} &[4(2F_{T,1}+F_{T,2})(4F_{T,8}+3F_{T,9}) - (2F_{T,6}+F_{T,7})|2F_{T,11}+4F_{T,5}+F_{T,7}|] \\ &\quad \times (-|2F_{T,11}+4F_{T,5}+F_{T,7}| + 2F_{T,6} + F_{T,7}) \geq 0 \\ &\text{or } 4F_{T,0} + 2F_{T,1} + 2F_{T,2} + 4F_{T,10} \\ &\qquad \geq \frac{(2F_{T,1}+F_{T,2})(2F_{T,6}+F_{T,7}-|2F_{T,11}+4F_{T,5}+F_{T,7}|)^2}{4(2F_{T,1}+F_{T,2})(4F_{T,8}+3F_{T,9}) - (2F_{T,6}+F_{T,7})^2} \end{aligned} \tag{4.29}$$

JHEP01(2021)095

As a check, we have also obtained the explicit values of u, v vectors for each bound. This information specifies the elastic channel from which a positivity bound can be derived. For the nine linear conditions, the corresponding elastic channels are

Bounds	Channels ($\|1\rangle + \|2\rangle \to \|1\rangle \ + \|2\rangle$)
$2F_{T,0} + 2F_{T,1} + F_{T,2} \geq 0,$	$\|1\rangle = \|W_x^1\rangle\,,\ \|2\rangle = \|W_x^1\rangle$
$F_{T,2} + 4F_{T,10} \geq 0,$	$\|1\rangle = \|W_x^1\rangle\,,\ \|2\rangle = \|W_y^1\rangle$
$4F_{T,1} + F_{T,2} \geq 0,$	$\|1\rangle = \|W_x^1\rangle\,,\ \|2\rangle = \|W_x^2\rangle$
$F_{T,2} \geq 0,$	$\|1\rangle = \|W_x^1\rangle\,,\ \|2\rangle = \|W_y^2\rangle$
$2F_{T,0} + F_{T,1} + F_{T,2} + 2F_{T,10} \geq 0,$	$\|1\rangle = \|W_L^-\rangle\,,\ \|2\rangle = \|W_L^+\rangle$
$2F_{T,8} + F_{T,9} \geq 0,$	$\|1\rangle = \|B_x\rangle\,,\ \|2\rangle = \|B_x\rangle$
$F_{T,9} \geq 0,$	$\|1\rangle = \|B_x\rangle\,,\ \|2\rangle = \|B_y\rangle$
$4F_{T,6} + F_{T,7} \geq 0,$	$\|1\rangle = \|B_x\rangle\,,\ \|2\rangle = \|W_x^1\rangle$
$F_{T,7} \geq 0,$	$\|1\rangle = \|B_x\rangle\,,\ \|2\rangle = \|W_y^1\rangle$

(4.30)

Similar results for quadratic and cubic conditions are given in appendix A.

The above results are derived with a factorization assumption on u, v, and so they are incomplete and should be considered as a set of conservative bounds. The constraining power is reflected by the solid angle of these bounds, $\Omega(\mathcal{C}_{AF}^{el}) = 0.891\%$. This is obtained by 10^9 Monte Carlo sampling points. Surprisingly, we see that more than 99% of the naive aQGC parameter space is already ruled out, even with this conservative approach.

4.1.1 Comparison with previous results

The bounds we have obtained in eqs. (4.17)–(4.28), although incomplete, are sufficient to cover all previous results on the transversal aQGC bounds presented in ref. [5] and ref. [7]. In this section we will make a comparison and demonstrate this coverage. All other approaches that we will consider in this work give even better results, and so for the rest of the paper we will make no further comparisons.

Let us start with ref. [7]. In the gauge-boson sector, the authors have considered superpositions in the helicity space, but not those in the gauge space. The resulting bounds are linear, and are the same as our eqs. (4.17), (4.18), (4.22), (4.23), (4.24), and (4.25). In particular, among the 5 bounds we have obtained in the W-boson sector, only the first two in eq. (4.30) were presented in ref. [7], as the other three require the two incoming particles to be orthogonal in the gauge space. In addition, quadratic and cubic bounds were also not obtained, as these require superposing both W- and B-bosons.[3]

Now consider the results in ref. [5]. In that work, superpositions have been considered in the helicities space with complex coefficients, and with W^+ and W^- used as particle basis, instead of W^1 and W^2. In addition, Z and γ were used instead of W^3 and B, Finally,

[3] A set of quadratic bounds were presented in eq. (96) of ref. [7], constraining the potential sizes of CP-violating operators. They arise from the superposition in the helicity space. In this work we have focused on CP-conserving operators.

JHEP01(2021)095

the operators $O_{T,10}$ and $O_{T,11}$ were missed. The bounds obtained for the $4W$ operators are:

$$\begin{matrix} W_x^- W_y^- \\ W_R^- W_R^- \\ W_R^- W_L^- \\ W_x^- W_x^- \end{matrix} \begin{pmatrix} 0 & 0 & 1 \\ 0 & 2 & 1 \\ 2 & 1 & 1 \\ 8 & 12 & 5 \end{pmatrix} \begin{pmatrix} F_{T,0} \\ F_{T,1} \\ F_{T,2} \end{pmatrix} \geq 0. \tag{4.31}$$

The corresponding scattering channel is shown on the left side of each bound.[4] For comparison, we set $F_{T,10} = 0$. The first one in eq. (4.31) can be identified as our eqs. (4.18) and (4.20). The second one can be obtained by adding our eqs. (4.19) and (4.20). The third one is the same as our eqs. (4.21). This correspondence is clear because

$$\left|W_R^{\pm}\right\rangle = \frac{1}{\sqrt{2}}\left(\left|W_R^1\right\rangle \mp i\left|W_R^2\right\rangle\right). \tag{4.32}$$

Finally, the fourth one is obtained from 4 times eqs. (4.17) plus (4.19).

Additional results in ref. [5], obtained from the ZZ, WZ, $W\gamma$, $Z\gamma$, and $\gamma\gamma$ channels, are also covered by positive linear combinations of our constraints (4.19), (4.20), (4.23), (4.24), (4.25), and by relaxing the quadratic constraint, eq. (4.26) (or eq. (A.51) and eq. (A.54)). The latter can be done with the inequality of arithmetic and geometric means (AM-GM inequality). For example, the $\gamma\gamma$ scattering with the same polarization gives

$$8F_{T,0} + 8F_{T,1} + 4F_{T,2} + 4F_{T,5} + 4F_{T,6} + 2F_{T,7} + 2F_{T,8} + F_{T,9} \geq 0. \tag{4.33}$$

This condition is covered by our condition eq. (4.26) (or (A.51)). To derive this, we use the AM-GM inequality

$$4\sqrt{ab} \leq 4a + b, \quad \forall a, b \geq 0 \tag{4.34}$$

Applying this to the l.h.s. of eq. (4.26) (or (A.51)) with

$$a = 2(F_{T,0} + F_{T,1}) + F_{T,2}, \quad b = 2F_{T,8} + F_{T,9}, \tag{4.35}$$

relaxes eq. (4.26) (or (A.51)) to eq. (4.33). In fact, all similar bounds obtained by scattering channels involving Z or γ with definite polarizations can be covered by our results, because eq. (4.32) together with $\left|W^3\right\rangle = c_W\left|Z\right\rangle + s_W\left|\gamma\right\rangle$ and $\left|B\right\rangle = -s_W\left|Z\right\rangle + c_W\left|\gamma\right\rangle$ (with $c_W \equiv \cos\theta_W$ and $s_W \equiv \sin\theta_W$, the cosine and sine of the Weinberg angle, respectively) allows us to represent all these channels by a pair of properly chosen u, v vectors, which are factorizable under our assumption.

4.2 General bounds

In this section we solve the problem without any assumptions on u and v vectors. We allow arbitrary superposition between the following 8 states:

$$W_x^1, W_y^1, W_x^2, W_y^2, W_x^3, W_y^3, B_x, B_y \tag{4.36}$$

[4] $W^{\pm}W^{\pm}$ and $W^{\pm}W^{\mp}$ channels give equivalent bounds. For simplicity we only use the W^- component.

JHEP01(2021)095

with $u, v \in \mathbb{R}^8$. We proceed as follows. First, in section 4.2.1 we only include the W-boson components $W^{1,2}_{x,y}$, but neglect $W^3_{x,y}$. We will show that in this case $\mathcal{Q}_P$ is a polyhedral cone, and we can determine the elastic positivity bounds by finding its ERs. Then in section 4.2.2 we include the hypercharge boson modes, $B_{x,y}$. Finally, in section 4.2.3 we show that adding the $W^3_{x,y}$ components does not lead to new results. Note that the last point is not true if the extremal positivity approach is used, as we will see later. In section 4.2.2 we will see that our approach is unfortunately still not complete, so the resulting bounds, which we dub $\mathcal{C}^{el}_A$, is slightly conservative.

4.2.1 Analytical bounds for W-boson only

The W-boson has two set of indices: polarization and the $\mathrm{SU}(2)_L$ gauge group index. We use a, b, c, d for the former and $\alpha, \beta, \gamma, \sigma$ for the latter. $\alpha, \beta, \gamma, \sigma$ run from 1 to 3, but we consider the first two components for the moment. The particle indices i, j, k, l each correspond to a pair of indices from the two sets, i.e. $i = (a, \alpha)$, $j = (b, \beta)$ etc. The physical space $\mathcal{S}$ must be invariant under the rotation around the beam axis, the global $\mathrm{SU}(2)_L$ transformation, and the $j \leftrightarrow l$ exchange. A basis for the amplitude can be chosen as

$$M_1^{ijkl} = \frac{1}{2}[\delta^{\alpha\beta}\delta^{ab}\delta^{\gamma\sigma}\delta^{cd} + (s \leftrightarrow u)]\,, \tag{4.37}$$

$$M_2^{ijkl} = \frac{1}{2}[\delta^{\alpha\beta}\epsilon^{ab}\delta^{\gamma\sigma}\epsilon^{cd} + (s \leftrightarrow u)]\,, \tag{4.38}$$

$$M_3^{ijkl} = \frac{1}{2}[\epsilon^{\alpha\beta}\delta^{ab}\epsilon^{\gamma\sigma}\delta^{cd} + (s \leftrightarrow u)]\,, \tag{4.39}$$

$$M_4^{ijkl} = \frac{1}{2}[\epsilon^{\alpha\beta}\epsilon^{ab}\epsilon^{\gamma\sigma}\epsilon^{cd} + (s \leftrightarrow u)]\,, \tag{4.40}$$

$$M_5^{ijkl} = -\epsilon^{\alpha\gamma}\epsilon^{ac}\epsilon^{\beta\delta}\epsilon^{bd}\,, \tag{4.41}$$

where $s \leftrightarrow u$ represents swapping b and d, and β and σ, simultaneously. An amplitude in this basis, written as $M^{ijkl} = \sum_{\alpha=1}^{5} C_\alpha M_\alpha^{ijkl} = \vec{C} \cdot \vec{M}$, can be matched to the SMEFT amplitude, and we can identify the $\vec{C}$ vector as combinations of the dim-8 aQGC coefficients and the dim-6 coefficient a_W:

$$C_1 = 4(2F_{T,0} + 2F_{T,1} + F_{T,2})\,, \tag{4.42}$$

$$C_2 = 2(F_{T,2} + 4F_{T,10})\,, \tag{4.43}$$

$$C_3 = 4F_{T,1} + F_{T,2} - 36\bar{a}_W^2, \tag{4.44}$$

$$C_4 = F_{T,2}\,, \tag{4.45}$$

$$C_5 = 2(2F_{T,1} + F_{T,2})\,, \tag{4.46}$$

where a common factor $16\alpha^2\pi^2/s_W^4\Lambda^4$ has been factored out. The $\bar{a}_W^2$ contribution comes from the dim-6 operator O_W, which we will neglect in this section. We will come back to this contribution in section 6.

We now need to study the cone $\mathcal{Q}_P = \mathrm{cone}(\vec{p}(u, v))$ and find its ERs. First, since $p_\alpha(u, v) = M_\alpha^{ijkl} u^i v^j u^k v^l$, we observe a number of complete squares that can be constructed

JHEP01(2021)095

with the components of $\vec{p}(u,v)$:

$$p_1 = (u^{a\alpha}v^{a\alpha})^2 \tag{4.47}$$
$$p_2 = (u^{a\alpha}v^{b\alpha}\epsilon^{ab})^2 \tag{4.48}$$
$$p_3 = (u^{a\alpha}v^{a\beta}\epsilon^{\alpha\beta})^2 \tag{4.49}$$
$$p_4 = (u^{a\alpha}v^{b\beta}\epsilon^{ab}\epsilon^{\alpha\beta})^2 \tag{4.50}$$
$$p_1+p_2+p_5 = (u^{a\alpha}v^{b\alpha}\sigma_3^{ab})^2 + (u^{a\alpha}v^{b\alpha}\sigma_1^{ab})^2 \tag{4.51}$$
$$p_1+p_3+p_5 = (u^{a\alpha}v^{a\beta}\sigma_3^{\alpha\beta})^2 + (u^{a\alpha}v^{a\beta}\sigma_1^{\alpha\beta})^2 \tag{4.52}$$
$$p_2+p_4+p_5 = (u^{a\alpha}v^{b\beta}\epsilon^{ab}\sigma_3^{\alpha\beta})^2 + (u^{a\alpha}v^{b\beta}\epsilon^{ab}\sigma_1^{\alpha\beta})^2 \tag{4.53}$$
$$p_3+p_4+p_5 = (u^{a\alpha}v^{b\beta}\sigma_3^{ab}\epsilon^{\alpha\beta})^2 + (u^{a\alpha}v^{b\beta}\sigma_1^{ab}\epsilon^{\alpha\beta})^2 \tag{4.54}$$

The fact that these squares or sums of squares are non-negative defines a polyhedral cone, $\mathcal{Q}_R$, in the space of $\vec{p}$, with 8 facets represented by the following $\vec{k}_i$ vectors:

$$\mathcal{Q}_R = \left\{\vec{p}\,|\vec{p}\cdot\vec{k}_i \geq 0\right\}, \qquad \text{with} \tag{4.55}$$

$$\begin{aligned} \vec{k}_1 &= (1,0,0,0,0) & \vec{k}_5 &= (1,1,0,0,1) \\ \vec{k}_2 &= (0,1,0,0,0) & \vec{k}_6 &= (1,0,1,0,1) \\ \vec{k}_3 &= (0,0,1,0,0) & \vec{k}_7 &= (0,1,0,1,1) \\ \vec{k}_4 &= (0,0,0,1,0) & \vec{k}_8 &= (0,0,1,1,1) \end{aligned} \tag{4.56}$$

and we have $\mathcal{Q}_P \subseteq \mathcal{Q}_R$ since $\vec{p}(u,v) \in \mathcal{Q}_R\ \forall u,v \in \mathbb{R}^n$. Later we will see that $\mathcal{Q}_P = \mathcal{Q}_R$.

The next step is to find the set of ERs, $\mathcal{E}_P$. Since Q_R is polyhedral with known facets, a vertex enumeration immediately leads to 7 edges:

$$\vec{E}_i = \hat{e}_i, \qquad \text{for } i = 1,\ldots,5\,, \tag{4.57}$$
$$\vec{E}_6 = (1,0,0,1,-1), \qquad \vec{E}_7 = (0,1,1,0,-1) \tag{4.58}$$

where $\hat{e}_i$ are the unit vectors along the 5 axes. One can check that each $\vec{E}_i$ can be written as $\vec{p}_i(u,v)$ for some $u,v \in \mathbb{R}^n$. This means that $\mathcal{Q}_R = \text{conv}(\mathcal{E}_P) \subseteq \text{cone}(\vec{p}(u,v)) = \mathcal{Q}_P$, and so $\mathcal{Q}_P = \mathcal{Q}_R$. The ERs of $\mathcal{Q}_R$ are also those of $\mathcal{Q}_P$. Therefore, the full set of the bounds for $\mathcal{C}_S^{el} = \mathcal{Q}_P^*$ are then given by $\vec{C}\cdot\vec{E}_i \geq 0,\ \forall \vec{E}_i \in \mathcal{E}_P$.

Finally, we plug in eqs. (4.42)–(4.46), which further reduces the 7 inequalities to 4. They are given by

bounds	channel ($\|1\rangle + \|2\rangle \to \|1\rangle\ + \|2\rangle$)
$F_{T,2} \geq 0,$	$\|1\rangle = \|W_x^1\rangle\,,\ \|2\rangle = \|W_y^2\rangle$
$4F_{T,1} + F_{T,2} \geq 0,$	$\|1\rangle = \|W_x^1\rangle\,,\ \|2\rangle = \|W_x^2\rangle$
$F_{T,2} + 8F_{T,10} \geq 0,$	$\|1\rangle = \|W_x^1\rangle + \|W_y^2\rangle\,,\ \|2\rangle = \|W_y^1\rangle - \|W_x^2\rangle$
$8F_{T,0} + 4F_{T,1} + 3F_{T,2} \geq 0,$	$\|1\rangle = \|W_x^1\rangle + \|W_y^2\rangle\,,\ \|2\rangle = \|W_x^1\rangle + \|W_y^2\rangle$

(4.59)

From the values of u,v that actually generate the $\vec{E}_i$, we could also derive the specific superpositions of states whose scattering amplitudes lead to the above bounds. This information is also listed above, to the right of each bound.

JHEP01(2021)095

One can easily check that these bounds already supersede those presented in the previous section, based on the factorization assumption, i.e. eqs. (4.17)–(4.21). In fact, eqs. (4.20) and (4.19) are the same as the first two bounds shown above; eqs. (4.18) is a sum of the first and the third bounds; eq. (4.17) is a sum of the second and the fourth bounds; and finally eq. (4.21) is a sum of the third and the fourth bounds. On the other hand, these bounds are still weaker than those obtained from the extremal approach in section 3.4: while they can all be reproduced by the extremal approach, the latter also gives eqs. (3.47) and (3.48), which cannot be obtained by the elastic approach.

4.2.2 Analytical bounds for W-boson and B-boson

We have seen that, for the W-boson case, the elastic positivity problem can be nicely solved by finding the ERs of the polyhedral cone Q_P. This is because the symmetries of the problem are sufficient to restrict the number of ERs to be finite. Adding the hypercharge boson B, the set of ERs becomes infinite. This significantly increases the difficulty of the problem.

Following a similar approach, we first specify a basis for $\mathcal{S}$, whose elements are invariant under both gauge transformations and rotations along the beam axis. Instead of the amplitude basis, we directly give all $\vec{p}(u,v)$. We denote $u^i = (r^{a\alpha}, p^c)$, $v^j = (s^{b\beta}, q^d)$, etc., where a, b are the polarization indices of the W-boson modes, α, β are the gauge indices for the W-boson modes, and c, d are the polarization indices for the B-boson modes. We found that the following $p_\alpha(u,v)$

$$p_1(u,v) = (r^{a\alpha}s^{a\alpha})^2 \tag{4.60}$$
$$p_2(u,v) = (r^{a\alpha}s^{b\alpha}\epsilon^{ab})^2 \tag{4.61}$$
$$p_3(u,v) = (r^{a\alpha}s^{a\beta}\epsilon^{\alpha\beta})^2 \tag{4.62}$$
$$p_4(u,v) = (r^{a\alpha}s^{b\beta}\epsilon^{ab}\epsilon^{\alpha\beta})^2 \tag{4.63}$$
$$p_5(u,v) = -4\left(r^{a\alpha}r^{b\beta}\epsilon^{ab}\epsilon^{\alpha\beta}\right)\left(s^{a\alpha}s^{b\beta}\epsilon^{ab}\epsilon^{\alpha\beta}\right) \tag{4.64}$$
$$p_6(u,v) = (p^c q^c)\,(r^{a\alpha}s^{a\alpha}) \tag{4.65}$$
$$p_7(u,v) = \left(p^c q^d \epsilon^{cd}\right)\left(r^{a\alpha}s^{b\alpha}\epsilon^{ab}\right) \tag{4.66}$$
$$p_8(u,v) = \sum_{\alpha=1,2}(r^{a\alpha}q^a + s^{a\alpha}p^a)^2 \tag{4.67}$$
$$p_9(u,v) = \sum_{\alpha=1,2}\left(r^{a\alpha}q^b\epsilon^{ab} + s^{a\alpha}p^b\epsilon^{ab}\right)^2 \tag{4.68}$$
$$p_{10}(u,v) = \left(p^a q^b \sigma_1^{ab}\right)\left(r^{a\alpha}s^{b\alpha}\sigma_1^{ab}\right) + \left(p^a q^b \sigma_3^{ab}\right)\left(r^{a\alpha}s^{b\alpha}\sigma_3^{ab}\right) \tag{4.69}$$
$$p_{11}(u,v) = (p^a q^a)^2 \tag{4.70}$$
$$p_{12}(u,v) = \left(p^a q^b \epsilon^{ab}\right)^2 \tag{4.71}$$

can be constructed from a set of basis amplitudes that are sufficient to describe the SMEFT amplitudes. Similar to the previous case, the corresponding coefficients $C_1, \cdots C_{12}$ can be

JHEP01(2021)095

mapped to the Wilson coefficients:

$$\begin{aligned}
C_1 &= \frac{16}{s_W^4}\left(2F_{T,0}+2F_{T,1}+F_{T,2}\right) & C_7 &= \frac{2}{c_W^2 s_W^2}\left(F_{T,7}+4F_{T,11}\right)\\
C_2 &= \frac{8}{s_W^4}\left(F_{T,2}+4F_{T,10}\right) & C_8 &= \frac{1}{c_W^2 s_W^2}\left(4F_{T,6}+F_{T,7}\right)\\
C_3 &= \frac{4}{s_W^4}\left(4F_{T,1}+F_{T,2}\right) & C_9 &= \frac{1}{c_W^2 s_W^2}F_{T,7}\\
C_4 &= \frac{4}{s_W^4}F_{T,2} & C_{10} &= \frac{2}{c_W^2 s_W^2}F_{T,7}\\
C_5 &= \frac{8}{s_W^4}\left(2F_{T,1}+F_{T,2}\right) & C_{11} &= \frac{4}{c_W^4}\left(2F_{T,8}+F_{T,9}\right)\\
C_6 &= \frac{2}{c_W^2 s_W^2}\left(8F_{T,5}+F_{T,7}\right) & C_{12} &= \frac{2}{c_W^4}F_{T,9}
\end{aligned} \tag{4.72}$$

with a common factor $4\alpha^2\pi^2/\Lambda^4$ divided.

We now need to study the boundary of the set of all possible $\vec{p}(u,v)$. To this end, we notice that a number of inequalities need to be satisfied by $\vec{p}$. First, the following p_i's are non-negative, as they are themselves complete squares or sums of complete squares:

$$p_i \geq 0, \text{ for } i = 1,2,3,4,8,9,11,12 \tag{4.73}$$

In addition, same as the W-boson case, four combinations of $p_1, \cdots p_5$ are non-negative:

$$\begin{aligned}
&p_1+p_2+p_5 \geq 0, && p_1+p_3+p_5 \geq 0,\\
&p_2+p_4+p_5 \geq 0, && p_3+p_4+p_5 \geq 0\,.
\end{aligned} \tag{4.74}$$

Also, a few other complete squares that are linear in $\vec{p}$ can be formed:

$$\begin{aligned}
p_8+p_9-4p_6 &= \sum_{\alpha=1,2}\left(r^{a1}q^b\sigma_1^{ab}-s^{a1}p^b\sigma_1^{ab}\right)^2\\
&\quad+\sum_{\alpha=1,2}\left(r^{a1}q^b\sigma_3^{ab}-s^{a1}p^b\sigma_3^{ab}\right)^2 &(4.75)\\
p_1+2r_1p_6+r_1^2p_{11} &= \left[r_1\left(p^cq^c\right)+\left(r^{a\alpha}s^{a\alpha}\right)\right]^2 &(4.76)\\
p_2+2r_2p_7+r_2^2p_{12} &= \left[r_2\left(p^cq^d\epsilon^{cd}\right)+\left(r^{a\alpha}s^{b\alpha}\epsilon^{ab}\right)\right]^2 &(4.77)\\
p_1+p_2+p_5+2r_3p_{10}+r_3^2(p_{11}+p_{12}) &= \sum_{I=1,3}\left[r_3\left(p^cq^d\sigma_I^{cd}\right)+\left(r^{a\alpha}s^{b\alpha}\sigma_I^{ab}\right)\right]^2 &(4.78)
\end{aligned}$$

Here, r_1, r_2, r_3 are free parameters. These squares lead to the following inequalities

$$\begin{aligned}
&-4p_6+p_8+p_9 \geq 0, && p_1p_{11}-p_6^2 \geq 0, && p_2p_{12}-p_7^2 \geq 0,\\
&(p_1+p_2+p_5)(p_{11}+p_{12})-p_{10}^2 \geq 0\,.
\end{aligned} \tag{4.79}$$

Note that the last three inequalities are quadratic. They come from the fact that, for example, $p_1+2r_1p_6+r_1^2p_{11}=0$ cannot have two distinct real solutions for r_1. Finally, one

JHEP01(2021)095

additional nonlinear inequality can be written down:

$$\begin{aligned}
&p_8+p_9-2\sqrt{p_1+p_2+p_3+p_4+p_5}\sqrt{p_{11}+p_{12}}\\
&-2\left(r^{a\alpha}s^{a\alpha}\right)\left(p^cq^c\right)+2\left(r^{a\alpha}s^{b\alpha}\epsilon^{ab}\right)\left(p^cq^d\epsilon^{cd}\right)=\left(\|r\|\,\|q\|-\|s\|\,\|p\|\right)^2\\
\Rightarrow\quad &p_8+p_9-2\sqrt{p_1+p_2+p_3+p_4+p_5}\sqrt{p_{11}+p_{12}}+2\left(\sqrt{p_1p_{11}}+\sqrt{p_2p_{12}}\right)\geq 0
\end{aligned}\tag{4.80}$$

Similar to the previous case, all these inequalities together define a region $\mathcal{Q}_R$. A difference however is that $\mathcal{Q}_R$ itself is not a convex cone, because eq. (4.80) does not describe a convex boundary. Therefore, instead of $\mathcal{Q}_R$, we should consider $\text{conv}(\mathcal{Q}_R)$. Due to the free parameters r_i and the nonlinear inequalities, $\text{conv}(\mathcal{Q}_R)$ is not polyhedral. Also, unlike the W-boson case, $\text{conv}(\mathcal{Q}_R)$ is not equal to Q_P. Its ERs cannot always be written as $\vec{p}_i(u,v)$, so they are not always in Q_P. This may imply that additional inequalities about p_i may be derived to further restrict $\mathcal{Q}_R$, but we have not been able to identify them. We will only use the inequalities in eqs. (4.73), (4.74), (4.79), (4.80), and for the ERs of $\text{conv}(\mathcal{Q}_R)$, we will only keep the ones that are inside $\mathcal{Q}_P$, to avoid over constraining $\mathcal{C}_S^{el}$. For this reason, our approach does not enumerate all the ERs of $\mathcal{Q}_P$, and so our $\mathcal{C}_A^{el}$ is slightly conservative.

To find the ERs of $\text{conv}(\mathcal{Q}_R)$, we simply follow the definition of ERs, and search in the set $\mathcal{Q}_R$. We first notice that p_8 and p_9 are only bounded from below. Given $p_8\geq 0$ and $p_9\geq 0$, one can easily check:

$$\vec{E}_{0,1}=(0,0,0,0,0,0,0,1,0,0,0,0)\tag{4.81}$$

$$\vec{E}_{0,2}=(0,0,0,0,0,0,0,0,1,0,0,0)\tag{4.82}$$

are extremal. The rest inequalities only involve p_8+p_9. Therefore, we shall first remove p_8 and p_9 from the problem, find the ERs of the rest p_i's, and then for each ER check the minimum value of p_8+p_9, allowed by all inequalities. Let $x=\min(p_8+p_9)$. If $x\leq 0$, setting $p_8=p_9=0$ is extremal in $\mathcal{Q}_R$; if $x>0$, setting $p_8=x, p_9=0$ and $p_8=0, p_9=x$ leads to two ERs in $\mathcal{Q}_R$.

For the rest p_i's, according to the definition of an ER, if $\vec{p}\in\mathcal{Q}_R$ is extremal (with $p_{8,9}$ removed), then if we write

$$\vec{p}=\vec{p}_a+\vec{p}_b,\ \ \vec{p}_{a,b}\in\mathcal{Q}_R\tag{4.83}$$

the only possible solutions are those $\vec{p}_{a,b}\parallel\vec{p}$. One possibility for this to happen is that $\vec{p}$ saturates 9 linear bounds, of the form $\vec{p}\cdot\vec{k}_i=0$, because

$$\vec{p}_{a,b}\in\mathcal{Q}_R\qquad\Rightarrow\qquad\vec{p}_a\cdot\vec{k}_i\geq 0,\ \vec{p}_b\cdot\vec{k}_i\geq 0,\tag{4.84}$$

$$\vec{p}\cdot\vec{k}_i=0\qquad\Rightarrow\qquad\vec{p}_a\cdot\vec{k}_i+\vec{p}_b\cdot\vec{k}_i=0\qquad\Rightarrow\qquad\vec{p}_{a,b}\cdot\vec{k}_i=0\tag{4.85}$$

and since the dimension of $\vec{p}$ is 10 (with $p_{8,9}$ removed), 9 such constraints will leave only one possible solution for $p_{a,b}$, up to a scalar multiplication.

Alternatively, a quadratic inequality, if saturated, counts two constraints. To see this, notice that there are 3 such inequalities in eqs. (4.79), which all have the form (if saturated):

$$(\vec{p}\cdot\vec{k}_1)(\vec{p}\cdot\vec{k}_2)=(\vec{p}\cdot\vec{k}_3)^2,\quad\text{with}\ \left(\vec{p}\cdot\vec{k}_1\right)\geq 0,\ \left(\vec{p}\cdot\vec{k}_2\right)\geq 0\tag{4.86}$$

JHEP01(2021)095

where $\left(\vec{p}\cdot\vec{k}_{1,2}\right)\geq 0$ are due to other linear bounds in $\mathcal{Q}_R$. Splitting $\vec{p}$ into $\vec{p}_a+\vec{p}_b$,

$$\begin{aligned}
&\vec{p}_{a,b}\in\mathcal{Q}_R\ \Rightarrow\ (\vec{p}_{a,b}\cdot\vec{k}_1)(\vec{p}_{a,b}\cdot\vec{k}_2)\geq(\vec{p}_{a,b}\cdot\vec{k}_3)^2,\ \left(\vec{p}_{a,b}\cdot\vec{k}_{1,2}\right)\geq 0,\\
&0\leq\left[\sqrt{\left(\vec{p}_1\cdot\vec{k}_1\right)\left(\vec{p}_2\cdot\vec{k}_2\right)}-\sqrt{\left(\vec{p}_2\cdot\vec{k}_1\right)\left(\vec{p}_1\cdot\vec{k}_2\right)}\right]^2\\
&=\left[\vec{p}_1\cdot\vec{k}_1+\vec{p}_2\cdot\vec{k}_1\right]\left[\vec{p}_1\cdot\vec{k}_2+\vec{p}_2\cdot\vec{k}_2\right]-\left[\sqrt{\left(\vec{p}_1\cdot\vec{k}_1\right)\left(\vec{p}_1\cdot\vec{k}_2\right)}+\sqrt{\left(\vec{p}_2\cdot\vec{k}_1\right)\left(\vec{p}_2\cdot\vec{k}_2\right)}\right]^2\\
&\leq\left(\vec{p}\cdot\vec{k}_1\right)\left(\vec{p}\cdot\vec{k}_2\right)-\left(\left|\vec{p}_1\cdot\vec{k}_3\right|+\left|\vec{p}_2\cdot\vec{k}_3\right|\right)^2\leq\left(\vec{p}\cdot\vec{k}_1\right)\left(\vec{p}\cdot\vec{k}_2\right)-\left(\vec{p}\cdot\vec{k}_3\right)^2=0\,,
\end{aligned}\tag{4.87}$$

so all inequalities between the two zeros on both sides are all saturated, which implies

$$\frac{\vec{p}_{1,2}\cdot\vec{k}_1}{\vec{p}\cdot\vec{k}_1}=\frac{\vec{p}_{1,2}\cdot\vec{k}_2}{\vec{p}\cdot\vec{k}_2}=\frac{\vec{p}_{1,2}\cdot\vec{k}_3}{\vec{p}\cdot\vec{k}_3}\tag{4.88}$$

This counts as two constraints, unless $\vec{p}\cdot\vec{k}_1=0$ or $\vec{p}\cdot\vec{k}_2=0$, in which case only $\vec{p}_{1,2}\cdot\vec{k}_3=0$ is required, i.e. the quadratic constraint is trivialized to one linear constraint (the other one requires $\vec{p}_{1,2}\cdot\vec{k}_1=0$ or $\vec{p}_{1,2}\cdot\vec{k}_2=0$, which will be already covered by other linear constraints).

With these in mind, we should consider all possibilities for $\vec{p}$ to saturate 9 such constraints. Also notice that p_6, p_7 and p_{10} are each constrained only by one quadratic inequality, which means that an ER always has to saturate these 3 inequalities in eqs. (4.79). Therefore we shall consider several cases, depending on how many of the 3 quadratic bounds are trivialized (i.e. either $\vec{p}_{1,2}\cdot\vec{k}_1=0$ or $\vec{p}_{1,2}\cdot\vec{k}_2=0$). For convenience, let us denote the 5-dimensional subspace $\{(p_1,p_2,\cdots,p_5)\}$ by $\mathcal{P}_W$, and the 2-dimensional subspace $\{(p_{11},p_{12})\}$ by $\mathcal{P}_B$. Note that in eqs. (4.73) and (4.74), there are 8 linear constraints that apply to $\mathcal{P}_W$ and 2 that apply to $\mathcal{P}_B$. Now let us consider the following cases.

1. All three quadratic bounds are trivially satisfied. Six additional linear bounds need to be saturated. We can take at most five in $\mathcal{P}_W$, or two in $\mathcal{P}_B$, otherwise they are not independent. If we take five in $\mathcal{P}_W$ with one in $\mathcal{P}_B$, all components in $\mathcal{P}_W$ will vanish, leaving two ERs:

$$\vec{E}_{0,3}=(0,0,0,0,0,0,0,0,0,0,1,0)\,,\tag{4.89}$$
$$\vec{E}_{0,4}=(0,0,0,0,0,0,0,0,0,0,0,1)\,,\tag{4.90}$$

while if we take four in $\mathcal{P}_W$ with two in $\mathcal{P}_B$, all components in $\mathcal{P}_B$ will vanish, leaving the seven ERs that we already found in the W-boson case:

$$\vec{E}_{0,5}=(1,0,0,0,0,0,0,0,0,0,0,0)\,,\tag{4.91}$$
$$\vec{E}_{0,6}=(0,1,0,0,0,0,0,0,0,0,0,0)\,,\tag{4.92}$$
$$\vec{E}_{0,7}=(0,0,1,0,0,0,0,0,0,0,0,0)\,,\tag{4.93}$$
$$\vec{E}_{0,8}=(0,0,0,1,0,0,0,0,0,0,0,0)\,,\tag{4.94}$$
$$\vec{E}_{0,9}=(0,0,0,0,1,0,0,0,0,0,0,0)\,,\tag{4.95}$$
$$\vec{E}_{0,10}=(1,0,0,1,-1,0,0,0,0,0,0,0)\,,\tag{4.96}$$
$$\vec{E}_{0,11}=(0,1,1,0,-1,0,0,0,0,0,0,0)\,.\tag{4.97}$$

JHEP01(2021)095

2. One quadratic constraint is non-trivial. Five additional linear constraints are needed. We can only take four in $\mathcal{P}_W$ and one in $\mathcal{P}_B$, otherwise all three quadratic constraints will be trivialized. After adding $p_{8,9}$ and discarding the ones that do not admit a solution for u, v satisfying $\vec{E} = \vec{p}(u, v)$, we find that the following rays are extremal, under the condition $r > 0$:

$$\vec{E}_{1,1} = (0, 0, 0, 0, 1, 0, 0, 2r, 0, r, r^2, 0) \tag{4.98}$$
$$\vec{E}_{1,2} = (0, 0, 0, 0, 1, 0, 0, 0, 2r, -r, r^2, 0) \tag{4.99}$$
$$\vec{E}_{1,3} = (0, 0, 0, 0, 1, 0, 0, 2r, 0, r, 0, r^2) \tag{4.100}$$
$$\vec{E}_{1,4} = (0, 0, 0, 0, 1, 0, 0, 0, 2r, -r, 0, r^2) \tag{4.101}$$
$$\vec{E}_{1,5} = (0, 1, 0, 0, 0, 0, 0, 2r, 0, r, r^2, 0) \tag{4.102}$$
$$\vec{E}_{1,6} = (0, 1, 0, 0, 0, 0, 0, 0, 2r, -r, r^2, 0) \tag{4.103}$$
$$\vec{E}_{1,7} = (0, 1, 1, 0, -1, 0, r, 0, 0, 0, 0, r^2) \tag{4.104}$$
$$\vec{E}_{1,8} = (0, 1, 1, 0, -1, 0, -r, 2r, 2r, 0, 0, r^2) \tag{4.105}$$
$$\vec{E}_{1,9} = (1, 0, 0, 0, 0, 0, 0, 0, 2r, 0, r, 0, r^2) \tag{4.106}$$
$$\vec{E}_{1,10} = (1, 0, 0, 0, 0, 0, 0, 0, 0, 2r, -r, 0, r^2) \tag{4.107}$$
$$\vec{E}_{1,11} = (1, 0, 0, 1, -1, r, 0, 2r, 2r, 0, r^2, 0) \tag{4.108}$$
$$\vec{E}_{1,12} = (1, 0, 0, 1, -1, -r, 0, 0, 0, 0, r^2, 0) \tag{4.109}$$

3. Two quadratic constraints are non-trivial, three linear constraints in $\mathcal{P}_W$ and one in $\mathcal{P}_B$ are saturated. We find the following ones parameterized by $r > 0$:

$$\vec{E}_{1,13} = \Big(1, 0, 0, 0, 0, -r, 0, 0, 0, r, r^2, 0\Big) \tag{4.110}$$
$$\vec{E}_{1,14} = \Big(1, 0, 0, 0, 0, -r, 0, 0, 0, -r, r^2, 0\Big) \tag{4.111}$$
$$\vec{E}_{1,15} = \Big(1, 0, 0, 0, 0, r, 0, 4r, 0, r, r^2, 0\Big) \tag{4.112}$$
$$\vec{E}_{1,16} = \Big(1, 0, 0, 0, 0, r, 0, 0, 4r, -r, r^2, 0\Big) \tag{4.113}$$
$$\vec{E}_{1,17} = \Big(0, 1, 0, 0, 0, 0, r, 0, 0, -r, 0, r^2\Big) \tag{4.114}$$
$$\vec{E}_{1,18} = \Big(0, 1, 0, 0, 0, 0, r, 0, 0, r, 0, r^2\Big) \tag{4.115}$$

and two additional ones parameterized by r, s, with $r \geq |s|$:

$$\vec{E}_{2,1} = \Big(r^2, 0, 0, r^2 - s^2, s^2 - r^2, -r, 0, 0, 0, s, 1, 0\Big) \tag{4.116}$$
$$\vec{E}_{2,2} = \Big(0, r^2, r^2 - s^2, 0, s^2 - r^2, 0, r, 0, 0, s, 0, 1\Big) \tag{4.117}$$

JHEP01(2021)095

4. Two quadratic constraints are non-trivial, four linear constraints in $\mathcal{P}_W$ and none in $\mathcal{P}_B$ are saturated. We find four ERs parameterized by r, s, with $r \geq |s|$:

$$\vec{E}_{2,3} = \Big(1,0,0,0,0,s,0,2(r+s),0,r,s^2,r^2-s^2\Big) \tag{4.118}$$

$$\vec{E}_{2,4} = \Big(1,0,0,0,0,s,0,0,2(r+s),-r,s^2,r^2-s^2\Big) \tag{4.119}$$

$$\vec{E}_{2,5} = \Big(0,1,0,0,0,0,-s,2(r+s),0,r,r^2-s^2,s^2\Big) \tag{4.120}$$

$$\vec{E}_{2,6} = \Big(0,1,0,0,0,0,-s,0,2(r+s),-r,r^2-s^2,s^2\Big) \tag{4.121}$$

5. Three quadratic constraints are non-trivial. We find that in this case all ERs that admit a solution of $\vec{E} = \vec{p}(u,v)$ reduce to the previous cases.

In total, we find 11 discrete ERs $\vec{E}_{0,i}$, 18 continuous sets of ERs parameterized by one free parameter, $\vec{E}_{1,i}(r)$ with $r > 0$, and 6 continuous sets of ERs parameterized by two free parameters, $\vec{E}_{2,i}(r,s)$ with $r > |s|$. Now positivity bounds are given by $\vec{C}\cdot\vec{E}_{a,i} \geq 0$. For $a = 0$ the bounds are straightforward. For $a = 1$, $\vec{C}\cdot\vec{E}_{1,i} \geq 0$ gives a quadratic polynomial in r, because

$$Ar^2 + Br + C \geq 0,\ \forall r \geq 0 \quad \Rightarrow \quad A \geq 0 \text{ and } C \geq 0 \text{ and } -B \leq 2\sqrt{AC} \tag{4.122}$$

So the resulting bound is a quadratic one, $-B \leq 2\sqrt{AC}$, while $A \geq 0$ and $B \geq 0$ are covered by $\vec{E}_{0,i}$'s. For $a = 2$, $\vec{C}\cdot\vec{E}_{2,i} \geq 0$ gives a quadratic polynomial in r and s

$$Ar^2 + Bs^2 + Cr + Ds + E \geq 0,\ \forall r \geq |s| \tag{4.123}$$

which is equivalent to

$$A \geq 0 \text{ and } E \geq 0 \text{ and } -C \leq 2\sqrt{AE} \text{ and } A + B \geq 0 \tag{4.124}$$

$$\text{and } |D| - C \leq 2\sqrt{(A+B)E} \tag{4.125}$$

$$\text{and } (B \leq 0,\ \text{or } A|D| + BC \geq 0,\ \text{or } 4ABE \geq AD^2 + BC^2). \tag{4.126}$$

However, constraints in eq. (4.124) are already covered by $a = 0$ and $a = 1$ cases, so they can be discarded. Putting everything together, we obtain around 40 inequalities. Numerically, by a Monte Carlo sampling of the coefficient space we find that some of them are redundant, so in the following we only list the independent ones.

Linear.

$$F_{T,2} \geq 0 \tag{4.127}$$

$$4F_{T,1} + F_{T,2} \geq 0 \tag{4.128}$$

$$F_{T,2} + 8F_{T,10} \geq 0 \tag{4.129}$$

$$8F_{T,0} + 4F_{T,1} + 3F_{T,2} \geq 0 \tag{4.130}$$

$$4F_{T,6} + F_{T,7} \geq 0 \tag{4.131}$$

$$F_{T,7} \geq 0 \tag{4.132}$$

$$2F_{T,8} + F_{T,9} \geq 0 \tag{4.133}$$

$$F_{T,9} \geq 0 \tag{4.134}$$

JHEP01(2021)095

Quadratic.

$$F_{T,9}\left(F_{T,2}+4F_{T,10}\right)\geq F_{T,11}^2 \tag{4.135}$$

$$16\left(2\left(F_{T,0}+F_{T,1}\right)+F_{T,2}\right)\left(2F_{T,8}+F_{T,9}\right)\geq\left(4F_{T,5}+F_{T,7}\right)^2 \tag{4.136}$$

$$2\sqrt{2}\sqrt{F_{T,9}\left(F_{T,2}+8F_{T,10}\right)}+4F_{T,6}+F_{T,7}-4F_{T,11}\geq 0 \tag{4.137}$$

$$4\sqrt{\left(8F_{T,0}+4F_{T,1}+3F_{T,2}\right)\left(2F_{T,8}+F_{T,9}\right)}+8F_{T,5}+4F_{T,6}+3F_{T,7}\geq 0 \tag{4.138}$$

Cubic.

$$\begin{aligned}&\left(4F_{T,0}+F_{T,2}\right)F_{T,7}\geq 4\left(4F_{T,1}+F_{T,2}\right)F_{T,5}\\ &\text{or}\quad 4\left(4F_{T,1}+F_{T,2}\right)\left(8F_{T,0}+4F_{T,1}+3F_{T,2}\right)\left(2F_{T,8}+F_{T,9}\right)\\ &\geq 16\left(4F_{T,1}+F_{T,2}\right)F_{T,5}^2+4\left(4F_{T,1}+F_{T,2}\right)F_{T,7}F_{T,5}+\left[2\left(F_{T,0}+F_{T,1}\right)+F_{T,2}\right]F_{T,7}^2\end{aligned} \tag{4.139}$$

$$\begin{aligned}&F_{T,2}F_{T,7}+4F_{T,10}F_{T,7}+2F_{T,2}F_{T,11}\geq 0\\ &\text{or}\quad 4F_{T,2}^2F_{T,9}\geq 4F_{T,10}F_{T,7}^2+F_{T,2}\left[F_{T,7}^2+4F_{T,11}F_{T,7}+8\left(F_{T,11}^2-4F_{T,9}F_{T,10}\right)\right]\end{aligned} \tag{4.140}$$

The results derived above define our analytical elastic positivity bounds, $\mathcal{C}_A^{el}$. All linear and quadratic bounds from the factorization approach, presented in section 4.1, are superseded by these bounds. For the linear bounds, eqs. (4.19), (4.20), (4.22), (4.23), (4.24), and (4.25) in the factorization approach are the same as eqs. (4.128), (4.127), (4.133), (4.134), (4.131), and (4.132). Eq. (4.17) in the factorization approach is obtained by adding up eq. (4.128) and (4.130). Similarly, eq. (4.18) can be derived from eq. (4.127) and (4.129), and eq. (4.21) can be derived from eq. (4.129) and (4.130). Numerically, we can also confirm that the quadratic conditions (4.26)–(4.28) from the factorization approach are covered.

The cubic bound in eq. (4.29) in the factorization approach is however not fully covered. This demonstrates the incompleteness of this approach, namely the inexactness of our determination of $\mathcal{Q}_P$. The difference is tiny: a randomly chosen point has only $\sim 10^{-8}$ probability to satisfy all above bounds but violate eq. (4.29). Such a difference can be safely ignored in any realistic application of these bounds.

In terms of constraining power, our analytical elastic positivity bounds correspond to a solid angle of about $\Omega(\mathcal{C}_A^{el}) = 0.694\%$, which improves the elastic factorization bounds $\Omega(\mathcal{C}_{AF}^{el}) = 0.891\%$. In figure 2, we show $\Omega(\mathcal{C}_A^{el})$ computed from different samplings, each consisting of up to 10^8 points. The average of 15 samplings, with 10^8 points in each sampling, is

$$\Omega(\mathcal{C}_A^{el}) = (0.6937 \pm 0.00021)\% \tag{4.141}$$

where the statistical 1σ error quoted is the square root of the sampling variance.

4.2.3 Adding $W^3_{x,y}$

So far we have not used the third component of the W-boson in the $\mathrm{SU}(2)_L$ triplet space. The two modes W_x^3 and W_y^3 have been ignored. In the following we show that adding them in the elastic approach does not change the conclusion.

JHEP01(2021)095

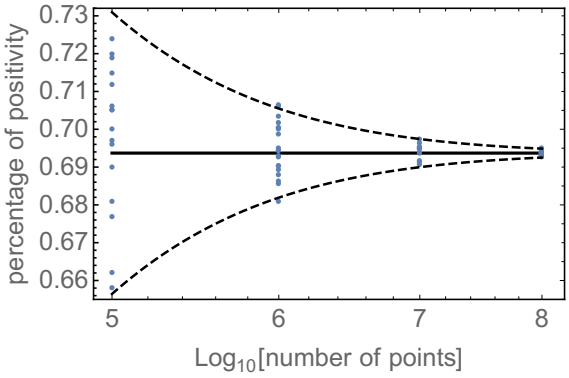

Figure 2. Percentages of the parameter space, or solid angle $\Omega(\mathcal{C}_A^{el})$, of analytical elastic positivity bounds, eqs. (4.127)–(4.140), computed from different samplings ($10^5, 10^6, 10^7$ or 10^8 points). Each blue point is a sampling. The horizontal axis is the number of sampling points, while the vertical axis is the resulting $\Omega(\mathcal{C}_A^{el})$. The solid line (0.6937%) is the average of 15 largest samplings, each with 10^8 points, while the dashed lines are 2σ errors.

First, we need to extend the basis in eqs. (4.60)–(4.71) in order to describe the $P(u,v)$ in this more general case. This can be done by the following operation:

- For $p_i(u,v)$ with $i = 1,2,6,7,8,9,10$, simply extend the summation of the α index to $\sum_{\alpha=1}^{3}$.
- For $p_i(u,v)$ with $i = 3,4,5$, cycle the α and β index and take the sum, e.g.

$$p_i(u,v) \to p_i(u,v) + p_i(u,v)(1\to 2\to 3\to 1) + p_i(u,v)(1\to 3\to 2\to 1) \tag{4.142}$$

  where $1\to 2\to 3\to 1$ or $1\to 3\to 2\to 1$ means that the values of the α,β indices are cycled.

- For $p_i(u,v)$ with $i = 11,12$, use the same $p_i(u,v)$.

With this new $p_i(u,v)$ and the same C_i values in eq. (4.72), one again has $p_\alpha(u,v) = M_\alpha^{ijkl}u^iv^ju^kv^l$, and $P(u,v) = C_\alpha p_\alpha(u,v) \geq 0$. We need to investigate how Q_R is changed with the above operation. First, the new components in u,v are r^{13}, r^{23}, s^{13}, s^{23}. Using the $\mathrm{SU}(2)_L$ rotations around the first and the second axes, together with the SO(2) rotation of the polarization space, one can eliminate 3 of them. Let us keep the r^{13} component. By expanding the new $p_i(u,v)$'s, we see that only the following ones are changed:

$$p_3(u,v) \to p_3(u,v) + \left(r^{13}\right)^2\left[\left(s^{11}\right)^2 + \left(s^{12}\right)^2\right] \tag{4.143}$$

$$p_4(u,v) \to p_4(u,v) + \left(r^{13}\right)^2\left[\left(s^{21}\right)^2 + \left(s^{22}\right)^2\right] \tag{4.144}$$

$$p_8(u,v) \to p_8(u,v) + \left(r^{13}\right)^2\left(q^1\right)^2 \tag{4.145}$$

$$p_9(u,v) \to p_9(u,v) + \left(r^{13}\right)^2\left(q^2\right)^2 \tag{4.146}$$

JHEP01(2021)095

These shifts are a positively weighed sum of $\vec{E}_{0,7}$, $\vec{E}_{0,8}$, $\vec{E}_{0,1}$, and $\vec{E}_{0,2}$, which themselves are already in Q_R. Therefore these shifts do not create any elements outside cone(Q_R). As a result, the ERs of cone(Q_R) remain unchanged, and so the resulting bounds are the same.

4.3 Numerical bounds

For a given set of Wilson coefficients, it is possible to numerically verify whether the full set of elastic positivity bounds is satisfied, for arbitrary polarizations and superpositions of gauge modes. Sampling the entire space with Monte Carlo method allows us to numerically determine the region $\mathcal{C}_S^{el}$, and to compute its solid angle $\Omega(\mathcal{C}_S^{el})$. By comparing the latter with $\Omega(\mathcal{C}_A^{el})$, we will see that the analytical bounds obtained in section 4.2 are extremely close to the full positivity bounds.

To decide whether a given set of Wilson coefficients satisfy the full elastic positivity bound, we plug the set of Wilson coefficients into the constraint $P(u,v) \geq 0$, which should hold for all $u, v \in \mathbb{R}^8$. The naive way forward is to let u^i and v^j randomly sample the 8-sphere for many times, and check whether $P(u,v) \geq 0$ holds. This method however becomes inefficient if we want to scan the full parameter space or even a continuous sub-region. To speed up the process, we recast the problem as an autonomous dynamical system [27].

To see how this works, we combine u^i and v^j into a 16-component vector $x^I = (u^i, v^j)$, and relax the normalization constraints on u^i and v^j. We let x^I depend on some fictitious "time" t and evolve according to an autonomous dynamical system

$$\frac{dx^I}{dt} = -\frac{dP}{dx^I}, \tag{4.147}$$

where $P = P(u,v) \geq 0$ is the full elastic positivity bound. Then we generate an initial value for x^I, whose components take random values in the interval $[-1,1]$, and evolve the dynamical system for some time (say $\Delta t = 100$). If the value of P at the final time becomes negative, we know that this set of Wilson coefficients violates positivity. If the value of P at the final time is positive, we re-run the autonomous system for more randomly chosen initial x^I's, to see whether P can become negative. If all these attempts fail, we declaim that the full elastic positivity bound is satisfied for this set of Wilson coefficients.

The reason why this dynamical system approach can guide us to the choices of u^i and v^j that violate the positivity can be seen from the fact that P is always decreasing with time t:

$$\frac{dP}{dt} = \sum_I \frac{dP}{dx^I}\frac{dx^I}{dt} = -\sum_I \frac{dP}{dx^I}\frac{dP}{dx^I} < 0. \tag{4.148}$$

away from $x^I = 0$ ($dP/dt \neq 0$ because P is a quartic form). It is prudent that we run the autonomous system for several time as the autonomous system can have several equilibria in its phase space and also there can be numerical errors in the evolution.

The numerical bounds obtained by this approach, denoted by C_N^{el}, can in principle still be conservative if P has some local positive minima (thus multiple attractors in the phase space of the dynamical system) and all the initial x^I seeds are accidentally trapped in the attracting basins of these local minima. We have however checked our results, by varying

JHEP01(2021)095

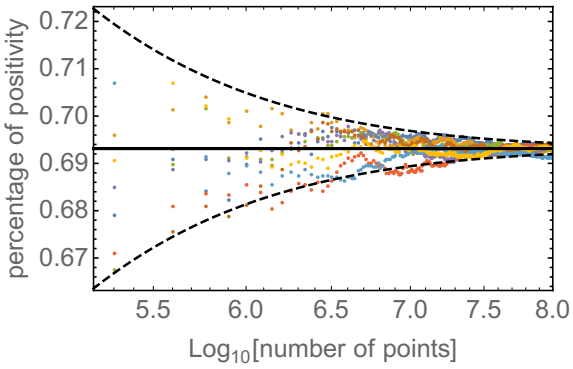

Figure 3. Numerical results for the percentages of the parameter space that satisfy the full elastic positivity bounds. Each point in the plot represents a sampling, and points with the same color come from the same 10^8 sampling. The horizontal axis is the number of points used for the sampling and the vertical axis is the percentage of these points satisfying the full elastic positivity bounds. The horizontal solid line (0.6937%) is the average of ten 10^8-points samplings, while the dashed lines are 2σ errors (square root of the sampling variance) for the samplings.

Δt and increasing the number of the initial x^I seeds used for the evolutions, and found that the resulting $\Omega(\mathcal{C}_N^{el})$ is stable. Therefore, our C_N^{el} should give an accurate description of C_S^{el}.

With this approach, it is straightforward to sample the parameter space and compute $\Omega(\mathcal{C}_N^{el})$ following the discussion in section 3.2. The average of the ten 10^8 samplings is

$$\Omega(\mathcal{C}_N^{el}) = (0.6931 \pm 0.00026)\% \tag{4.149}$$

where the statistical 1σ error quoted is the square root of the sampling variance. With the same method, we have also explicitly verified that $\mathcal{C}_A^{el} \supsetneq \mathcal{C}_N^{el}$, which consists of two facts: 1) there are no Wilson coefficients that satisfy the full elastic positivity but violate the analytical bounds $\mathcal{C}_A^{el}$, which means $\mathcal{C}_A^{el}$ is indeed conservative, providing a consistency check for our results obtained in section 4.2; and 2) there are sets of Wilson coefficients that satisfy the analytical bounds $\mathcal{C}_A^{el}$ but violate the numerical elastic positivity bounds. Instances of the latter indeed occur with a probability consistent with the difference between eq. (4.141) and eq. (4.149), $\sim 0.0006\%$.

To conclude, we have demonstrated that the our analytical results for $\mathcal{C}_A^{el}$ are extremely close to the full elastic positivity bounds, with a relative difference of about 0.1%. We thus conclude that our analytical approach presented in section 4.2 is, even though incomplete in principle, accurate enough to capture the full elastic positivity bounds in all practical applications.

5 The extremal positivity bounds

In this section, we adopt the extremal positivity approach. While the case for the W-boson operators have been discussed already in section 3.4, here we will need to include the hypercharge boson B as well. We will see that, similar to the elastic positivity case, this makes the problem more difficult. In particular, the PERs, from which we construct

JHEP01(2021)095

the convex cone of the physically allowed region $\mathcal{C}_S$, are continuously distributed. The resulting cone is not polyhedral anymore. We will briefly discuss a general solution to this kind of problems, and then present both analytical and numerical results.

Recall that in the W-boson case, the PERs are constructed by combining the projection operators of both the SU(2) and SO(2) group. Adding the $B_{x,y}$ modes induces more projectors. Since B lives in the same representation as W in the SO(2) rotational group, the corresponding projectors of this group remain the same. We however need to modify the gauge group projectors. Since the **5** irrep cannot be formed by two B's or one W and one B, we can keep the corresponding projector $P^{(3)}$. As for $P^{(1)}$ and $P^{(2)}$, we will ignore their normalization, as this has no effect on the determination of the parameter space. The $P^{(1)}$ projector can now be constructed for any linear combination of the singlet in WW and the singlet in BB:

$$P^{(1)}(r)_{\alpha\beta\gamma\sigma} = \frac{1}{3} d_{\alpha\beta}(r) d_{\gamma\sigma}(r) \tag{5.1}$$

$$d_{\alpha\beta}(r) = \begin{cases} 1 & \alpha = \beta = 1,2,3 \\ r & \alpha = \beta = 4 \\ 0 & \text{otherwise} \end{cases} \tag{5.2}$$

where the indices $\alpha, \beta, \gamma, \sigma$ represent the 3 components of W and the B-boson, for values $1, 2, 3, 4$ respectively. r is a real number that parameterizes the mixing between the WW and BB singlets. This means that there is an infinite set of $P^{(1)}$, parameterized by a free parameter r.

The $P^{(2)}$ can be written in a similar way, for any linear combination of triplets in WW, WB and BW:

$$P_S^{(2)}(r_1, r_2)_{\alpha\beta\gamma\sigma} = \frac{1}{2} \sum_{i=1}^{3} f^i_{\{\alpha,\beta\}}(r_1, r_2) f^i_{\{\gamma,\sigma\}}(r_1, r_2) \tag{5.3}$$

$$P_A^{(2)}(r_1, r_2)_{\alpha\beta\gamma\sigma} = \frac{1}{2} \sum_{i=1}^{3} f^i_{[\alpha,\beta]}(r_1, r_2) f^i_{[\gamma,\sigma]}(r_1, r_2) \tag{5.4}$$

$$f^1_{\alpha\beta}(r_1, r_2) = \begin{pmatrix} 0 & 0 & 0 & r_1 \\ 0 & 0 & 1 & 0 \\ 0 & -1 & 0 & 0 \\ r_2 & 0 & 0 & 0 \end{pmatrix}, \qquad f^2_{\alpha\beta}(r_1, r_2) = \begin{pmatrix} 0 & 0 & -1 & 0 \\ 0 & 0 & 0 & r_1 \\ 1 & 0 & 0 & 0 \\ 0 & r_2 & 0 & 0 \end{pmatrix},$$

$$f^3_{\alpha\beta}(r_1, r_2) = \begin{pmatrix} 0 & 1 & 0 & 0 \\ -1 & 0 & 0 & 0 \\ 0 & 0 & 0 & r_1 \\ 0 & 0 & r_2 & 0 \end{pmatrix} \tag{5.5}$$

which are freely parameterized by two real numbers, r_1 and r_2. The PERs are constructed from the symmetrized projector $P_S^{(2)}$ and the anti-symmetrized $P_A^{(2)}$, which are obtained by further symmetrizing the β and δ indices. They essentially depend on at most one free

JHEP01(2021)095

parameter ($r_1 + r_2$ or $r_1 - r_2$), which we will simply denote as r and use the notation $P^{(2)}_{S,A}(r)$ instead.

Among all the PERs, there are in total 13 linearly independent terms. We choose the following ones to form a basis:

$$B_1 = (1,3), \quad B_2 = (3,3), \quad B_3 = (1,2)_S, \quad B_4 = (3,2)_S, \quad B_5 = (1,1)^0, \tag{5.6}$$
$$B_6 = (1,1)^1, \quad B_7 = (1,1)^2, \quad B_8 = (3,1)^0, \quad B_9 = (3,1)^1, \tag{5.7}$$
$$B_{10} = (3,1)^2, \quad B_{11} = (2,2)^0_S, \quad B_{12} = (2,2)^1_S, \quad B_{13} = (2,2)^2_S. \tag{5.8}$$

where (m,n) represents that the projectors $P^{(m)}$ for SO(2) and $P^{(n)}$ for SU(2) are combined. The subscript S indicates that we take the symmetric components (i.e. $P^{(2)}_S$ is used if $m = 1, 3$, or $P^{(2)}_A$ is used if $m = 2$.) The superscript $0, 1, 2$ means that the free parameter r is present, and we take the coefficient of the r^0, r^1, or r^2 term, respectively. All PERs are at most a quadratic function of r. With this basis, the full set of PERs can be written as a set of 13-vectors:

$$\vec{e}_1 = (1,0,0,0,0,0,0,0,0,0,0,0,0) \tag{5.9}$$
$$\vec{e}_2 = (0,1,0,0,0,0,0,0,0,0,0,0,0) \tag{5.10}$$
$$\vec{e}_3 = (0,0,1,0,0,0,0,0,0,0,0,0,0) \tag{5.11}$$
$$\vec{e}_4 = (0,0,0,1,0,0,0,0,0,0,0,0,0) \tag{5.12}$$
$$\vec{e}_5 = \left(-\frac{1}{6}, \frac{1}{6}, 0, 0, -\frac{5}{3}, 0, 0, \frac{5}{3}, 0, 0, \frac{5}{6}, 0, 0\right) \tag{5.13}$$
$$\vec{e}_6 = \left(0, 0, -1, 1, 0, -\frac{3}{4}, 0, 0, \frac{3}{4}, 0, 0, 0, 1\right) \tag{5.14}$$
$$\vec{e}_7(r) = \left(0,0,0,0,1,r,r^2,0,0,0,0,0,0\right) \tag{5.15}$$
$$\vec{e}_8(r) = \left(0,0,0,0,0,0,0,1,r,r^2,0,0,0\right) \tag{5.16}$$
$$\vec{e}_9(r) = \left(0,0,0,0,0,0,0,0,0,0,1,r,r^2\right) \tag{5.17}$$
$$\vec{e}_{10}(r) = \left(-\frac{1}{3}, \frac{1}{3}, -\frac{4r}{3}, \frac{4r}{3}, -\frac{1}{3}, 0, -r^2, \frac{1}{3}, 0, r^2, -\frac{1}{3}, 0, -\frac{4r}{3}\right) \tag{5.18}$$
$$\vec{e}_{11}(r) = \left(\frac{1}{2}, \frac{1}{2}, \frac{r^2}{2}, \frac{r^2}{2}, -1, -\frac{3r^2}{8}, 0, -1, -\frac{3r^2}{8}, 0, -\frac{1}{2}, r, -\frac{r^2}{2}\right) \tag{5.19}$$
$$\vec{e}_{12}(r) = \left(1, 0, r^2, 0, -2, -\frac{3r^2}{4}, 0, 0, 0, 0, 1, -2r, r^2\right) \tag{5.20}$$

Their conical hull defines the cone $\mathcal{C}$.

To find its intersection with the physical subspace, $\mathcal{C}_S$, one can write the amplitude as $M = \sum_i f_i B_i$, and a comparison with $M^{ijkl} = \sum_\alpha C_\alpha M^{ijkl}_\alpha$ gives the following relations

JHEP01(2021)095

between the operator coefficients and f_i's:

$$\begin{aligned}
f_1 &= 4s_W^{-4}\left(8F_{T,1}+F_{T,2}-8F_{T,10}\right) & f_8 &= 16s_W^{-4}\left(F_{T,2}+2F_{T,10}\right)\\
f_2 &= 4s_W^{-4}\left(F_{T,2}+8F_{T,10}\right) & f_9 &= 3s_W^{-2}c_W^{-2}F_{T,7}\\
f_3 &= 4s_W^{-2}c_W^{-2}\left(8F_{T,6}+F_{T,7}-4F_{T,11}\right) & f_{10} &= 6c_W^{-4}F_{T,9}\\
f_4 &= 4s_W^{-2}c_W^{-2}\left(F_{T,7}+4F_{T,11}\right) & f_{11} &= 4s_W^{-4}\left(F_{T,2}-8F_{T,10}\right)\\
f_5 &= 16s_W^{-4}\left(6F_{T,0}+2F_{T,1}+F_{T,2}-2F_{T,10}\right) & f_{12} &= 0\\
f_6 &= 3s_W^{-2}c_W^{-2}\left(8F_{T,5}+F_{T,7}\right) & f_{13} &= 4s_W^{-2}c_W^{-2}\left(F_{T,7}-4F_{T,11}\right),\\
f_7 &= 6c_W^{-4}\left(4F_{T,8}+F_{T,9}\right)
\end{aligned} \tag{5.21}$$

(a common factor $4\alpha^2\pi^2/\Lambda^4$ has been divided.) These relations can be use to convert the bounds of $\mathcal{C}$ to those of $\mathcal{C}_S$. Now we have the cone $\mathcal{C}$ determined through the extremal representation, with all PERs given in eq. (5.9)–(5.20), while $\mathcal{C}_S$ is the set of points in $\mathcal{S}$ which, after substituting into the above relations, are inside $\mathcal{C}$.

Our goal is to find the inequality representation so that the positivity bounds can be extracted. While the conversion to this representation can be easily done in the case of polyhedral cones, the problem is nontrivial for our non-polyhedral cone $\mathcal{C}$, as obviously the bounds cannot be described by a finite number of linear inequalities. Obtaining the full set of analytical bounds is indeed difficult due to the 6 free parameters in $\vec{e}_7(r)$ to $\vec{e}_{12}(r)$. Nevertheless, analytical bounds up to the quadratic level is relatively simple to obtain, and, as an incomplete set of bounds, they give a conservative description of the allowed physical parameter space. We will denote these bounds by $\mathcal{C}_A$, and will show how they can be derived in section 5.1. Alternatively, in section 5.2, the numerical bounds $\mathcal{C}_N$ will be obtained, by sampling $\vec{e}_i(r)$ with a sufficiently large number of r values. In section 5.3, we will see that both approaches lead to a very good approximation of the full set of extremal positivity bounds.

5.1 Analytical bounds

Recall that finding the bounds of $\mathcal{C}$ is equivalent to finding the ERs of $\mathcal{C}^*$, as $\mathcal{C}$ is given by the collection of points $\vec{f}$ that satisfy $\vec{E}_i\cdot\vec{f}\geq 0$, where $\{\vec{E}_i\}$ is the ERs of $\mathcal{C}^*$. If $\mathcal{C}$ were polyhedral, this would be a normal vertex enumeration problem. Unfortunately, due to the r parameters, we need to solve, in some sense, a continuous version of vertex enumeration.

For illustration, let us first consider a polyhedral case in which $\mathcal{C}$ is a d-dimensional cone constructed from a set of discrete PERs, $\vec{e}_i$, which are constant vectors. In this case, the ERs of $\mathcal{C}^*$ can be obtained by constructing all possible combinations of $d-1$ $\vec{e}_i$, i.e.

$$E^\alpha=\epsilon^{\alpha_1\alpha_2\ldots\alpha_{d-1}\alpha}e_{i_1}^{\alpha_1}e_{i_2}^{\alpha_2}\ldots e_{i_{d-1}}^{\alpha_{d-1}} \tag{5.22}$$

that satisfy the following condition:

$$E^\alpha e_i^\alpha=\epsilon^{\alpha_1\alpha_2\ldots\alpha_{d-1}\alpha}e_{i_1}^{\alpha_1}e_{i_2}^{\alpha_2}\ldots e_{i_{d-1}}^{\alpha_{d-1}}e_i^\alpha\equiv\langle e_{i_1},e_{i_2},\ldots,e_{i_{d-1}},e_i\rangle\geq 0,\quad\forall\ \vec{e}_i \tag{5.23}$$

where ϵ is the d-dimensional Levi-Civita tensor, and $\{\vec{e}_{i_1},\vec{e}_{i_2},\ldots,\vec{e}_{i_{d-1}}\}$ is any combination of $d-1$ $\vec{e}_i$'s. This is simply because a facet of $\mathcal{C}$ is always in a hyperplane spanned by a combination of $d-1$ edges, such that the entire cone is on one side of this hyperplane; the

JHEP01(2021)095

latter condition is guaranteed by eq. (5.23), because any point $\vec{f}$ in $\mathcal{C}$ can be written as a positive sum of $\vec{e}_i$. It's also easy to check that E^α is extremal in $\mathcal{C}^*$, using the fact that $E^\alpha e^\alpha_{i_1} = E^\alpha e^\alpha_{i_2} = \cdots = 0$, i.e. it saturates $d-1$ bounds of $\mathcal{C}^*$. If a PER which is not really extremal is included in the combination, it will not give an independent bound. Therefore, the positivity bounds can be written as

$$\langle e_{i_1}, e_{i_2}, \ldots, e_{i_{d-1}}, f\rangle \geq 0 \tag{5.24}$$

subject to eq. (5.23). This is in fact how vertex enumeration can be solved by brute force.

If some of the $\vec{e}_i$'s are functions of a free parameter r, the procedure above still works in principle, but with some notable differences:

- If $\vec{e}_i(r_1)$ is included in the combination, then $\vec{e}_i{}'(r_1)$, the derivative w.r.t. r at r_1, must also be included, unless it is not linearly independent of the rest vectors in the combination. This is because $\vec{E}$ needs to be also orthogonal to its neighboring ERs.
- The r parameters in all $\vec{e}_i$'s can be chosen independently.
- The condition $\langle e_{i_1}, e_{i_2}, \ldots, e_{i_{d-1}}, e_i\rangle \geq 0$ should be satisfied for any e_i with any choices of r.

For example, one might construct an ER that depends on 3 independent parameters:

$$E^\alpha(r_1, r_2, r_3) = \epsilon^{\alpha_1\alpha_2\ldots\alpha_{d-1}\alpha} e^{\alpha_1}_{i_1}(r_1) e'_{i_1}{}^{\alpha_2}(r_1) e^{\alpha_3}_{i_2}(r_2) e'_{i_2}{}^{\alpha_4}(r_2) e^{\alpha_5}_{i_3}(r_3) e'_{i_3}{}^{\alpha_6}(r_3)\ldots \tag{5.25}$$

and this has to satisfy

$$E^\alpha(r_1, r_2, r_3) e^\alpha_i(r) \geq 0 \tag{5.26}$$

for all $\vec{e}_i$ and all $r \in \mathbb{R}$, in order to represent a faithful bound. If an $\vec{e}_i$ is a quadratic function of r, eq. (5.26) defines a quadratic condition on the components of $E^\alpha(r_1, r_2, r_3)$ (i.e. $Ar^2 + Br + C \geq 0 \Rightarrow A \geq 0,\ C \geq 0,\ B^2 \leq 4AC$). Therefore, the resulting bound has the following form: an up to 6-order polynomial (of r_1, r_2, r_3) needs to be PSD, namely $\vec{E}\cdot\vec{f} \geq 0$, in a range constrained by the inequalities (5.26).

In our problem, $d = 13$ and there are 6 ERs that depend on free r parameters. From the discussion above, we know that obtaining the full analytical results is difficult, as it involves the determination of high-degree PSD polynomials subject to nonlinear constraints. In fact, as soon as $\vec{e}_i$ depends on a second independent free parameter, the bound involves the determination of 4th order PSD polynomials, which is already difficult. To avoid over complicating this problem, we consider combinations of $\vec{e}_i$'s that depend, in total, on at most one common parameter r_0, through at most a quadratic function. In particular, each $\vec{e}_i(r)$ is only allowed to take either $\vec{e}_i(0)$, $\vec{e}_i(\infty)$, or $\vec{e}_i(\pm r_0)$, in the construction of E^α. Note that this is different from sampling $\vec{e}_i(r)$ with only 4 values, not only because $\vec{e}_i{}'(0)$, $\vec{e}_i{}'(\infty)$, $\vec{e}_i{}'(\pm r_0)$ are also used in the construction, but also because $E^\alpha(r_0)e^\alpha_i(r) \geq 0$ is satisfied for all r values, which are not sampled but solved analytically. This means that $E^\alpha \in \mathcal{C}^*$ holds strictly, so the resulting bounds are conservative.

We adopt the above simplified approach and find 10 linear bounds and 59 quadratic bounds. Furthermore, the 59 quadratic bounds are very well-approximated by a subset,

JHEP01(2021)095

constituted by 9 quadratic bounds: a randomly chosen point only has a chance smaller than 10^{-6} to satisfy the subset while violating the complete set. We will thus replace the 59 quadratic bounds by the subset. Together, these bounds define our analytical extremal positivity bounds $\mathcal{C}_A$. We list our results as follows:

Linear.

$$F_{T,2} \geq 0 \tag{5.27}$$
$$4F_{T,1} + F_{T,2} \geq 0 \tag{5.28}$$
$$F_{T,2} + 8F_{T,10} \geq 0 \tag{5.29}$$
$$8F_{T,0} + 4F_{T,1} + 3F_{T,2} \geq 0 \tag{5.30}$$
$$12F_{T,0} + 4F_{T,1} + 5F_{T,2} + 4F_{T,10} \geq 0 \tag{5.31}$$
$$4F_{T,0} + 4F_{T,1} + 3F_{T,2} + 12F_{T,10} \geq 0 \tag{5.32}$$
$$4F_{T,6} + F_{T,7} \geq 0 \tag{5.33}$$
$$F_{T,7} \geq 0 \tag{5.34}$$
$$2F_{T,8} + F_{T,9} \geq 0 \tag{5.35}$$
$$F_{T,9} \geq 0 \tag{5.36}$$

Quadratic.

$$F_{T,9}\left(F_{T,2} + 4F_{T,10}\right) \geq F_{T,11}^2 \tag{5.37}$$
$$16\left(2\left(F_{T,0} + F_{T,1}\right) + F_{T,2}\right)\left(2F_{T,8} + F_{T,9}\right) \geq \left(4F_{T,5} + F_{T,7}\right)^2 \tag{5.38}$$
$$32\left(2F_{T,8} + F_{T,9}\right)\left(3F_{T,0} + F_{T,1} + 2F_{T,2} + 4F_{T,10}\right) \geq 3\left(4F_{T,5} + F_{T,7}\right)^2 \tag{5.39}$$
$$2\sqrt{2}\sqrt{F_{T,9}\left(F_{T,2} + 8F_{T,10}\right)} \geq \max\left(-F_{T,7} - 4F_{T,11}, -4F_{T,6} - F_{T,7} + 4F_{T,11}\right) \tag{5.40}$$
$$\begin{aligned} &4\sqrt{\left(8F_{T,0} + 4F_{T,1} + 3F_{T,2}\right)\left(2F_{T,8} + F_{T,9}\right)} \\ &\quad \geq \max\left(-8F_{T,5} - 4F_{T,6} - 3F_{T,7}, 8F_{T,5} + F_{T,7}\right) \end{aligned} \tag{5.41}$$
$$\begin{aligned} &4\sqrt{F_{T,9}\left(12F_{T,0} + 4F_{T,1} + 5F_{T,2} + 4F_{T,10}\right)} \\ &\quad \geq \max\left(-F_{T,7} - 4F_{T,11}, -4F_{T,6} - F_{T,7} + 4F_{T,11}\right) \end{aligned} \tag{5.42}$$
$$\begin{aligned} &4\sqrt{6}\sqrt{\left(2F_{T,8} + F_{T,9}\right)\left(12F_{T,0} + 4F_{T,1} + 5F_{T,2} + 4F_{T,10}\right)} \\ &\quad \geq \max\left[3\left(8F_{T,5} + F_{T,7}\right), -3\left(8F_{T,5} + 4F_{T,6} + 3F_{T,7}\right)\right] \end{aligned} \tag{5.43}$$
$$\begin{aligned} &\sqrt{6}\sqrt{\left(4F_{T,8} + 3F_{T,9}\right)\left(6F_{T,0} + 2F_{T,1} + 3F_{T,2} + 6F_{T,10}\right)} \\ &\quad \geq \max\left(3\left(2F_{T,5} + F_{T,11}\right), -3\left(2F_{T,5} + F_{T,7} + F_{T,11}\right)\right) \end{aligned} \tag{5.44}$$
$$\begin{aligned} &2\sqrt{\left(12F_{T,8} + 7F_{T,9}\right)\left(12F_{T,0} + 4F_{T,1} + 5F_{T,2} + 4F_{T,10}\right)} \\ &\quad \geq \max\left(-12F_{T,5} - 4F_{T,6} - 5F_{T,7} - 2F_{T,11}, 12F_{T,5} + F_{T,7} - 2F_{T,11},\right. \\ &\qquad \left. 12F_{T,5} + F_{T,7} + 2F_{T,11}, 12F_{T,5} - 4F_{T,6} + F_{T,7} + 2F_{T,11}\right) \end{aligned} \tag{5.45}$$

The first 6 linear bounds are the same as the W-boson-only case, which is expected. The solid angle $\Omega(\mathcal{C}_A)$ is 0.687%, smaller than the elastic positivity case.

JHEP01(2021)095

What can we expect if we gradually relax our restriction (that all $\vec{e}_i$'s depend on at most a common r)? Since E^α will become higher degree polynomials, it is likely that we will obtain a series of polynomial inequalities with increasing degrees, i.e. eqs. (5.27)–(5.45) followed by cubic bounds, quartic bounds, and so on. In this sense, what we have obtained here is the leading and the next-to-leading bounds of this series. However, strictly speaking, we cannot claim that the full set of linear and quadratic bounds are included in eqs. (5.27)–(5.45), as it is always possible to decompose a degree-d bound to an infinite number of degree-$(d-1)$ bounds. In any case, one always needs to find a balance between the accuracy of the results and the complexity of the method. While the above truncation at the quadratic level is manageable, the resulting bounds are already very close to the exact extremal positivity bounds, with only $\sim 1\%$ relative difference. We will demonstrate this in the next two sections.

5.2 Numerical bounds

Our numerical approach to the extremal positivity bounds proceeds by sampling the continuous PERs, numerically, by a discrete set of rays. Specifically, we sample an ER $\vec{e}_i(r)$ by the following $2N$ values of r:

$$r_i = \begin{cases} \tan\frac{i\pi}{2N}, & \text{for } -N+1 \le i \le N-1 \\ \infty, & i = N \end{cases} \tag{5.46}$$

where for $r_N = \infty$ we define $\vec{e}_i(\infty) \equiv \lim_{r\to\infty} r^{-2}\vec{e}_i(r)$. Collecting the values of $\vec{e}_7(r) \sim \vec{e}_{12}(r)$ at the above $2N$ points, together with the $\vec{e}_1 \sim \vec{e}_6$ that do not depend on r, we have in total $12N+6$ numerical PERs, which we denote by $\vec{e}_{\text{num},i}$. Their conical hull, after taking an intersection with the physical subspace $\mathcal{S}$, defines the numerical bound $\mathcal{C}_N$. It is inscribed in and therefore smaller than $\mathcal{C}_S$, but the difference decreases as we increase N, and so the error due to this numerical approximation can be taken under control.

Let us first estimate how well this approximation is. Note that the conical hull of a continuous set of ERs of the form $(1, \sqrt{2}r, r^2)$ represents a circular cone: by rotating the x and z directions by 45°, the rays become $((1+r^2)/\sqrt{2}, \sqrt{2}r, (1-r^2)/\sqrt{2})$, which satisfy

$$\left(\frac{1+r^2}{\sqrt{2}}\right)^2 = \left(\sqrt{2}r\right)^2 + \left(\frac{1-r^2}{\sqrt{2}}\right)^2 \tag{5.47}$$

The r_i values chosen according to eq. (5.46) generate a set of ERs that uniformly distribute on this circular cone. In figure 4 we show the case for $N = 4$. In this case the eight ER samples form a regular octagonal cone that is inscribed to the circular cone, $(1, \sqrt{2}r, r^2)$. To estimate the difference between the circular cone and the inscribed polyhedral cone with $2N$ edges, we note that the ratio of the volumes, or the solid angles, between the two objects, is given by $\frac{n}{2\pi}\sin\left(\frac{2\pi}{n}\right)$, with $n = 2N$. Since we have 6 continuous sets of ERs, as a rough estimation, we expect

$$\frac{\Omega(\mathcal{C}_N)}{\Omega(\mathcal{C}_S)} \approx \left[\frac{n}{2\pi}\sin\left(\frac{2\pi}{n}\right)\right]^6 = 1 - \frac{\pi^2}{N^2} + \mathcal{O}(N^{-4}) \tag{5.48}$$

JHEP01(2021)095

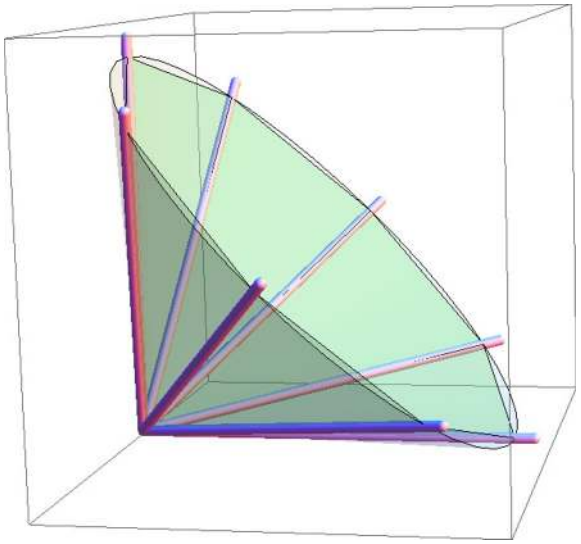

Figure 4. A circular cone, $(1, \sqrt{2}r, r^2)$, and its inscribed octagonal cone, by taking $N = 4$ in eq. (5.46).

This tells us that, to approximate $\mathcal{C}_S$ at the per mille level, taking $N \sim 50$ or 100 would be sufficient.

Since $\mathcal{C}_N$ is polyhedral, one might think that the most straightforward way to determine whether a given point $\vec{f}$ is included in $\mathcal{C}_N$, is to first obtain its facets, as a set of inequalities, and then check them one by one. For $N \sim \mathcal{O}(100)$, finding the facets of $\mathcal{C}_N$ is, however, not realistic. For $N = 5$, with only 66 $\vec{e}_{\text{num},i}$, we already have about 400,000 linear inequalities, thanks to the large dimension of the problem. We thus take an alternative approach. A vector $\vec{f} = (f_1, f_2, \ldots f_{13})$ is included in $\mathcal{C}_N$, if and only if there exists a set of $12N+6$ real numbers $w_i \geq 0$, such that $\sum_i w_i \vec{e}_{\text{num},i} = \vec{f}$ for the set of the $12N + 6$ numerical PERs, $\vec{e}_{\text{num},i}$, determined by eq. (5.46). In other words, $\vec{f}$ is a positively weighted sum of $\vec{e}_{\text{num},i}$'s. This can be written as a linear programming problem:

$$\begin{array}{ll} \text{minimize} & 0 \\ \text{subject to} & \sum_i w_i \vec{e}_{\text{num},i} = \vec{f},\ w_i \geq 0 \end{array} \tag{5.49}$$

which can be efficiently solved by existing algorithms, such as the simplex method or the interior point method. Since the objective function is a constant, there is essentially no minimization, and the algorithm just checks if $\vec{f}$ is included in $\mathcal{C}_N$. For example, taking $N = 50$, $\mathcal{C}_N$ has 606 ERs. Using the LinearProgramming function in Mathematica, checking the inclusion of 10^5 points takes less than one minute on a 4-core laptop. The fraction of points inside $\mathcal{C}_N$ is around 0.68%, which is already a good approximation.

5.3 Comparison

The analytical bounds defines a cone $\mathcal{C}_A$ which contains $\mathcal{C}_S$, because by construction all the $\vec{E}$ vectors are inside $\mathcal{C}^*$. On the other hand, the $\mathcal{C}_N$ given by the numerical approach

JHEP01(2021)095

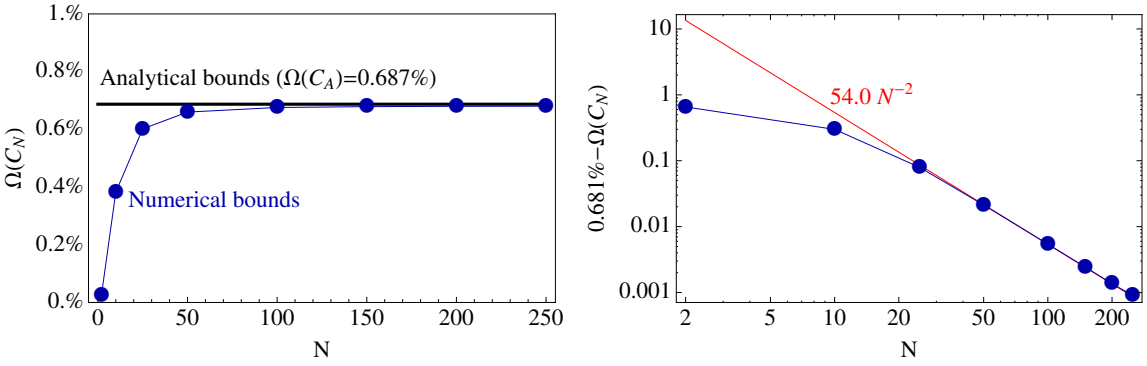

Figure 5. Solid angle $\Omega(\mathcal{C}_N)$ for different N values.

is inscribed in $\mathcal{C}_S$. So we have

$$\mathcal{C}_N \subset \mathcal{C}_S \subset \mathcal{C}_A, \quad \Omega(\mathcal{C}_N) < \Omega(\mathcal{C}_S) < \Omega(\mathcal{C}_A) \tag{5.50}$$

and thus a comparison between $\mathcal{C}_N$ and $\mathcal{C}_A$, in terms of solid angles, gives us an idea where exactly $\mathcal{C}_S$ lies, and how close $\mathcal{C}_N$ and $\mathcal{C}_A$ are to the exact bound. In particular, for $N = 250$, we find

$$\Omega(\mathcal{C}_A) = 0.687\%, \quad \Omega(\mathcal{C}_N) = 0.680\% \tag{5.51}$$

This means that we have a good estimate of $\mathcal{C}_S$, at least at the 1% level, in relative errors.

We may also estimate $\Omega(\mathcal{C}_S)$ by investigating the behaviour of $\Omega(\mathcal{C}_N)$ as N increases. In the left plot of figure 5, we show how $\Omega(\mathcal{C}_N)$ changes with N, and we also compare it with $\Omega(\mathcal{C}_A)$. The solid angle of $\mathcal{C}_S$ is constrained between the black and the blue lines. In addition, for large N, eq. (5.48) suggests that the asymptotic form of $\Omega(\mathcal{C}_N)$ is $\Omega(\mathcal{C}_S)(1 - aN^{-2})$ for some constant a. By fitting $\Omega(\mathcal{C}_N)$ with $N = 100, 150, 200, 250$ to this expression, we find that $a\Omega(\mathcal{C}_S) = 54.0$ and $\Omega(\mathcal{C}_S) = 0.681\%$, i.e.

$$\Omega(\mathcal{C}_N) \approx 0.681\% \left(1 - \frac{79.3}{N^2}\right), \quad \text{for large } N. \tag{5.52}$$

In the right plot of figure 5, we show the differences between $\Omega(\mathcal{C}_N)$ and 0.681%, and we see that, indeed, the above expression agrees very well with our numerical result. This not only indicates that we can confidently extrapolate N to infinity and obtain

$$\Omega(\mathcal{C}_S) = 0.681\%\,, \tag{5.53}$$

but also, it illustrates that our numerical approach is reliable and the fluctuation is well under control. In practice, the numerical error due to a finite N is $54.0N^{-2}$, so taking $N = 100$ is already a very accurate approximation, as it leads to a relative error below 1%.

6 Quadratic dimension-6 contribution

So far we have not considered the quadratic contribution from the dim-6 operator O_W. In this section we will briefly discuss how the inclusion of this operator changes the bounds. Since O_W only enters the WW scattering amplitudes, we will focus on these amplitudes.

JHEP01(2021)095

First consider the elastic positivity. One can simply restore the $\bar{a}_W^2$ term in eq. (4.44), which leads to

bounds	channel ($\|1\rangle + \|2\rangle \to \|1\rangle \ + \|2\rangle$)
$F_{T,2} \geq 0,$	$\|1\rangle = \|W_x^1\rangle\,,\ \|2\rangle = \|W_y^2\rangle$
$4F_{T,1} + F_{T,2} \geq 36\bar{a}_W^2,$	$\|1\rangle = \|W_x^1\rangle\,,\ \|2\rangle = \|W_x^2\rangle$
$F_{T,2} + 8F_{T,10} \geq 36\bar{a}_W^2,$	$\|1\rangle = \|W_x^1\rangle + \|W_y^2\rangle\,,\ \|2\rangle = \|W_y^1\rangle - \|W_x^2\rangle$
$8F_{T,0} + 4F_{T,1} + 3F_{T,2} \geq 00,$	$\|1\rangle = \|W_x^1\rangle + \|W_y^2\rangle\,,\ \|2\rangle = \|W_x^1\rangle + \|W_y^2\rangle$

(6.1)

Comparing with eq. (4.59), obviously, the only difference is that the r.h.s. of the last two bounds become a non-negative number. Roughly speaking, the dim-6 coefficients give a positive lower bound on the dim-8 coefficients. On the one hand, this means that the bounds in eq. (4.59), obtained by neglecting $\bar{a}_W$, are conservative and valid in general. On the other hand, if the coefficient of O_W is found to be nonzero in the future, VBS and tri-boson processes will be the next interesting channels to confirm this, as both $F_{T,2}+8F_{T,10}$ and $8F_{T,0}+4F_{T,1}+3F_{T,2}$ will have to be non-vanishing. These observations are consistent with what we found in refs. [4, 5].

Now we turn to the extremal approach. While the ERs remain the same, the mapping to the physical space $\mathcal{S}$ will be different, as the latter will now have one more dimension, which corresponds to the contribution from $\bar{a}_W^2$. Specifically, the following relations are modified:

$$f_1 = 4s_W^{-4}\left(8F_{T,1} + F_{T,2} - 8F_{T,10} - 36\bar{a}_W^2\right) \tag{6.2}$$

$$f_2 = 4s_W^{-4}\left(F_{T,2} + 8F_{T,10} - 36\bar{a}_W^2\right) \tag{6.3}$$

$$f_5 = 16s_W^{-4}\left(6F_{T,0} + 2F_{T,1} + F_{T,2} - 2F_{T,10} + 18\bar{a}_W^2\right) \tag{6.4}$$

$$f_8 = 16s_W^{-4}\left(F_{T,2} + 2F_{T,10} + 18\bar{a}_W^2\right) \tag{6.5}$$

$$f_{11} = 4s_W^{-4}\left(F_{T,2} - 8F_{T,10} + 36\bar{a}_W^2\right) \tag{6.6}$$

To focus on WW scattering, one simply takes the 9 ERs: $\vec{e}_1$, $\vec{e}_2$, $\vec{e}_5$, $\vec{e}_7(0)$, $\vec{e}_8(0)$, $\vec{e}_9(0)$, $\vec{e}_{10}(0)$, $\vec{e}_{11}(0)$, $\vec{e}_{12}(0)$, whose conical hull forms a polyhedral cone with 8 edges. A vertex enumeration gives the following set of bounds:

$$F_{T,2} \geq 0, \tag{6.7}$$

$$4F_{T,1} + F_{T,2} \geq 36\bar{a}_W^2, \tag{6.8}$$

$$F_{T,2} + 8F_{T,10} \geq 36\bar{a}_W^2, \tag{6.9}$$

$$8F_{T,0} + 4F_{T,1} + 3F_{T,2} \geq 0, \tag{6.10}$$

$$12F_{T,0} + 4F_{T,1} + 5F_{T,2} + 4F_{T,10} \geq 0, \tag{6.11}$$

$$4F_{T,0} + 4F_{T,1} + 3F_{T,2} + 12F_{T,10} \geq 72\bar{a}_W^2. \tag{6.12}$$

Comparing with the extremal bounds in section 3.4, the difference is that several inequalities become stronger, as the lower bounds become a positive number ($\bar{a}_W^2$) rather

JHEP01(2021)095

than 0. The consequence is similar to the case of elastic positivity, namely that the removal of dim-6 contributions is conservative, and that a nonzero dim-6 coefficient could also imply non-vanishing dim-8 effects. It is likely that this is a general feature of the dim-6 quadratic contributions in positivity bounds.

7 Discussion

Recall that the main goals of this work are: 1) to establish the methodology to obtain complete positivity bounds; 2) to compare the elastic and extremal positivity approaches; and 3) to get physical results, i.e. bounds on aQGC coefficients. Let us discuss these three topics one by one.

Methodology. We first summarize the methods that we have adopted in this work.

- Elastic positivity:
  - The "factorized" analytical approach ($\mathcal{C}^{el}_{AF}$): assuming that the superposition of the helicity states can be factorized from those of the additional quantum numbers. This reduces the problem to a set of quadratically-constrained quadratic programming problems. The latter is still NP-hard, but if the number of modes is not large, they can be solved analytically.
  - General analytical approach ($\mathcal{C}^{el}_{A}$): First construct a basis for M^{ijkl} using the symmetries of the system, and obtain the $\vec{p}(u,v)$ vectors. Then the boundary of $\{\vec{p}(u,v)\}$ can be identified by inspection (e.g. by finding/constructing complete squares), which defines a region $\mathcal{Q}_R$. Finding the ERs of cone($\mathcal{Q}_R$) gives a set of analytical bounds.
  - Numerical approach ($\mathcal{C}^{el}_{N}$): for a given point in the Wilson coefficient space, minimize $P(u,v)$ w.r.t. u,v, by casting the problem into a dynamical system and evolve the dynamical system. The sign of the minimum determines whether the point satisfies positivity bounds.
- Extremal positivity:
  - Analytical approach ($\mathcal{C}_A$): first construct the full set of ERs of $\mathcal{C}$ via group theoretical considerations. Some of the ERs are continuously parameterized by free parameters. To get the linear and quadratic bounds, enumerate all "facets" determined by a combination of ERs, which altogether depend on at most one common free parameter.
  - Numerical approach ($\mathcal{C}_N$): sample a continuous set of ERs, numerically, with a discrete set of rays. With order $\mathcal{O}(10^3)$ sampling rays, use linear programming methods to determine the inclusion of a given point in the conical hull of these rays.

JHEP01(2021)095

Comparison of elastic and extremal positivity. There are several aspects to be compared. The first is the constraining power, i.e. how tight these bounds are. This is quantified by the solid angle Ω. Below we summarize the solid angles we found for all approaches, in *percentage*.

$\mathcal{C}_S^{el}$	$\mathcal{C}_{AF}^{el}$	$\mathcal{C}_A^{el}$	$\mathcal{C}_N^{el}$	$\mathcal{C}_S$	$\mathcal{C}_A$	$\mathcal{C}_N$
0.693	0.891	0.694	0.693	0.681	0.687	$0.681 - 54.0N^{-2}$

(7.1)

where N in the last column is one half of the number of sampling rays for each continuous set of ERs. Clearly, in all cases, more than 99% of the full parameter space can be excluded by positivity, because the corresponding SMEFTs cannot be UV-completed.

In principle, the extremal positivity $\mathcal{C}_S$ gives the tightest bounds that can be set on the SMEFT dim-8 operators by using the axiomatic QFT principles. The conventional approach based on elasticity, $\mathcal{C}_S^{el}$, is a relaxation of $\mathcal{C}_S$, as we have showed in section 3.3. We see that in our problem the relaxation is small in terms of the solid angle of the positive region, which amounts to $\Omega(C_S^{el}) = 0.693\%$ compared with $\Omega(\mathcal{C}_S) = 0.681\%$. This is however maybe related with the large dimension of the parameter space, which dilutes the differences that mainly arise in the W sector. In the relevant subspaces, the differences may be larger, as for example shown in figure 1.

In practice, due to the complexity of the problem, our analytical approaches are conservative and do not describe exactly the full bounds. We however see that $\mathcal{C}_A^{el}$ and $\mathcal{C}_A$ are accurate at the 0.1% and 1% level, compared with $\mathcal{C}_S^{el}$ and $\mathcal{C}_S$ respectively, which should be sufficient in many circumstances. The "factorized" analytical elastic bounds, $\mathcal{C}_{AF}^{el}$, are more conservative, which is also expected as the factorization assumption used there is a strong one. This remains an interesting result thanks to the simplicity of the approach, and may be useful when the exactness of the bounds is not important. Finally, the numerical approach for the elastic positivity $\mathcal{C}_N^{el}$ should describe $\mathcal{C}_S^{el}$ exactly, while that for the extremal positivity $\mathcal{C}_N$ can be over-constraining, if N is not sufficiently large. This effect becomes negligible as soon as we take $N \gtrsim 100$.

A second aspect, which may be even more important, is whether an approach can be systematically algorithmized, i.e. clearly defined as a set of procedures that definitely lead to the answer. An approach with this feature is more valuable as it is applicable to more complicated problems, for example to derive bounds for more SMEFT operators. Our numerical approaches clearly satisfy this criteria. For the analytical approaches, the extremal positivity $\mathcal{C}_A$ wins in this aspect, as the enumeration of both the projective operators and the "facets" can be algorithmized. We are not able to algorithmize the elastic positivity $\mathcal{C}_A^{el}$, mainly because of the difficulty in identifying the boundary of $\{\vec{p}(u,v)\}$. We are not aware of a systematic way for doing this, and in this work this was done by inspection: we searched for various kinds of complete squares by trying different combinations. This is neither systematic nor complete, and is tedious. While in this work it has worked adequately, as the resulting bound is only 0.1% weaker than the exact one, it is more likely to be insufficient for more complicated problems, as for example for the full set of aQGCs including longitudinal modes, because further increasing the number of modes seems to significantly

JHEP01(2021)095

increase the difficulty. On the other hand, the $\mathcal{C}^{el}_{AF}$ approach has a clearly defined set of procedures which turns the problem into a quadratically-constrained quadratic programming problem. Solving the latter, however, is analytically realistic only when the number of modes is not large, so this approach is also not suitable for more complicated cases.

What exactly is the origin of the difficulty in $\mathcal{C}^{el}_{A}$? We have showed that elastic positivity corresponds to a relaxation of the $\mathcal{C}_S$ cone to $\mathcal{Q}^*_P = \text{cone}(\{\vec{M}^{ijkl}u^iv^ju^kv^l\})^*$. Naively, one might think that a relaxation should reduce the difficulty of the problem. This is true if our goal was to obtain some positivity bounds: one can easily plug in random values of u, v and get a bound; but this is not true if our goal was to extract the complete set of bounds: the set $\mathcal{Q}_P$ is more difficult to describe than $\mathcal{C}^*$, due to the quartic nature of its elements. In this work we had to first extract the boundaries by searching for complete square relations, and then search for the ERs. On the other hand, comparing with the extremal approach, the boundaries of $\mathcal{C}^*$ is known from the beginning, as they are just the ERs of $\mathcal{C}$, which we directly wrote down using group theory as a guideline. Therefore, this relaxation is not efficient: it actually increases the difficulty of the problem, and at the same time only gives weaker results. It does have the advantage of connecting the bounds to a clear physics picture, i.e. the elastic scattering. However, to obtain an exact description of all bounds, this approach is certainly not suitable. We emphasize that having the exact set of bounds is important not only for testing the axiomatic principles of QFT, but also for inferring or excluding possible UV states using positivity, see ref. [10].

One last aspect to compare is the speed of the two numerical approaches. Below we show the average time it takes to check numerically whether a given point in the space of Wilson coefficients satisfies positivity bounds, on a single core (obviously the problem can be easily parallelized when checking many points). For the extremal approach, we use the simplex method to solve the linear programming, eq. (5.49).

Single-core time	Elastic	Extremal $\mathcal{C}_N$		
[second]	$\mathcal{C}^{el}_N$	$N = 50$	$N = 100$	$N = 200$
No filter	0.1	0.002	0.004	0.007
With filter	0.001	0.00019	0.00021	0.00023
Error on $\Omega(\mathcal{C}_N)$	N/A	3%	0.8%	0.2%

(7.2)

The time used for numerical extremal bounds depends on N, one half of the number of sampling rays per a continuous set of ERs. "Filter" refers to whether we first test a given point against the analytical elastic bounds $\mathcal{C}^{el}_A$, so that we only run the numerical determination if these analytical bounds are satisfied. This procedure significantly accelerates the determination for a randomly chosen point, and should always be used in a practical application (or with $\mathcal{C}^{el}_A$ replaced by $\mathcal{C}_A$). Clearly, the extremal approach drastically improves the speed. For $N = 50$, the speed of the extremal approach is almost 2 orders of magnitude faster. The bounds in that case are about $\approx 3\%$ over-constraining. For $N = 200$ this error is reduced to $\approx 0.2\%$, while the speed is still more than one order of magnitude faster. Furthermore, the difference in speed is still large after applying the "filter".

JHEP01(2021)095

Physics result. We have obtained positivity bounds on the full set of the transversal aQGC operators, and these results provide guidance to the ongoing VBS and tri-boson measurements at the LHC. Our results represent the best that can be derived from the axiomatic principles of QFT, and supersede those presented in the literature whenever relevant. For practical application, we have provided bounds in terms of analytical inequalities, which are convenient to use. We recommend using the extremal analytical bounds $\mathcal{C}_A$, in eqs. (5.27)–(5.45), for reasons discussed above. While they are slightly weaker than the exact extremal bounds, by about 1% (relative) in solid angle, one can also resort to the numerical bounds $\mathcal{C}_N$, if better accuracy is needed, along with a sampling number $N \gtrsim 100$ to ensure the desired accuracy.

Positivity bounds on the full set of aQGC operators, including longitudinal modes, is likely to be too difficult in the elastic approach. The extremal approach should be feasible, but we will leave it to a future work.

8 Summary and outlook

There are at least two ways to derive positivity bounds in the forward limit for SMEFT operators: the conventional elastic positivity approach uses elastic scattering amplitudes from a pair of arbitrarily superposed SM fields, while a more recently proposed approach, which we dub extremal positivity approach, directly constructs the allowed parameter space using the extremal representation of convex cones. We have provided a unified picture to understand and connect both approaches, based on the geometry of the coefficient space and using several concepts from convex geometry. We have shown that the extremal positivity approach always describes the best bounds available from the axiomatic principles of QFT, while the elastic positivity approach relaxes these bounds and are thus often weaker.

As a case study, we have applied both approaches to the scattering amplitude of the transversal electroweak gauge bosons. Aiming at obtaining the complete set of bounds, we have established the methodology for both approaches, identified the main difficulties that arise due to the large number of low-energy modes involved in the problem, and provided both analytical and numerical solutions, which are generally applicable to the SMEFT positivity problems and beyond. We have further compared the two approaches in several aspects. Our main conclusions are

- Extremal positivity gives better bounds than elastic positivity. The improvement in the considered case is small, but can become sizable when focusing on specific sets of operators.
- Analytical solutions are available for both elastic and extremal positivity bounds. They are based on certain approximations, but the final results can reach an accuracy level of 0.1% and 1%, respectively.
- Analytically, the extremal approach can be easily implemented algorithmically and thus applicable to more complicated problems (e.g. bounds involving more operators and more fields). The elastic approach does not seem to have this feature, and so it is less suitable for a more complicated application.

JHEP01(2021)095

- Numerically, to determine if a given point in the Wilson coefficient space is excluded by positivity, the extremal approach is significantly faster than the elastic approach, by about one or two orders of magnitude, while the error can be controlled at the per mille level.

- Neglecting dim-6 operators leads to conservative bounds in both approaches. Non-zero dim-6 coefficients, on the other hand, could imply that certain linear combinations of dim-8 coefficients must be non-vanishing.

For these reasons, we conclude that the extremal positivity approach is always the better option, for extracting the full set of forward limit positivity bounds in SMEFT. These conclusions should also apply to other EFTs with a large number of low energy modes, connected with some symmetry groups.

Physically, this study gives the best positivity bounds on the transversal aQGC couplings. The analytical results of these bounds have been explicitly displayed in the relevant sections. Interested readers should be able to directly dive into these sections and find these results for direct application. These bounds should be obeyed by any SMEFT that admits a UV completion consistent with the axiomatic principles of QFT. By excluding more than 99% of the transversal aQGC parameter space, these bounds will provide useful guidance to both experimental and theoretical studies of the VBS and tri-boson processes.

While these results already represent a significant improvement over the existing literature, we can foresee several further developments, which we leave for future studies:

- The full set of aQGC couplings including the longitudinal modes. The extremal approach discussed in this work should be applicable to this problem.

- Methodology: there is still room to improve for all approaches we have provided in this work. In particular, higher-order bounds (beyond the quadratic ones) will further improve the analytical results, provided that an efficient method exists to find them.

- A comprehensive study of the SMEFT bounds. This study will pave the way towards further applications of positivity bounds in collider physics. While the most obvious application is to provide guidance to experimental searches wherever relevant, there are other more interesting possibilities, such as testing the axiomatic QFT principles in colliders, and inferring/excluding the existence of UV states by using precision measurements. For the last two possibilities, we refer to [10] for a recent application in e^+e^- scattering.

Acknowledgments

We thank G. Durieux, G. Remmen, F. Riva, and N. Rodd for helpful discussions and comments. We also thank X. Li for numerically checking the extremal bounds including the dim-6 coefficient. KY is supported by the Chinese Academy of Sciences (CAS)

JHEP01(2021)095

President's International Fellowship Initiative under Grant No. 2020PM0018. CZ is supported by IHEP under Contract No. Y7515540U1, and by National Natural Science Foundation of China (NSFC) under grant No. 12035008 and 12075256. SYZ acknowledges support from the starting grants from University of Science and Technology of China under grant No. KY2030000089 and GG2030040375, and is also supported by National Natural Science Foundation of China under grant No. 11947301, 12075233 and 12047502, and supported by the Fundamental Research Funds for the Central Universities under grant No. WK2030000036.

A Some details for the analytical elastic positivity with factorization

Here we present more details about deriving the bounds in section 4.1. In eq. (4.16) we have removed the a_i dependence and determined 4 linear inequalities. In terms of C_{kl}, they are

$$C_{1l}b_l \geq 0, \qquad C_{2l}b_l \geq 0, \tag{A.1}$$

$$(C_{1l}+C_{3l})b_l \geq 0, \qquad (C_{2l}+C_{3l})b_l \geq 0 \tag{A.2}$$

and we can write them collectively as

$$\sum_j M^i_{bj}b_j \geq 0, \quad \text{for } i=1,2,3,4 \tag{A.3}$$

with M^i_{bj}'s given by:

$i=1$:

$$M^1_{b1}=\frac{16F_{T,0}+8F_{T,1}+6F_{T,2}}{s_W^4}, \quad M^1_{b2}=\frac{16F_{T,0}+8F_{T,1}+6F_{T,2}}{s_W^4}, \quad M^1_{b3}=\frac{4(4F_{T,1}+F_{T,2})}{s_W^4},$$
$$M^1_{b4}=\frac{8F_{T,5}+4F_{T,6}+3F_{T,7}}{2c_W^2s_W^2}, \quad M^1_{b5}=\frac{8F_{T,5}+4F_{T,6}+3F_{T,7}}{2c_W^2s_W^2}, \quad M^1_{b6}=\frac{4F_{T,6}+F_{T,7}}{c_W^2s_W^2},$$
$$M^1_{b7}=\frac{4(2F_{T,8}+F_{T,9})}{c_W^4}. \tag{A.4}$$

$i=2$:

$$M^2_{b1}=\frac{4(4F_{T,10}+4F_{T,0}+F_{T,2})}{s_W^4}, \quad M^2_{b2}=\frac{4(2F_{T,1}+F_{T,2})}{s_W^4}, \quad M^2_{b3}=\frac{4(2F_{T,1}+F_{T,2})}{s_W^4},$$
$$M^2_{b4}=\frac{2F_{T,11}+4F_{T,5}+F_{T,7}}{c_W^2s_W^2}, \quad M^2_{b5}=\frac{2F_{T,6}+F_{T,7}}{c_W^2s_W^2}, \quad M^2_{b6}=\frac{2F_{T,6}+F_{T,7}}{c_W^2s_W^2},$$
$$M^2_{b7}=\frac{4F_{T,8}+3F_{T,9}}{c_W^4}. \tag{A.5}$$

$i=3$:

$$M^3_{b1}=\frac{4(2F_{T,1}+F_{T,2})}{s_W^4}, \quad M^3_{b2}=\frac{4(4F_{T,10}+4F_{T,0}+F_{T,2})}{s_W^4}, \quad M^3_{b3}=\frac{4(2F_{T,1}+F_{T,2})}{s_W^4},$$
$$M^3_{b4}=\frac{2F_{T,6}+F_{T,7}}{c_W^2s_W^2}, \quad M^3_{b5}=\frac{2F_{T,11}+4F_{T,5}+F_{T,7}}{c_W^2s_W^2}, \quad M^3_{b6}=\frac{2F_{T,6}+F_{T,7}}{c_W^2s_W^2},$$
$$M^3_{b7}=\frac{4F_{T,8}+3F_{T,9}}{c_W^4}. \tag{A.6}$$

JHEP01(2021)095

$$
\begin{aligned}
&i=4: \\
&M^4_{b1}=\frac{2(8F_{T,10}+F_{T,2})}{s^4_W}, \qquad M^4_{b2}=\frac{2(8F_{T,10}+F_{T,2})}{s^4_W}, \qquad M^4_{b3}=\frac{4F_{T,2}}{s^4_W}, \\
&M^4_{b4}=\frac{4F_{T,11}+F_{T,7}}{2c^2_W s^2_W}, \qquad M^4_{b5}=\frac{4F_{T,11}+F_{T,7}}{2c^2_W s^2_W}, \qquad M^4_{b6}=\frac{F_{T,7}}{c^2_W s^2_W}, \\
&M^4_{b7}=\frac{2F_{T,9}}{c^4_W}.
\end{aligned} \tag{A.7}
$$

The first observation here is that the $i=2$ case and the $i=3$ case are in fact identical: they are related by swapping b_1 with b_2, and b_4 with b_5. This simply amounts to taking $\beta_i \to \beta_i^*$. Since β_i are allowed to take any complex 4-vectors, $i=2$ and $i=3$ lead to identical bounds, and thus we can omit the $i=3$ case. A second observation is that not all M^i_{bj}'s are independent. In fact, the following equations hold:

$$
i=1,4: \qquad M^1_{b1}=M^1_{b2}, \qquad M^1_{b4}=M^1_{b5}, \tag{A.8}
$$

$$
i=2: \qquad M^2_{b2}=M^2_{b3}, \qquad M^2_{b5}=M^2_{b6}, \tag{A.9}
$$

i.e. there are only 5 independent M^i_{bj} coefficients. This means that we need to solve the following two positivity conditions for all b_i's:

$$
i=1,4: \qquad (b_1+b_2)M_{b1}+b_3M_{b3}+(b_4+b_5)M_{b4}+b_6M_{b6}+b_7M_{b7}\geq 0 \tag{A.10}
$$

$$
i=2: \qquad b_1M_{b1}+(b_2+b_3)M_{b2}+b_4M_{b4}+(b_5+b_6)M_{b5}+b_7M_{b7}\geq 0 \tag{A.11}
$$

Here we omit the superscript i for M_{bj}.

Since the b_i's are quartic polynomials of α and β, they cannot take arbitrary values. We need to find the range of b_i, as we should only require eqs. (A.10) and (A.11) to hold for b_i within this range. It is easy to identify the following bounds for b_i's:

$$
b_7\geq 0, \qquad 0\leq b_1\leq b_3, \qquad 0\leq b_2\leq b_3, \tag{A.12}
$$

$$
|b_4|\leq 2\sqrt{b_1b_7}, \qquad |b_5|\leq 2\sqrt{b_2b_7}, \qquad b_6\geq 2\sqrt{b_3b_7}. \tag{A.13}
$$

$b_i\geq 0$ for $i=1,2,3,6,7$ are simply by definitions. $b_1\leq b_3$ and $b_2\leq b_3$ are obtained from the Cauchy-Schwarz inequality: $|\langle \vec{u_1},\vec{u_2}\rangle|^2\leq \langle \vec{u_1},\vec{u_1}\rangle\langle \vec{u_2},\vec{u_2}\rangle$, where $\vec{u_1}$ and $\vec{u_2}$ are arbitrary vectors in an inner product space over $\mathbb{C}$. Eq. (A.13) can be derived from:

$$
4b_1b_7-|b_4|^2=4\left[\mathrm{Im}(\alpha_1\beta_1\left\langle \vec{u},\vec{v^*}\right\rangle)\right]^2\geq 0, \tag{A.14}
$$

$$
4b_2b_7-|b_5|^2=4\left[\mathrm{Im}(\alpha_1\beta_1^*\langle \vec{u},\vec{v}\rangle)\right]^2\geq 0. \tag{A.15}
$$

$$
b_6^2-4b_3b_7=(|\beta_1|^2|\vec{u}|^2-|\alpha_1|^2|\vec{v}|^2)^2\geq 0. \tag{A.16}
$$

Now the inequalities (A.12) and (A.13) specify the boundary of the possible range for the b_i parameters. One still needs to show that this boundary is tight, i.e. for all b_i' parameters that satisfy these bounds, there exist a set of α_i and β_i parameters such that $b_i(\alpha_1,\cdots,\alpha_4,\beta_1,\cdots,\beta_4)=b_i'$, or in other words, all points within this range can be

JHEP01(2021)095

achieved by some superposition in the gauge space. In fact, for all b'_i that satisfy eqs. (A.12) and (A.13), defining the following variables:

$$\theta_1 = \cos^{-1}\left(\frac{b'_4}{2\sqrt{b'_1 b'_7}}\right), \qquad \theta_2 = \cos^{-1}\left(\frac{b'_5}{2\sqrt{b'_2 b'_7}}\right), \tag{A.17}$$

$$\phi_1 = \cos^{-1}\left(\frac{2b'_1 - b'_3}{b'_3}\right), \qquad \phi_2 = \cos^{-1}\left(\frac{2b'_2 - b'_3}{b'_3}\right), \tag{A.18}$$

$$r^2 = \frac{1}{2}\left(\frac{b'_6}{\sqrt{b'_3 b'_7}} + \sqrt{\frac{b'^2_6}{b'_3 b'_7} - 4}\right), \tag{A.19}$$

the following α_i and β_i should give the desired b'_i's:

$$\begin{aligned}
&\alpha_1 = r b_7'^{1/4} \exp\left[i\left(\frac{\theta_1+\theta_2}{2} + \frac{\phi_1+\phi_2}{4}\right)\right], \quad \beta_1 = \frac{b_7'^{1/4}}{r} \exp\left[i\left(\frac{\theta_1-\theta_2}{2} + \frac{\phi_1-\phi_2}{4}\right)\right], \\
&\alpha_2 = \frac{b_3'^{1/4}}{\sqrt{2}}, \quad \beta_2 = \frac{b_3'^{1/4}}{\sqrt{2}}, \quad \alpha_3 = \frac{b_3'^{1/4}}{\sqrt{2}} \exp\left[i\left(\frac{\phi_1+\phi_2}{2}\right)\right], \quad \beta_3 = \frac{b_3'^{1/4}}{\sqrt{2}} \exp\left[i\left(\frac{\phi_1-\phi_2}{2}\right)\right], \\
&\alpha_4 = 0, \qquad \beta_4 = 0,
\end{aligned} \tag{A.20}$$

which means that all b_i's that satisfy eqs. (A.12) and (A.13) correspond to some α_i and β_i parameters. The fact that $(\alpha_4, \beta_4) = (0, 0)$ implies that including W^3 states in this "factorized" elastic positivity approach does not give rise to new bounds.

It is now clear that, for $i = 1, 4$, we should require that eq. (A.10) holds, subject to the inequalities (A.12) and (A.13); and for $i = 2$ (and equivalently $i = 3$), we require eq. (A.11) to hold, subject to the same set of inequalities. In terms of $\sqrt{b_1}, \sqrt{b_2}, \sqrt{b_3}, b_4, b_5, b_6, \sqrt{b_7}$, these are two quadratically constrained quadratic programming (QCQP) problems, i.e. we essentially need to minimize the l.h.s. eqs. (A.10) and (A.11), which are quadratic polynomials, subject to a set of quadratic constraints. We can further simplify these problems. For $i = 1, 4$, for any b_i within the constraints, one can always change the values of b_1 and b_2 to $(b_1 + b_2)/2$, and the values of b_4 and b_5 to $(b_4 + b_5)/2$, without changing the l.h.s. of eq. (A.10). At the same time the constraints in eqs. (A.12) and (A.13) are still satisfied, due to $2(b_1 + b_2) \geq (\sqrt{b_1} + \sqrt{b_2})^2$. Therefore the first QCQP problem can be written as

$$\begin{aligned}
&\text{QCQP-1}: \\
&\text{minimize} \quad 2b_1 M_{b1} + b_3 M_{b3} + 2b_4 M_{b4} + b_6 M_{b6} + b_7 M_{b7} \\
&\text{subject to} \quad b_7 \geq 0, 0 \leq b_1 \leq b_3, |b_4| \leq 2\sqrt{b_1 b_7}, b_6 \geq 2\sqrt{b_3 b_7}
\end{aligned} \tag{A.21}$$

For the $i = 2$ case, we can redefine $b_5 + b_6$ as b_6, and write the problem as:

$$\begin{aligned}
&\text{QCQP-2}: \\
&\text{minimize} \quad b_1 M_{b1} + (b_2 + b_3) M_{b2} + b_4 M_{b4} + b_6 M_{b5} + b_7 M_{b7} \\
&\text{subject to} \quad b_7 \geq 0, 0 \leq b_1 \leq b_3, 0 \leq b_2 \leq b_3, |b_4| \leq 2\sqrt{b_1 b_7}, \\
&\qquad\qquad b_6 \geq 2\sqrt{b_3 b_7} - 2\sqrt{b_2 b_7}
\end{aligned} \tag{A.22}$$

In the following, we will show how QCQP-1 can be solved analytically.

JHEP01(2021)095

Our goal is to find the conditions under which the two QCQP problems: 1) admit a minimum value, and 2) the minimum value is positive. We will see that each condition corresponds to the target function being positive at a specific point in the b_i space. In the following, we will always list the conditions, along with the corresponding b_i points shown in a pair of parentheses. The conditions will become our positivity bounds, while the b_i values correspond the scattering channels, from which these bounds are derived.

First of all, two conditions can be derived by examining the $b_3 = 0$ case, for which we also have $b_1 = b_4 = 0$:

$$\text{Condition: } M_{b6} \geq 0 \tag{A.23}$$
$$(b_6 > 0, \quad \text{other } b_i = 0)$$
$$\text{Condition: } M_{b7} \geq 0 \tag{A.24}$$
$$(b_7 > 0, \quad \text{other } b_i = 0)$$

Now we consider $b_3 > 0$. Since the problem is homogeneous in b_i, we set $b_3 = 1$ without loss of generality. Knowing $M_{b6} \geq 0$, and using $|M_{b4}| \geq 0$, we further minimize the amplitude by taking $b_6 \to 2\sqrt{b_7}$ and the b_4 term to $-4\sqrt{b_1 b_7}|M_{b4}|$. Now the problem has two variables:

$$\begin{aligned} &\text{minimize} \quad 2x^2 M_{b1} + M_{b3} - 4xy|M_{b4}| + 2yM_{b6} + y^2 M_{b7} \\ &\text{subject to} \quad y \geq 0, 0 \leq x \leq 1 \end{aligned} \tag{A.25}$$

where we have let $b_1 = x^2$ and $b_7 = y^2$, as they are both positive. The rest is simply to find the (x, y) value that minimize the function. Note that since x is bounded in $[0, 1]$, M_{b1} does not have to be positive for the target function to admit a minimum. To proceed, consider two cases, $M_{b1} < 0$ and $M_{b1} \geq 0$. For the first case:

$$\text{QCQP-1-1: } M_{b1} < 0 \tag{A.26}$$
$$\bullet \text{ If } M_{b6} \geq 2|M_{b4}| : \tag{A.27}$$
$$\text{Condition: } 2M_{b1} + M_{b3} \geq 0 \tag{A.28}$$
$$((x, y) = (1, 0))$$
This condition is required even when $M_{b1} \geq 0$ and/or $M_{b_6} \leq 2|M_{b4}|$.
$$\bullet \text{ If } M_{b6} \leq 2|M_{b4}| : \tag{A.29}$$
$$\text{Condition: } 2M_{b1} + M_{b3} - \frac{(2|M_{b4}| - M_{b6})^2}{M_{b7}} \geq 0 \tag{A.30}$$
$$\left((x, y) = \left(1, \frac{2|M_{b4}| - M_{b6}}{M_{b7}}\right)\right)$$
This condition is required even when $M_{b1} \geq 0$.

Here, condition (A.28) needs to be satisfied regardless of conditions (A.26) and (A.27), because the target function needs to be positive for $(x, y) = (1, 0)$, which is in the proper range, i.e. eq. (A.25), eqs. (A.26) and (A.27) simply give the conditions for this point to be the true minimum. In contrast, eq. (A.29) should be kept, as it is required for $y \geq 0$ in

JHEP01(2021)095

eq. (A.25). For QCQP-1-2 (i.e. $M_{b1} \geq 0$), we can obtain similar results:

$$\text{QCQP-1-2:}\quad M_{b1} \geq 0 \tag{A.31}$$

- Condition: $M_{b3} \geq 0$ (A.32)

  $((x, y) = (0, 0))$

- If $M_{b6} \leq 2|M_{b4}|$: (A.33)

  $$\text{Condition: } 2M_{b1} + M_{b3} - \frac{(2|M_{b4}| - M_{b6})^2}{M_{b7}} \geq 0 \tag{A.34}$$

  $$\left((x, y) = \left(1, \frac{2|M_{b4}| - M_{b_6}}{M_{b_7}}\right)\right)$$

Collecting all conditions, and converting (x, y) to $\{b_i\}$, the final result for QCQP-1 is

- Condition: $M_{b6} \geq 0$ (A.35)

  $(b_6 > 0, \quad \text{other } b_i = 0)$

- Condition: $M_{b7} \geq 0$ (A.36)

  $(b_7 > 0, \quad \text{other } b_i = 0)$

- Condition: $M_{b3} \geq 0$ (A.37)

  $(b_3 > 0, \quad \text{other } b_i = 0)$

- Condition: $2M_{b1} + M_{b3} \geq 0$ (A.38)

  $(b_1 = b_3 > 0, \quad \text{other } b_i = 0)$

- Condition: If $-2M_{b4} \geq M_{b6}$ then $M_{b7}(2M_{b1} + M_{b3}) - (2M_{b4} + M_{b6})^2 \geq 0$ (A.39)

  $$\left(b_1 = b_3 = 1, b_4 = b_6 = 2\left(\frac{-2M_{b4} - M_{b6}}{M_{b7}}\right), b_7 = \frac{b_4^2}{4}\right)$$

- Condition: If $2M_{b_4} \geq M_{b_6}$ then $M_{b7}(2M_{b1} + M_{b3}) - (2M_{b4} - M_{b6})^2 \geq 0$ (A.40)

  $$\left(b_1 = b_3 = 1, b_4 = -b_6 = -2\left(\frac{2M_{b4} - M_{b6}}{M_{b7}}\right), b_7 = \frac{b_4^2}{4}\right)$$

For QCQP-2, which can be solved similarly, we simply present the results as below

- Condition: $M_{b2} \geq 0$ (A.41)

  $(b_2 = b_3 > 0, \quad \text{other } b_i = 0)$

- Condition: $M_{b1} + M_{b2} \geq 0$ (A.42)

  $(b_1 = b_3 > 0, \quad \text{other } b_i = 0)$

- Condition: $M_{b7} \geq 0$ (A.43)

  $(b_7 > 0, \quad \text{other } b_i = 0)$

- Condition: $M_{b5} \geq 0$ (A.44)

  $(b_6 > 0, \quad \text{other } b_i = 0)$

- Condition: $M_{b7}(M_{b1} + 2M_{b2}) - M_{b4}^2 \geq 0$ (A.45)

  $$\left(b_1 = b_2 = b_3 = 1, b_4 = -2\frac{M_{b4}}{M_{b7}}, b_6 = 0, b_7 = \frac{b_4^2}{4}\right)$$

JHEP01(2021)095

- Condition: if $(-M_{b4}-M_{b5})(M_{b2}M_{b7}+M_{b4}M_{b5})\geq 0$ (A.46)

  then $M_{b1}+M_{b2}-\dfrac{M_{b2}}{M_{b2}M_{b7}-M_{b5}^2}(M_{b4}+M_{b5})^2\geq 0$ (A.47)

  $$\left(b_1=b_3=1, b_2=\left(\frac{M_{b5}(M_{b4}+M_{b5})}{M_{b2}M_{b7}-M_{b5}^2}\right)^2, b_4=2\frac{M_{b2}(-M_{b4}-M_{b5})}{M_{b2}M_{b7}-M_{b5}^2},\right.$$
  $$\left. b_6=2\frac{M_{b2}(-M_{b4}-M_{b5})(M_{b2}M_{b7}+M_{b4}M_{b5})}{(M_{b2}M_{b7}-M_{b5}^2)^2}, b_7=\frac{b_4^2}{4}\right)$$

- Condition: if $(M_{b4}-M_{b5})(M_{b2}M_{b7}-M_{b4}M_{b5})\geq 0$ (A.48)

  then $M_{b1}+M_{b2}-\dfrac{M_{b2}}{M_{b2}M_{b7}-M_{b5}^2}(M_{b4}-M_{b5})^2\geq 0$ (A.49)

  $$\left(b_1=b_3=1, b_2=\left(\frac{M_{b5}(M_{b4}-M_{b5})}{M_{b2}M_{b7}-M_{b5}^2}\right)^2, b_4=-2\frac{M_{b2}(M_{b4}-M_{b5})}{M_{b2}M_{b7}-M_{b5}^2},\right.$$
  $$\left. b_6=2\frac{M_{b2}(M_{b4}-M_{b5})(M_{b2}M_{b7}-M_{b4}M_{b5})}{(M_{b2}M_{b7}-M_{b5}^2)^2}, b_7=\frac{b_4^2}{4}\right)$$

Once the programming problems are solved, what is left is simply to plug in eqs. (A.4) and (A.7), respectively, into the conditions of QCQP-1, and similarly, eq. (A.5) into QCQP-2. This will give the positivity bounds in terms of the Wilson coefficients $F_{T,i}$. To identify the actual elastic channel and the polarization for each bound, since we have kept track of $a_i(i=1,2,3)$ and $b_j(j=1,\cdots,7)$, the (x_i,y_i) and (α_i,β_i) parameters can be solved using eqs. (4.6)–(4.11). The solution is not unique, but for illustration purposes it suffices to show just one solution. For the nine linear bounds, this information is shown in eq. (4.30). Below, we give the same information for the quadratic and cubic bounds.

The three quadratic bounds in eqs. (4.26)–(4.28) are constructed by the following five conditions, with the corresponding scatterings channels ($|1\rangle+|2\rangle\to|1\rangle+|2\rangle$) and helicities as follows. Again, subscripts R and L indicate positive and negative helicity states respectively, while superscripts for the W-boson are SU(2) indices.

1. Under the conditions eqs. (4.17), (4.22), and $2F_{T,5}+2F_{T,6}+F_{T,7}\leq 0$, the following elastic channel:

   $$|1\rangle=|2\rangle=\frac{c_W}{s_W}\sqrt{\frac{-(2F_{T,5}+2F_{T,6}+F_{T,7})}{2F_{T,8}+F_{T,9}}}(|B_R\rangle+|B_L\rangle)+\left|W_R^1\right\rangle+\left|W_L^1\right\rangle \quad \text{(A.50)}$$

   gives the bound

   $$2\sqrt{[2(F_{T,0}+F_{T,1})+F_{T,2}]\,(2F_{T,8}+F_{T,9})}\geq -(2F_{T,5}+2F_{T,6}+F_{T,7}) \quad \text{(A.51)}$$

   which is also satisfied when $2F_{T,5}+2F_{T,6}+F_{T,7}\geq 0$.

JHEP01(2021)095

2. Under the conditions eqs. (4.17), (4.22), and $4F_{T,5}+F_{T,7}\geq 0$, the following elastic channel:

$$|1\rangle = \frac{c_W}{s_W}\sqrt{\frac{4F_{T,5}+F_{T,7}}{2(2F_{T,8}+F_{T,9})}}(|B_R\rangle+|B_L\rangle)+\left|W_R^1\right\rangle+\left|W_L^1\right\rangle \tag{A.52}$$

$$|2\rangle = -\frac{c_W}{s_W}\sqrt{\frac{4F_{T,5}+F_{T,7}}{2(2F_{T,8}+F_{T,9})}}(|B_R\rangle+|B_L\rangle)+\left|W_R^1\right\rangle+\left|W_L^1\right\rangle \tag{A.53}$$

gives the bound

$$4\sqrt{[2(F_{T,0}+F_{T,1})+F_{T,2}]\,(2F_{T,8}+F_{T,9})}\geq 4F_{T,5}+F_{T,7} \tag{A.54}$$

which is also satisfied when $4F_{T,5}+F_{T,7}\leq 0$.

The combination of (A.51) and (A.54) gives condition (4.26).

3. Under the conditions eqs. (4.18), (4.23), and $2F_{T,11}+F_{T,7}\leq 0$, the following elastic channel:

$$|1\rangle = \frac{c_W}{s_W}\sqrt{\frac{-(2F_{T,11}+F_{T,7})}{F_{T,9}}}(|B_R\rangle-|B_L\rangle)+\left|W_R^1\right\rangle-\left|W_L^1\right\rangle \tag{A.55}$$

$$|2\rangle = \frac{c_W}{s_W}\sqrt{\frac{-(2F_{T,11}+F_{T,7})}{F_{T,9}}}(|B_R\rangle+|B_L\rangle)+\left|W_R^1\right\rangle+\left|W_L^1\right\rangle \tag{A.56}$$

gives the bound

$$2\sqrt{F_{T,9}(F_{T,2}+4F_{T,10})}\geq -(2F_{T,11}+F_{T,7}) \tag{A.57}$$

which is also satisfied when $2F_{T,11}+F_{T,7}\geq 0$.

4. Under the conditions eqs. (4.18), (4.23) and $F_{T,11}\geq 0$, the following elastic channel:

$$|1\rangle = \frac{c_W}{s_W}\sqrt{\frac{2F_{T,11}}{F_{T,9}}}(|B_R\rangle-|B_L\rangle)+\left|W_R^1\right\rangle-\left|W_L^1\right\rangle \tag{A.58}$$

$$|2\rangle = -\frac{c_W}{s_W}\sqrt{\frac{2F_{T,11}}{F_{T,9}}}(|B_R\rangle+|B_L\rangle)+\left|W_R^1\right\rangle+\left|W_L^1\right\rangle \tag{A.59}$$

gives the bound

$$\sqrt{F_{T,9}(F_{T,2}+4F_{T,10})}\geq F_{T,11} \tag{A.60}$$

which is also satisfied when $F_{T,11}\leq 0$.

The combination of (A.57) and (A.60) gives the condition (4.27).

5. Eqs. (4.19), (4.20), and (4.21) lead to $4(F_{T,0}+F_{T,1})+3F_{T,2}+4F_{T,10}\geq 0$; and eqs. (4.22), (4.23) lead to $4F_{T,8}+3F_{T,9}\geq 0$. With these two conditions satisfied, the following elastic channel:

$$|1\rangle = \frac{c_W}{s_W}\sqrt{\frac{2F_{T,11}+4F_{T,5}+F_{T,7}}{4F_{T,8}+3F_{T,9}}}\,|B_L\rangle+\left|W_L^1\right\rangle \tag{A.61}$$

$$|2\rangle = \frac{c_W}{s_W}\sqrt{\frac{2F_{T,11}+4F_{T,5}+F_{T,7}}{4F_{T,8}+3F_{T,9}}}\,|B_L\rangle-\left|W_L^1\right\rangle \tag{A.62}$$

JHEP01(2021)095

gives the bound

$$2\sqrt{[4F_{T,10}+4(F_{T,0}+F_{T,1})+3F_{T,2}](4F_{T,8}+3F_{T,9})} \geq |2F_{T,11}+4F_{T.5}+F_{T,7}| \quad \text{(A.63)}$$

While all quadratic bounds involve some superposition between the B and the W^1 modes, the cubic bound in (4.29) involves a superposition of three states: B, W^1, and W^2. Using $2F_{T,1}+F_{T,2} \geq 0$ and $2F_{T,6}+F_{T,7} \geq 0$ derived from the conditions eqs. (4.19), (4.20), (4.24), and (4.25), the cubic bound is constructed by the following two cubic conditions.

1. Under the conditions

$$[4(2F_{T,1}+F_{T,2})(4F_{T,8}+3F_{T,9})+(2F_{T,6}+F_{T,7})(4F_{T,5}+F_{T,7}+2F_{T,11})] \times(2F_{T,5}+F_{T,6}+F_{T,7}+F_{T,11}) \leq 0$$

the following elastic channel:

$$\begin{aligned}
|1\rangle &= |2\rangle^* \qquad \text{(A.64)}\\
&= i2\sqrt{2}c_W\sqrt{(2F_{T,1}+F_{T,2})|2F_{T,5}+F_{T,6}+F_{T,7}+F_{T,11}|}\,|B_L\rangle\\
&\quad +\frac{1}{2}s_W\\
&\quad \times\Big(\sqrt{|4(2F_{T,1}+F_{T,2})(4F_{T,8}+3F_{T,9})-(2F_{T,6}+F_{T,7})(4(F_{T,5}+F_{T,6})+3F_{T,7}+2F_{T,11})|}\\
&\qquad +i\sqrt{|4(2F_{T,1}+F_{T,2})(4F_{T,8}+3F_{T,9})+(2F_{T,6}+F_{T,7})(4F_{T,5}+F_{T,7}+2F_{T,11})|}\Big)\,|W_L^1\rangle\\
&\quad +\frac{1}{2}s_W\\
&\quad \times\Big(\sqrt{|4(2F_{T,1}+F_{T,2})(4F_{T,8}+3F_{T,9})-(2F_{T,6}+F_{T,7})(4(F_{T,5}+F_{T,6})+3F_{T,7}+2F_{T,11})|}\\
&\qquad -i\sqrt{|4(2F_{T,1}+F_{T,2})(4F_{T,8}+3F_{T,9})+(2F_{T,6}+F_{T,7})(4F_{T,5}+F_{T,7}+2F_{T,11})|}\Big)\,|W_L^2\rangle
\end{aligned}$$

gives the bound

$$2F_{T,0}+F_{T,1}+F_{T,2}+2F_{T,10} \geq \frac{2(2F_{T,1}+F_{T,2})(2F_{T,5}+F_{T,6}+F_{T,7}+F_{T,11})^2}{4(2F_{T,1}+F_{T,2})(4F_{T,8}+3F_{T,9})-(2F_{T,6}+F_{T,7})^2} \quad \text{(A.65)}$$

2. Under the conditions

$$[4(2F_{T,1}+F_{T,2})(4F_{T,8}+3F_{T,9})-(2F_{T,6}+F_{T,7})(4F_{T,5}+F_{T,7}+2F_{T,11})] \times(-2F_{T,5}+F_{T,6}-F_{T,11}) \leq 0$$

JHEP01(2021)095

the following elastic channel:

$$
\begin{aligned}
|1\rangle = {} & 2\sqrt{2}c_W\sqrt{(2F_{T,1}+F_{T,2})|2F_{T,5}-F_{T,6}+F_{T,11}|}\,|B_L\rangle \\
& +\frac{1}{2}s_W \\
& \times\Bigg(\sqrt{|4(2F_{T,1}+F_{T,2})(4F_{T,8}+3F_{T,9})+(2F_{T,6}+F_{T,7})(4(F_{T,5}-F_{T,6})-F_{T,7}+2F_{T,11})|} \\
& \quad +i\sqrt{|4(2F_{T,1}+F_{T,2})(4F_{T,8}+3F_{T,9})-(2F_{T,6}+F_{T,7})(4F_{T,5}+F_{T,7}+2F_{T,11})|}\Bigg)\,|W_L^1\rangle \\
& +\frac{1}{2}s_W \\
& \times\Bigg(\sqrt{|4(2F_{T,1}+F_{T,2})(4F_{T,8}+3F_{T,9})+(2F_{T,6}+F_{T,7})(4(F_{T,5}-F_{T,6})-F_{T,7}+2F_{T,11})|} \\
& \quad -i\sqrt{|4(2F_{T,1}+F_{T,2})(4F_{T,8}+3F_{T,9})-(2F_{T,6}+F_{T,7})(4F_{T,5}+F_{T,7}+2F_{T,11})|}\Bigg)\,|W_L^2\rangle
\end{aligned}
\tag{A.66}
$$

$$
\begin{aligned}
|2\rangle = {} & -2\sqrt{2}c_W\sqrt{(2F_{T,1}+F_{T,2})|2F_{T,5}-F_{T,6}+F_{T,11}|}\,|B_L\rangle \\
& +\frac{1}{2}s_W \\
& \times\Bigg(\sqrt{|4(2F_{T,1}+F_{T,2})(4F_{T,8}+3F_{T,9})+(2F_{T,6}+F_{T,7})(4(F_{T,5}-F_{T,6})-F_{T,7}+2F_{T,11})|} \\
& \quad -i\sqrt{|4(2F_{T,1}+F_{T,2})(4F_{T,8}+3F_{T,9})-(2F_{T,6}+F_{T,7})(4F_{T,5}+F_{T,7}+2F_{T,11})|}\Bigg)\,|W_L^1\rangle \\
& +\frac{1}{2}s_W \\
& \times\Bigg(\sqrt{|4(2F_{T,1}+F_{T,2})(4F_{T,8}+3F_{T,9})+(2F_{T,6}+F_{T,7})(4(F_{T,5}-F_{T,6})-F_{T,7}+2F_{T,11})|} \\
& \quad +i\sqrt{|4(2F_{T,1}+F_{T,2})(4F_{T,8}+3F_{T,9})-(2F_{T,6}+F_{T,7})(4F_{T,5}+F_{T,7}+2F_{T,11})|}\Bigg)\,|W_L^2\rangle
\end{aligned}
\tag{A.67}
$$

gives the bound

$$
2F_{T,0}+F_{T,1}+F_{T,2}+2F_{T,10} \geq \frac{2(2F_{T,1}+F_{T,2})(2F_{T,5}-F_{T,6}+F_{T,11})^2}{4(2F_{T,1}+F_{T,2})(4F_{T,8}+3F_{T,9})-(2F_{T,6}+F_{T,7})^2} \tag{A.68}
$$

B Polarization dependence in VBS amplitudes

In eq. (4.4), we have observed that the amplitude depends on polarization parameters x and y only through the three combinations, a_1, a_2 and a_3, as defined in eq. (4.6). In this section, we will demonstrate that this is a consequence of angular momentum conservation and parity conservation. For illustration, we consider the case of BB scattering, but the same reasoning applies in general.

We consider the forward elastic scattering $|1\rangle + |2\rangle \to |1\rangle + |2\rangle$ with the superposed states

$$
|1\rangle = x_1\,|B_R\rangle + x_2\,|B_L\rangle \tag{B.1}
$$

$$
|2\rangle = y_1\,|B_R\rangle + y_2\,|B_L\rangle \tag{B.2}
$$

JHEP01(2021)095

where R and L denote positive and negative helicity states, respectively. The matrix element can be expanded in the components of x and y:

$$\begin{aligned}
&\langle 1,2|\mathcal{M}|1,2\rangle \\
&\quad = (x_1^* y_1^* \langle B_R, B_R| + x_1^* y_2^* \langle B_R, B_L| + x_2^* y_1^* \langle B_L, B_R| + x_2^* y_2^* \langle B_L, B_L|) \\
&\qquad \mathcal{M}(x_1 y_1 |B_R, B_R\rangle + x_1 y_2 |B_R, B_L\rangle + x_2 y_1 |B_L, B_R\rangle + x_2 y_2 |B_L, B_L\rangle) \qquad \text{(B.3)} \\
&\quad = |x_1|^2 |y_1|^2 \langle B_R, B_R \,|\, \mathcal{M} \,|\, B_R, B_R\rangle + |x_2|^2 |y_2|^2 \langle B_L, B_L \,|\, \mathcal{M} \,|\, B_L, B_L\rangle \\
&\qquad + x_2 y_2 x_1^* y_1^* \langle B_R, B_R \,|\, \mathcal{M} \,|\, B_L, B_L\rangle + x_1 y_1 x_2^* y_2^* \langle B_L, B_L \,|\, \mathcal{M} \,|\, B_R, B_R\rangle \\
&\qquad + |x_1|^2 |y_2|^2 \langle B_R, B_L \,|\, \mathcal{M} \,|\, B_R, B_L\rangle + |x_2|^2 |y_1|^2 \langle B_L, B_R \,|\, \mathcal{M} \,|\, B_L, B_R\rangle \qquad \text{(B.4)} \\
&\quad = (|x_1|^2 |y_1|^2 + |x_2|^2 |y_2|^2) \langle B_R, B_R \,|\, \mathcal{M} \,|\, B_R, B_R\rangle \\
&\qquad + (x_2 y_2 x_1^* y_1^* + x_1 y_1 x_2^* y_2^*) \langle B_R, B_R \,|\, \mathcal{M} \,|\, B_L, B_L\rangle \\
&\qquad + (|x_1|^2 |y_2|^2 + |x_2|^2 |y_1|^2) \langle B_R, B_L \,|\, \mathcal{M} \,|\, B_R, B_L\rangle \qquad \text{(B.5)} \\
&\quad = \left(a_2 + \frac{a_1 - a_3}{2}\right) \langle B_R, B_R \,|\, \mathcal{M} \,|\, B_R, B_R\rangle + \frac{1}{2}(a_1 - a_3) \langle B_R, B_R \,|\, \mathcal{M} \,|\, B_L, B_L\rangle \\
&\qquad + \frac{1}{2}(a_1 + a_3) \langle B_R, B_L \,|\, \mathcal{M} \,|\, B_R, B_L\rangle \,, \qquad \text{(B.6)}
\end{aligned}$$

where, to obtain eq. (B.4), 10 terms that violate angular momentum conservation in the forward limit have been dropped (such as $\langle B_R, B_R \,|\, \mathcal{M} \,|\, B_R, B_L\rangle$ and $\langle B_L, B_R \,|\, \mathcal{M} \,|\, B_R, B_L\rangle$, etc.); to obtain eq. (B.5), parity conservation has been use, as all operators considered in this work conserve parity.

Eq. (B.6) shows that the elastic forward amplitude, superposed in the helicity space, depends on the superposition parameters x and y only through the three a_i parameters.

References

[1] B. Henning, X. Lu, T. Melia and H. Murayama, 2, 84, 30, 993, 560, 15456, 11962, 261485, ...: *higher dimension operators in the SM EFT*, *JHEP* **08** (2017) 016 [*Erratum ibid.* **09** (2019) 019] [arXiv:1512.03433] [INSPIRE].

[2] C.W. Murphy, *Dimension-8 operators in the Standard Model effective field theory*, *JHEP* **10** (2020) 174 [arXiv:2005.00059] [INSPIRE].

[3] H.-L. Li, Z. Ren, J. Shu, M.-L. Xiao, J.-H. Yu and Y.-H. Zheng, *Complete set of dimension-8 operators in the Standard Model effective field theory*, arXiv:2005.00008 [INSPIRE].

[4] C. Zhang and S.-Y. Zhou, *Positivity bounds on vector boson scattering at the LHC*, *Phys. Rev. D* **100** (2019) 095003 [arXiv:1808.00010] [INSPIRE].

[5] Q. Bi, C. Zhang and S.-Y. Zhou, *Positivity constraints on aQGC: carving out the physical parameter space*, *JHEP* **06** (2019) 137 [arXiv:1902.08977] [INSPIRE].

[6] B. Bellazzini and F. Riva, *New phenomenological and theoretical perspective on anomalous ZZ and Zγ processes*, *Phys. Rev. D* **98** (2018) 095021 [arXiv:1806.09640] [INSPIRE].

JHEP01(2021)095

[7] G.N. Remmen and N.L. Rodd, *Consistency of the Standard Model effective field theory*, *JHEP* **12** (2019) 032 [arXiv:1908.09845] [INSPIRE].

[8] G.N. Remmen and N.L. Rodd, *Flavor constraints from unitarity and analyticity*, *Phys. Rev. Lett.* **125** (2020) 081601 [arXiv:2004.02885] [INSPIRE].

[9] C. Zhang and S.-Y. Zhou, *Convex geometry perspective on the (Standard Model) effective field theory space*, *Phys. Rev. Lett.* **125** (2020) 201601 [arXiv:2005.03047] [INSPIRE].

[10] B. Fuks, Y. Liu, C. Zhang and S.-Y. Zhou, *Positivity in electron-positron scattering: testing the axiomatic quantum field theory principles and probing the existence of UV states*, arXiv:2009.02212 [INSPIRE].

[11] A. Adams, N. Arkani-Hamed, S. Dubovsky, A. Nicolis and R. Rattazzi, *Causality, analyticity and an IR obstruction to UV completion*, *JHEP* **10** (2006) 014 [hep-th/0602178] [INSPIRE].

[12] C. de Rham, S. Melville, A.J. Tolley and S.-Y. Zhou, *Positivity bounds for scalar field theories*, *Phys. Rev. D* **96** (2017) 081702 [arXiv:1702.06134] [INSPIRE].

[13] C. de Rham, S. Melville, A.J. Tolley and S.-Y. Zhou, *UV complete me: positivity bounds for particles with spin*, *JHEP* **03** (2018) 011 [arXiv:1706.02712] [INSPIRE].

[14] T.N. Pham and T.N. Truong, *Evaluation of the derivative quartic terms of the meson chiral Lagrangian from forward dispersion relation*, *Phys. Rev. D* **31** (1985) 3027 [INSPIRE].

[15] M.R. Pennington and J. Portoles, *The chiral Lagrangian parameters, l_1, l_2, are determined by the ρ resonance*, *Phys. Lett. B* **344** (1995) 399 [hep-ph/9409426] [INSPIRE].

[16] B. Ananthanarayan, D. Toublan and G. Wanders, *Consistency of the chiral pion pion scattering amplitudes with axiomatic constraints*, *Phys. Rev. D* **51** (1995) 1093 [hep-ph/9410302] [INSPIRE].

[17] J. Comellas, J.I. Latorre and J. Taron, *Constraints on chiral perturbation theory parameters from QCD inequalities*, *Phys. Lett. B* **360** (1995) 109 [hep-ph/9507258] [INSPIRE].

[18] A.V. Manohar and V. Mateu, *Dispersion relation bounds for $\pi\pi$ scattering*, *Phys. Rev. D* **77** (2008) 094019 [arXiv:0801.3222] [INSPIRE].

[19] I. Low, R. Rattazzi and A. Vichi, *Theoretical constraints on the Higgs effective couplings*, *JHEP* **04** (2010) 126 [arXiv:0907.5413] [INSPIRE].

[20] J.J. Sanz-Cillero, D.-L. Yao and H.-Q. Zheng, *Positivity constraints on the low-energy constants of the chiral pion-nucleon Lagrangian*, *Eur. Phys. J. C* **74** (2014) 2763 [arXiv:1312.0664] [INSPIRE].

[21] B. Bellazzini, *Softness and amplitudes' positivity for spinning particles*, *JHEP* **02** (2017) 034 [arXiv:1605.06111] [INSPIRE].

[22] N. Arkani-Hamed, T.-C. Huang and Y.-T. Huang, *The EFT-hedron*, arXiv:2012.15849 [INSPIRE].

[23] C. de Rham, S. Melville, A.J. Tolley and S.-Y. Zhou, *Positivity bounds for massive spin-1 and spin-2 fields*, *JHEP* **03** (2019) 182 [arXiv:1804.10624] [INSPIRE].

[24] C. de Rham, S. Melville, A.J. Tolley and S.-Y. Zhou, *Massive Galileon positivity bounds*, *JHEP* **09** (2017) 072 [arXiv:1702.08577] [INSPIRE].

[25] D. Baumann, D. Green, H. Lee and R.A. Porto, *Signs of analyticity in single-field inflation*, *Phys. Rev. D* **93** (2016) 023523 [arXiv:1502.07304] [INSPIRE].

JHEP01(2021)095

[26] B. Bellazzini, C. Cheung and G.N. Remmen, *Quantum gravity constraints from unitarity and analyticity*, *Phys. Rev. D* **93** (2016) 064076 [arXiv:1509.00851] [INSPIRE].

[27] C. Cheung and G.N. Remmen, *Positive signs in massive gravity*, *JHEP* **04** (2016) 002 [arXiv:1601.04068] [INSPIRE].

[28] J. Bonifacio, K. Hinterbichler and R.A. Rosen, *Positivity constraints for pseudolinear massive spin-2 and vector Galileons*, *Phys. Rev. D* **94** (2016) 104001 [arXiv:1607.06084] [INSPIRE].

[29] M.-L. Du, F.-K. Guo, U.-G. Meißner and D.-L. Yao, *Aspects of the low-energy constants in the chiral Lagrangian for charmed mesons*, *Phys. Rev. D* **94** (2016) 094037 [arXiv:1610.02963] [INSPIRE].

[30] B. Bellazzini, F. Riva, J. Serra and F. Sgarlata, *Beyond positivity bounds and the fate of massive gravity*, *Phys. Rev. Lett.* **120** (2018) 161101 [arXiv:1710.02539] [INSPIRE].

[31] K. Hinterbichler, A. Joyce and R.A. Rosen, *Massive spin-2 scattering and asymptotic superluminality*, *JHEP* **03** (2018) 051 [arXiv:1708.05716] [INSPIRE].

[32] B. Bellazzini, F. Riva, J. Serra and F. Sgarlata, *The other effective fermion compositeness*, *JHEP* **11** (2017) 020 [arXiv:1706.03070] [INSPIRE].

[33] J. Bonifacio and K. Hinterbichler, *Bounds on amplitudes in effective theories with massive spinning particles*, *Phys. Rev. D* **98** (2018) 045003 [arXiv:1804.08686] [INSPIRE].

[34] B. Bellazzini, M. Lewandowski and J. Serra, *Positivity of amplitudes, weak gravity conjecture, and modified gravity*, *Phys. Rev. Lett.* **123** (2019) 251103 [arXiv:1902.03250] [INSPIRE].

[35] S. Melville and J. Noller, *Positivity in the sky: constraining dark energy and modified gravity from the UV*, *Phys. Rev. D* **101** (2020) 021502 [*Erratum ibid.* **102** (2020) 049902] [arXiv:1904.05874] [INSPIRE].

[36] S. Melville, D. Roest and D. Stefanyszyn, *UV constraints on massive spinning particles: lessons from the gravitino*, *JHEP* **02** (2020) 185 [arXiv:1911.03126] [INSPIRE].

[37] C. de Rham and A.J. Tolley, *Speed of gravity*, *Phys. Rev. D* **101** (2020) 063518 [arXiv:1909.00881] [INSPIRE].

[38] L. Alberte, C. de Rham, A. Momeni, J. Rumbutis and A.J. Tolley, *Positivity constraints on interacting spin-2 fields*, *JHEP* **03** (2020) 097 [arXiv:1910.11799] [INSPIRE].

[39] L. Alberte, C. de Rham, A. Momeni, J. Rumbutis and A.J. Tolley, *Positivity constraints on interacting pseudo-linear spin-2 fields*, *JHEP* **07** (2020) 121 [arXiv:1912.10018] [INSPIRE].

[40] G. Ye and Y.-S. Piao, *Positivity in the effective field theory of cosmological perturbations*, *Eur. Phys. J. C* **80** (2020) 421 [arXiv:1908.08644] [INSPIRE].

[41] Y.-J. Wang, F.-K. Guo, C. Zhang and S.-Y. Zhou, *Generalized positivity bounds on chiral perturbation theory*, *JHEP* **07** (2020) 214 [arXiv:2004.03992] [INSPIRE].

[42] L. Alberte, C. de Rham, S. Jaitly and A.J. Tolley, *Positivity bounds and the massless spin-2 pole*, *Phys. Rev. D* **102** (2020) 125023 [arXiv:2007.12667] [INSPIRE].

[43] Y.-T. Huang, J.-Y. Liu, L. Rodina and Y. Wang, *Carving out the space of open-string S-matrix*, arXiv:2008.02293 [INSPIRE].

[44] J. Tokuda, K. Aoki and S. Hirano, *Gravitational positivity bounds*, *JHEP* **11** (2020) 054 [arXiv:2007.15009] [INSPIRE].

JHEP01(2021)095

[45] J. Distler, B. Grinstein, R.A. Porto and I.Z. Rothstein, *Falsifying models of new physics via WW scattering*, *Phys. Rev. Lett.* **98** (2007) 041601 [hep-ph/0604255] [INSPIRE].

[46] N. Arkani-Hamed, G.L. Kane, J. Thaler and L.-T. Wang, *Supersymmetry and the LHC inverse problem*, *JHEP* **08** (2006) 070 [hep-ph/0512190] [INSPIRE].

[47] S. Dawson, S. Homiller and S.D. Lane, *Putting Standard Model EFT fits to work*, *Phys. Rev. D* **102** (2020) 055012 [arXiv:2007.01296] [INSPIRE].

[48] J. Gu and L.-T. Wang, *Sum rules in the Standard Model effective field theory from helicity amplitudes*, arXiv:2008.07551 [INSPIRE].

[49] J. Ellis and S.-F. Ge, *Constraining gluonic quartic gauge coupling operators with $gg \to \gamma\gamma$*, *Phys. Rev. Lett.* **121** (2018) 041801 [arXiv:1802.02416] [INSPIRE].

[50] S. Alioli, R. Boughezal, E. Mereghetti and F. Petriello, *Novel angular dependence in Drell-Yan lepton production via dimension-8 operators*, *Phys. Lett. B* **809** (2020) 135703 [arXiv:2003.11615] [INSPIRE].

[51] CMS collaboration, *Search for anomalous electroweak production of vector boson pairs in association with two jets in proton-proton collisions at* 13 *TeV*, *Phys. Lett. B* **798** (2019) 134985 [arXiv:1905.07445] [INSPIRE].

[52] CMS collaboration, *Measurements of production cross sections of same-sign WW and WZ boson pairs in association with two jets in proton-proton collisions at $\sqrt{s} = 13$ TeV*, Tech. Rep. CMS-PAS-SMP-19-012, CERN, Geneva, Switzerland (2020).

[53] CMS collaboration, *Measurement of the cross section for electroweak production of a Z boson, a photon and two jets in proton-proton collisions at $\sqrt{s} = 13$ TeV and constraints on anomalous quartic couplings*, *JHEP* **06** (2020) 076 [arXiv:2002.09902] [INSPIRE].

[54] J. Ellis, S.-F. Ge, H.-J. He and R.-Q. Xiao, *Probing the scale of new physics in the $ZZ\gamma$ coupling at e^+e^- colliders*, *Chin. Phys. C* **44** (2020) 063106 [arXiv:1902.06631] [INSPIRE].

[55] J. Ellis, H.-J. He and R.-Q. Xiao, *Probing new physics in dimension-8 neutral gauge couplings at e^+e^- colliders*, *Sci. China Phys. Mech. Astron.* **64** (2021) 221062 [arXiv:2008.04298] [INSPIRE].

[56] M. Rauch, *Vector-boson fusion and vector-boson scattering*, arXiv:1610.08420 [INSPIRE].

[57] A. Azatov, R. Contino, C.S. Machado and F. Riva, *Helicity selection rules and noninterference for BSM amplitudes*, *Phys. Rev. D* **95** (2017) 065014 [arXiv:1607.05236] [INSPIRE].

[58] *Limits on anomalous triple and quartic gauge couplings webpage*, https://twiki.cern.ch/twiki/bin/view/CMSPublic/PhysicsResultsSMPaTGC.

[59] P. Azzi et al., *Report from working group* 1*: Standard Model physics at the HL-LHC and HE-LHC*, *CERN Yellow Rep. Monogr.* **7** (2019) 1 [arXiv:1902.04070] [INSPIRE].

[60] O.J.P. Eboli, M.C. Gonzalez-Garcia and J.K. Mizukoshi, *$pp \to jje^\pm\mu^\pm\nu\nu$ and $jje^\pm\mu^\mp\nu\nu$ at $O(\alpha_{\rm em}^6)$ and $O(\alpha_{\rm em}^4\alpha_s^2)$ for the study of the quartic electroweak gauge boson vertex at CERN LHC*, *Phys. Rev. D* **74** (2006) 073005 [hep-ph/0606118] [INSPIRE].

[61] C. Degrande et al., *Monte Carlo tools for studies of non-standard electroweak gauge boson interactions in multi-boson processes: a Snowmass white paper*, in *Community summer study* 2013*: Snowmass on the Mississippi*, (2013) [arXiv:1309.7890] [INSPIRE].

JHEP01(2021)095

[62] O.J.P. Éboli and M.C. Gonzalez-Garcia, *Classifying the bosonic quartic couplings*, *Phys. Rev. D* **93** (2016) 093013 [arXiv:1604.03555] [INSPIRE].

[63] B. Grzadkowski, M. Iskrzynski, M. Misiak and J. Rosiek, *Dimension-six terms in the Standard Model Lagrangian*, *JHEP* **10** (2010) 085 [arXiv:1008.4884] [INSPIRE].

[64] N.D. Christensen and C. Duhr, *FeynRules — Feynman rules made easy*, *Comput. Phys. Commun.* **180** (2009) 1614 [arXiv:0806.4194] [INSPIRE].

[65] A. Alloul, N.D. Christensen, C. Degrande, C. Duhr and B. Fuks, *FeynRules* 2.0 — *a complete toolbox for tree-level phenomenology*, *Comput. Phys. Commun.* **185** (2014) 2250 [arXiv:1310.1921] [INSPIRE].

[66] T. Hahn, *Generating Feynman diagrams and amplitudes with FeynArts* 3, *Comput. Phys. Commun.* **140** (2001) 418 [hep-ph/0012260] [INSPIRE].

[67] T. Hahn and M. Pérez-Victoria, *Automatized one loop calculations in four-dimensions and D-dimensions*, *Comput. Phys. Commun.* **118** (1999) 153 [hep-ph/9807565] [INSPIRE].

[68] D. Avis and K. Fukuda, *A pivoting algorithm for convex hulls and vertex enumeration of arrangements and polyhedra*, *Discrete Comput. Geom.* **8** (1992) 295.

[69] D. Avis, *lrs webpage*, http://cgm.cs.mcgill.ca/~avis/C/lrs.html.

JHEP01(2021)095